
**DOCUMENT DE RECHERCHE**

**EPEE**

**CENTRE D'ETUDES DES POLITIQUES ECONOMIQUES DE L'UNIVERSITE D'EVRY**

# Evolving Monetary Policy in the Aftermath of the Great Recession

**A. ORTMANS**

**20-01**

www.univ-evry.fr/EPEE

**Université d'Evry Val d'Essonne, 4 bd. F. Mitterrand, 91025 Evry CEDEX**

# Evolving Monetary Policy in the Aftermath of the Great Recession

Aymeric Ortmans*

November 16, 2020

**Abstract**

A Taylor-type monetary policy rule is estimated using a time-varying parameter vector autoregressive model to assess changes in central banks' behavior during and after the Great Recession. Based on US and euro area data, the results show that both the Fed and the ECB have changed their behavior after the 2008 crisis. Contemporaneous coefficients have increased with expansionary monetary policy at the ZLB. Although they do not indicate clear evidence of significant changes in the systematic component of monetary policy, estimated response coefficients suggest dramatic shifts in monetary policy shocks after the Global Financial Crisis. These departures from rule-based behavior – i.e. monetary policy discretion – are increasingly larger with the implementation of non-standard measures. Unconventional monetary policy shocks are shown to strongly affect the US macroeconomy and to contribute to the variance of inflation and output even more importantly when the Fed eased its monetary policy at the ZLB. This is not the case in the euro area, despite increasing monetary policy shocks in unconventional times. A counterfactual analysis shows however that the shift in the systematic component of monetary policy appears to be a key determinant of the level of inflation and output at the ZLB, especially in the euro area that would have suffered a continuous period of deflation from 2014:1 to 2018:1 without any change in ECB's behavior after the 2008 crisis.

**Keywords:** Federal Reserve, European Central Bank, Taylor rule, Time-varying parameter VAR, Shadow rate, Zero lower bound

**JEL Codes:** C32, E31, E32, E37, E43, E44, E52, E58

*Université Paris-Saclay, Univ Evry, EPEE, 91025, Evry-Courcouronnes, France.

*E-mail address:* aymeric.ortmans@univ-evry.fr

I wish to thank my supervisor Fabien Tripier for his extremely precious help, and Jean-Bernard Chatelain (discussant), Carl Grekou, Wenjiao Hu (discussant), Paul Hubert, Gary Koop, Stéphane Lhuissier, Thomas A. Lubik for helpful comments and discussion. I am particularly grateful to Peter N. Ireland for his valuable advice. I also thank all participants at EPEE seminar, 10th Thematic School on Public Policy Evaluation (TEPP - CNRS), 36th GdRE International Symposium on Money, Banking and Finance, 68th Annual meeting of the French Economic Association (AFSE) and ADRES Annual Doctoral Conference. All remaining errors are mine. This paper has previously been circulated as "Central Banks' Behavior in the Aftermath of the Great Recession".

# 1 Introduction

Central banks are in the spotlight since the 2008 financial crisis and the resulting 'Great Recession'. The global economic downturn spurred the main central banks to take drastic decisions, as cutting short-term interest rates to zero and adopting unconventional measures by implementing new monetary policy tools. Hitting the so-called zero lower bound (ZLB) on nominal interest rates, lots of central banks decided to use a large set of non-standard policy tools, including negative interest rate policy (NIRP), quantitative easing (QE), long-term refinancing operations (LTROs) or forward guidance (FG). Those operations have been conducted to foster economic activity by going beyond the traditional use of nominal short-term interest rates as the main policy instrument.

Figure 1: Policy rates and balance sheets

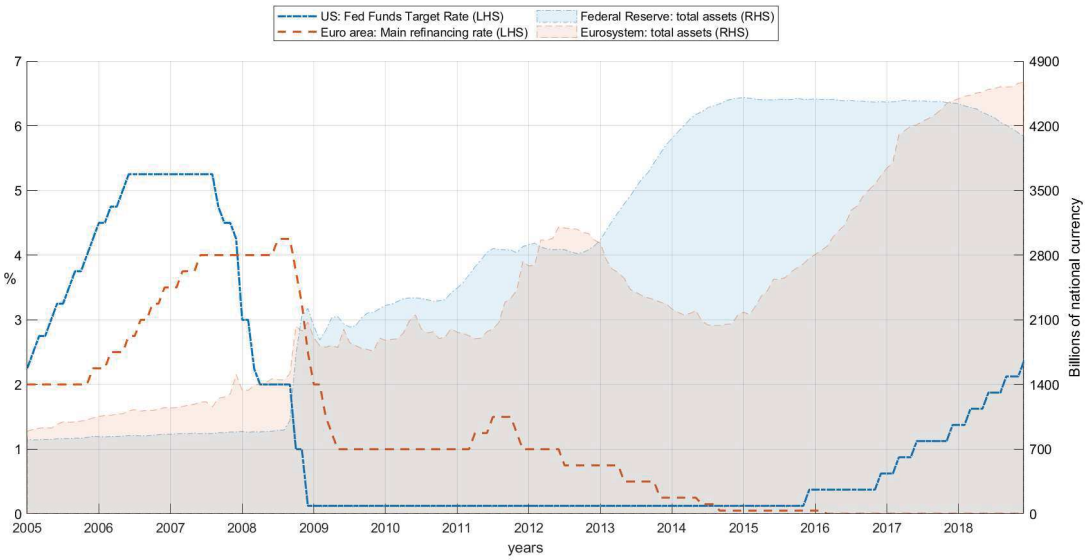


*Note:* Monthly data from Federal Reserve and European Central Bank. Left-hand side: policy rates in percentage. Right-hand side: central banks' total assets in billions of US dollars for the Federal Reserve and billions of euros for the Eurosystem.

Hence, as depicted in Figure 1, it seems that central banks were actually "not very constrained by the zero lower bound on nominal interest rates" after the crisis, to quote Swanson (2018).[1] Notwithstanding target nominal interest rates near or at 0%, explosive balance sheets show how the Federal Reserve and the European Central Bank (Fed and ECB hereafter, respectively) kept on acting strongly to lower long-term interest rates during the ZLB, for the purpose of stimulating the real economy by setting negative policy rates, purchasing

[1]Eric T. Swanson focuses on the Federal Reserve in his paper. He echoes Debortoli et al. (2019) and supports the view that macroeconomic performances were not affected by the binding ZLB constraint (known as the *ZLB empirical 'irrelevance hypothesis'*), through the effectiveness of Fed's unconventional monetary policy and its ability to influence interest rates all along the yield curve. Other recent papers suggest that the ZLB was not such a constraint on policy, such as Garín et al. (2019), Wieland (2019), Wu and Zhang (2019) and Lhuissier et al. (2020) for instance. This is consistent with earlier literature on unconventional monetary policy as a relatively effective substitute for the federal funds rate at the ZLB, including Vissing Jorgensen and Krishnamurthy (2011) for QE and Campbell et al. (2012) for FG, among many others. Recently, Kim et al. (2020) and Kortela and Nelimarkka (2020) use a structural VAR and support this view in the US and in the euro area, respectively, while Sims and Wu (2020) use a DSGE approach.

a huge amount of assets, directly lending to financial institutions, or communicating about the future path of short-term interest rates.[2] Despite their exceptional nature, these policies have been launched, above all, in order to pursue the standard objectives of stabilizing inflation or stimulating economic growth. However, the implementation of US and euro area monetary policy may have evolved in the sense that the Fed and the ECB could have adapted their response to changing macroeconomic conditions after the crisis. Has the conduct of Fed and ECB monetary policy evolved in the aftermath of the Great Recession? And if so, how has it affected macroeconomic performances in the US and in the euro area?

The present paper draws on the seminal work of Taylor (1993) and the well-known 'Taylor rule', according to which the central bank sets the policy rate considering inflation and output fluctuations. Since then, a huge literature has emerged to give further insights into central banks' behavior.[3] In the spirit of the standard Taylor rule, central bank's behavior may be defined by its emphasis on stabilizing inflation and output, but also by its willingness to depart from the behavior prescribed by the policy rule. This paper investigates in which extent changes in central banks' behavior may explain monetary policy decisions since the Great Recession, and how it may have influenced inflation and economic growth. Based on the methodology employed in Belongia and Ireland (2016), I use a time-varying parameters vector autoregressive (TVP-VAR) model with stochastic volatility to estimate a Taylor-type rule with drifting coefficients. I extend their work by focusing especially on the post-2008 decade, including the Great Recession and the ZLB, and by comparing the Fed and the ECB. To get rid of flat rates challenging monetary policy rule estimations in the ZLB era, I use the shadow rate constructed by Krippner (2013, 2019) as a proxy for the short-term nominal interest rate that captures the overall stance of monetary policy at the ZLB taking into account unconventional policy actions. Hence, a shadow Taylor rule with time-varying parameters is estimated on the ZLB sample period.[4]

Estimation results show that the Fed and the ECB have changed their behavior in the aftermath the Great Recession. Contemporaneous coefficients of the time-varying reaction function have increased with expansionary monetary policy at the ZLB. In the US, they peaked when the Fed started tapering in end-2013 and went back to pre-crisis levels around the time of the main policy rate lift-off. In the euro area, they went up around 2009 and are still large due to ongoing massive expansionary ECB's monetary policy. However, these results do not indicate clear evidence of significant changes in Fed's and ECB's responses to inflation and output. Importantly, the evolution of estimated response coefficients suggests dramatic shifts in monetary policy shocks during and after the Great Recession. The path of realized policy shocks volatility both in the US and in the euro area is statistically different from the pre-recession period, and support striking evidence of a change in monetary policy after the 2008 crisis. These departures from rule-like behavior during the ZLB are interpreted as more policy

[2]From 2008 to 2014, the Federal Reserve has implemented three successive QE programmes (Dec. 2008, Nov. 2010 and Sep. 2012). In late 2015, it began to normalize US monetary policy by raising the key policy rate, and by reducing its balance sheet in late 2017. The European Central Bank decided to improve credit support and bank lending (Oct. 2008 and June 2009), and launched its first asset purchase programme (APP) in July 2009. However, its balance sheet expanded a lot in 2012 due to very long-term refinancing operations (VLTROs), and especially in 2015 when it implemented an APP including both sovereign bonds and private-sector securities purchases. This point is also discussed in Section 4.

[3]Bernanke and Mishkin (1992) use the expression "central bank behavior" to mention the conduct and the performance of monetary policy.

[4]See pioneering papers using the shadow rate in VAR models (Wu and Xia, 2016) or DSGE models (Wu and Zhang, 2019). Based on the latter paper, the relevance of shadow Taylor rules is discussed in Appendix B (more references in Section 4).

discretion, and hugely increase with the launch of non-standard policy measures. Unconventional monetary policy shocks are shown to strongly affect the US macroeconomy and to contribute to the variance of inflation and output even more importantly when the Fed eased its monetary policy at the ZLB. Nevertheless, increasing monetary policy shocks at the ZLB do not transmit to the real economy as efficiently as in normal times in the euro area, and do not explain a large part of the variance of inflation and output. A counterfactual analysis shows in which extent changes in Fed's and ECB's behavior during and after the Great Recession have affected macroeconomic performances both in the US and in the euro area. Despite evidence of a significant change in the non-systematic component of monetary policy after the 2008 crisis, the shift in contemporaneous response coefficients of the time-varying policy rule appears to be a key determinant of the level of inflation and output at the ZLB, mainly in the euro area that would have suffered a large period of deflation from 2014:1 to 2018:1 without any change in ECB's behavior after the 2008 crisis.

The rest of the paper is organized as follows. Section 2 is dedicated to the literature review. Section 3 describes the methodology used for the modelling framework. Section 4 presents the data. Section 5 is devoted to the estimation results. Section 6 contains the counterfactual analysis based on the results. Finally, Section 7 is for the conclusion.

## 2 Related literature

The question of the conduct of monetary policy has been widely discussed in the literature. Since John B. Taylor's (1993) benchmark work, lots of papers have evaluated the conduct of monetary policy and have proposed improvements in the analysis of Taylor-type rules (see Clarida et al., 1999 and Woodford, 2001, 2003, among others). At the same time, a growing literature has emerged and found support to the use of Taylor rules as a practical tool to capture shifts in central banks' behavior across different monetary policy regimes.

Monetary policy rules have been used to identify changes in Fed's behavior across different monetary policy regimes in the US, by disentangling pre-Volcker (before Paul Volcker's appointment as Fed Chairman in 1979) and post-Volcker (including Paul Volcker's tenure) periods. Clarida et al. (2000) advocate that a shift in the systematic component of monetary policy has been the main source of macroeconomic stability during the post-Volcker period. Lubik and Schorfheide (2004) conduct a test for indeterminacy in the pre-Volcker and Volcker-Greenspan periods and confirm this result. Favero and Rovelli (2003), Ozlale (2003), Dennis (2006), and Surico (2007a) provide additional support for these findings, with a specific attention on interest rate smoothing in the reaction function.[5] Similarly, Stock and Watson (2002), Galí et al. (2003) and Ahmed et al. (2004) support the view that better Fed's performances has considerably reduced macroeconomic volatility during the Great Moderation. Using Bayesian methods to estimate a basic New Keynesian model, Ilbas (2012) also finds a break in the conduct of US monetary policy during the post-Volcker period. Interestingly, Coibion (2012) attributes a leading role to monetary policy shocks measured from estimated Taylor rules in significantly contributing to real economic fluctuations during the 1970s and early 1980s. Nikolsko-Rzhevskyy et al. (2014)

[5]Higher persistence of lagged interest rate in the conduct of monetary policy can be justified by misspecifications of the macroeconomic dynamics, as highlighted by Rudebusch (2001), Castelnuovo and Surico (2004), Castelnuovo (2006) and Givens (2012).

identify monetary policy regimes according to rules-based or discretionary eras. They provide further evidence of improving economic performance when central banks adhere to a monetary policy rule.

Since all of the papers cited above focus on Fed's behavior, other studies focus on the ECB (Taylor, 1999, Gerlach and Schnabel, 2000).[6] Relying on estimates of reaction functions, Gerdesmeier and Roffia (2004), Garcia-Iglesias (2007) and Surico (2007b) find a stronger interest rate response to inflation than to output fluctuations. However, other studies find a relatively high contemporaneous coefficient on output stabilization in a Taylor rule applied to the eurozone (see Fourçans and Vranceanu, 2007, Sauer and Sturm, 2007 for estimations on ex-post data, and Castelnuovo, 2007 and Gorter et al., 2008 for forward-looking estimations of monetary policy rules). Other papers do the same exercise including the ZLB and the financial crisis, as Gorter et al. (2010), Gerlach (2011), and more recently Gerlach and Lewis (2014a,b). Hutchinson and Smets (2017) advocate that the ECB has launched unconventional measures to respond to its communicated reaction function and fulfill its mandate, that is a key point in the present analysis.

Also, a strand of the literature proposes a comparative analysis of the conduct of monetary policy between the US and the euro area. Empirical estimates include Ullrich (2005) and Belke and Polleit (2007). In the latter, the authors find that the standard Taylor rule is a better tool for modelling Fed's monetary policy than ECB's. They also find a lower emphasis on inflation relative to the output gap in the euro area. However, higher interest rate smoothing in the US displays more cautiousness in Fed's behavior. Belke and Klose (2013) propose the same exercise during the Great Recession. Based on dynamic stochastic general equilibrium (DSGE) models, Christiano et al. (2008) and Sahuc and Smets (2008) show that differences in shocks largely explain the gap between Fed's and ECB's interest rate setting.

In line with early empirical advances in monetary policy rule estimations, the use of vector autoregressive (VAR) models has a long-lasting tradition of monetary analysis (Sims, 1980, 1992, Bernanke and Blinder, 1992, Christiano et al., 1996, among many others). This approach has been widely used to measure the effects of monetary policy shocks, relying on some critical identifying assumptions of monetary policy innovations in structural frameworks. As highlighted by Christiano et al. (1999) and Ramey (2016), lots of identification strategies have been developed since decades, and now allow a better understanding of the impact of monetary policy shocks as the exogenous part of central banks behavior.[7] However, and as stressed above, the conduct of monetary policy has been shown to be regime-dependent, and both response coefficients of the reaction function and monetary policy shocks are likely to change over time. Therefore, a large set of VAR specification has been developed to capture the non-linear dynamics of the whole central banks' behavior over a given sample period, including vector autoregressions with time-varying parameters and stochastic volatility (TVP-VAR).

TVP-VAR models allow for smooth and gradual changes in the parameters of the estimated monetary policy rule. In a seminal paper, Primiceri (2005) (see Del Negro and Primiceri, 2015 for a *corrigendum*) wonders whether monetary policy in the US has been less active against inflationary pressure during the Martin-Burns

[6] More recently, Hartmann and Smets (2018) look at the evolution of ECB's behavior during its first twenty years.

[7] Further analyses on the non-systematic component have been proposed to better understand changes in the conduct of monetary policy. Following on from Boivin and Giannoni (2006), Justiniano and Primiceri (2008), Benati and Surico (2009), and using both a structural VAR and a Bayesian estimation of DSGE models, recent papers investigate the impact of time-varying volatility of monetary policy shocks on the economy (Fernández-Villaverde et al., 2011 and Mumtaz and Zanetti, 2013).

period than during the Volcker-Greenspan era. He finds that the non-systematic part of US monetary policy was higher in the 1960s and 1970s, although monetary policy was more systematic under Greenspan in the US. Other influential studies such as Cogley and Sargent (2005), Boivin (2006), Kim and Nelson (2006), Benati and Mumtaz (2007) use a VAR with drifting coefficients and stochastic volatilities to analyze Fed's behavior during the post-World War II period in the US. All these papers agree on the improvement in the systematic component of monetary policy after Volcker's appointment. As a whole, time-varying parameters VAR methodology has been widely employed in monetary policy analyses. Benati and Surico (2008), Canova and Gambetti (2009), Cogley et al. (2010), Baxa et al. (2014) and Creel and Hubert (2015) use TVP-VARs to examine the evolution of inflation persistence and predictability. Mumtaz and Surico (2009) and Baumeister and Benati (2013) include the yield curve in their model. Koop et al. (2009), Canova and Pérez Forero (2015), Amir-Ahmadi et al. (2016) investigate possible structural breaks in the economy, but also attribute large macroeconomic implications to time-varying monetary policy shocks.

As an extension, the present paper replicates the same results as Belongia and Ireland (2016) on the common sample period of estimation: the Fed decreased the weight it placed on stabilizing inflation from 2000 to 2007, and deviated persistently from the estimated policy rule that had important implications for output and inflation. However, one of the main contributions of the present paper is to bring new evidence on the evolution of monetary policy in the US and in the euro area in the wake of the Global Financial Crisis.

# 3 Methodology

**The model.** The methodology used in this paper is similar to Belongia and Ireland (2016). Their empirical procedure is reproduced in this section and detailed in Appendix A. Indeed, a vector autoregressive model with time-varying parameters and stochastic volatility (TVP-VAR) is used to study the evolution of monetary policy on the period of estimation.[8] The main difference comes from the extension of the sample period of estimation, that henceforth covers unconventional times. Also, as an extension, the vector autoregression with time-varying coefficients and stochastic volatility is applied to euro area data. The model is based on Primiceri (2005) and Cogley and Sargent (2005), and its baseline version can be written as follows:

$$\mathbf{y}_t = \begin{bmatrix} \Pi_t & G_t & R_t^s \end{bmatrix}' \tag{1}$$

where $\Pi_t$ is the inflation rate, $G_t$ is the output gap and $R_t^s$ is the shadow rate at period $t$.[9] The three

[8] Stability of the simple VAR model is checked in Appendix C. Aastveit et al. (2017) examine the stability of VARs in the period since the Great Recession and provide evidence against stability of parameters.

[9] I am aware of Bognanni's (2018) criticism of vector autoregressive time series models with time-varying parameters and stochastic volatility developed by Primiceri (2005) and Cogley and Sargent (2005). According to him, this framework suffers from a fundamental ordering problem that makes it ill-suited for the structural analysis conducted in this paper. As shown later in this section, the methodology employed in the present paper is however slightly different from Primiceri (2005) and Cogley and Sargent (2005). Following Benati (2011) and Belongia and Ireland (2016), the choice of the calibration of prior distribution of coefficients and the identification strategy of structural disturbances are different from that of the baseline methodology. I am also conscious of the fact that the analysis does not include some financial measures that were likely to have played an important role in the transmission of monetary policy during and in the aftermath of the Great Recession, such as credit spreads (Caldara and Herbst,

endogenous variables are collected in the $3 \times 1$ vector $\mathbf{y}_t$. The model is assumed to follow a second-order time-varying parameters vector autoregressive model with time-varying coefficients in the reduced form:

$$\mathbf{y}_t = \mathbf{b}_t + \mathbf{B}_{1,t}\mathbf{y}_{t-1} + \mathbf{B}_{2,t}\mathbf{y}_{t-2} + \mathbf{u}_t \tag{2}$$

where $\mathbf{b}_t$ is a $3 \times 1$ vector of time-varying intercepts, $\mathbf{B}_{i,t}$ for $i = 1, 2$ are $3 \times 3$ matrices of time-varying autoregressive coefficients, and $\mathbf{u}_t$ is a $3 \times 1$ vector of heteroskedastic shocks with time-varying covariance matrix $\mathbf{\Omega}_t$, such that $\mathbb{E}\{\mathbf{u}_t\mathbf{u}_t'\} = \mathbf{\Omega}_t$.

Both intercepts and autoregressive coefficients in the $21 \times 1$ vectorized form are obtained from equation (2):

$$\mathbf{B}_t = \text{vec}\left(\begin{bmatrix} \mathbf{b}_t' \\ \mathbf{B}_{1,t}' \\ \mathbf{B}_{2,t}' \end{bmatrix}\right)$$

and decompose the covariance matrix $\mathbf{\Omega}_t$ by applying a Cholesky factorization as

$\mathbf{\Omega}_t = \mathbf{A}_t^{-1}\mathbf{\Sigma}_t\mathbf{\Sigma}_t'(\mathbf{A}_t')^{-1}$

where the $3 \times 3$ matrix $\mathbf{A}_t$ is lower triangular with ones along its diagonal:

$$\mathbf{A}_t = \begin{bmatrix} 1 & 0 & 0 \\ \alpha_{g\pi,t} & 1 & 0 \\ \alpha_{r\pi,t} & \alpha_{rg,t} & 1 \end{bmatrix}$$

and the $3 \times 3$ matrix $\mathbf{\Sigma}_t$ is diagonal:

$$\mathbf{\Sigma}_t = \begin{bmatrix} \sigma_{\pi,t} & 0 & 0 \\ 0 & \sigma_{g,t} & 0 \\ 0 & 0 & \sigma_{r,t} \end{bmatrix}$$

Hence, the reduced form of equation (2) can be rewritten in a matrix form as:

$$\mathbf{y}_t = \mathbf{X}_t'\mathbf{B}_t + \mathbf{A}_t^{-1}\mathbf{\Sigma}_t\varepsilon_t$$

where $\mathbf{X}_t = \mathbf{I}_3 \otimes \begin{bmatrix} 1 & \Pi_{t-1} & G_{t-1} & R_{t-1}^s & \Pi_{t-2} & G_{t-2} & R_{t-2}^s \end{bmatrix}$, and $\mathbb{E}\{\varepsilon_t\varepsilon_t'\} = \mathbf{I}_3$, where $\mathbf{I}_3$ is a $3 \times 3$ identity matrix.

Let $\alpha_t = \begin{bmatrix} \alpha_{g\pi,t} & \alpha_{r\pi,t} & \alpha_{rg,t} \end{bmatrix}'$ be $3 \times 1$ vector containing the elements of $\mathbf{A}_t$ different from zero or one, and

2019). However, despite the possible misleading approach to characterize central banks' behavior during the post-crisis period, and as raised above, the estimated monetary policy rule of the original Taylor type only include inflation and output objectives. Under these circumstances, I assume that the Fed and the ECB have launched unconventional measures purely in order to trigger inflation and to boost economic growth, according to their respective mandate. Putnam and Azzarello (2012), Gavin et al. (2015) and Debortoli et al. (2019) investigate the conduct and the effectiveness of US monetary policy through the lens of a dual mandate monetary policy rule. Moreover, along with its objective of price stability, "the ECB typically should avoid generating excessive fluctuations in output and employment if this is in line with the pursuit of its primary objective" (see ECB's objective of monetary policy).

$\sigma_t = \begin{bmatrix} \sigma_{\pi,t} & \sigma_{g,t} & \sigma_{r,t} \end{bmatrix}'$ be $3 \times 1$ vector collecting diagonal elements of $\mathbf{\Sigma}_t$. The dynamics of the time-varying parameters are governed by the following process:

$\mathbf{B}_t = \mathbf{B}_{t-1} + \nu_t$

$\alpha_t = \alpha_{t-1} + \zeta_t$

and

$log\ \sigma_t = log\ \sigma_{t-1} + \eta_t,$

where all the uncorrelated innovations are assumed to be jointly normally distributed, with the following assumptions on the variance covariance matrix:

$$\mathbf{V} = \mathbb{V}\mathrm{ar}\left(\begin{bmatrix} \varepsilon_t \\ \nu_t \\ \zeta_t \\ \eta_t \end{bmatrix}\right) = \begin{bmatrix} \mathbf{I}_3 & \mathbf{0} & \mathbf{0} & \mathbf{0} \\ \mathbf{0} & \mathbf{Q} & \mathbf{0} & \mathbf{0} \\ \mathbf{0} & \mathbf{0} & \mathbf{S} & \mathbf{0} \\ \mathbf{0} & \mathbf{0} & \mathbf{0} & \mathbf{W} \end{bmatrix}$$

where $\mathbf{0}$ denotes matrices of zeros, $\mathbf{Q}$ is $21 \times 21$, $\mathbf{S}$ is $3 \times 3$ and block-diagonal, and $\mathbf{W}$ is $3 \times 3$ and diagonal with elements $w_{i,i}$ for $i = 1, 2, 3$.

As a whole, $\mathbf{Q}$ has 231 distinct elements, $\mathbf{S}$ has four distinct non-zero elements, and $\mathbf{W}$ has three distinct non-zero elements.

**Estimation strategy.** Bayesian methods are often used to estimate large numbers of parameters in classical VAR models because of their strong explanatory and predictive powers. In this paper, I follow the same approach than in Primiceri (2005) and Cogley and Sargent (2005) to be able to deal with autoregressive models with time-varying coefficients. The aim of the estimation strategy is to assess the posterior distribution of the parameters, based on prior distributions calibrated with simple estimates on a training sample period consisting of the first ten years of data (equivalent to the first forty quarters) to a time-invariant coefficients version of the reduced form model presented above. The, posterior distributions of parameters can be simulated by Markov Chain Monte Carlo (MCMC) algorithm, as detailed in Primiceri (2005), Cogley and Sargent (2005) and in Appendix A. Following the same approach, prior distributions of parameters are obtained by running a constant-parameter version of the model in the form:

$$\mathbf{y}_t = \mathbf{X}_t'\mathbf{B} + \mathbf{A}^{-1}\mathbf{\Sigma}\varepsilon_t$$

Applying ordinary least squares (OLS) to each equation in this system, an estimate $\hat{\mathbf{B}}$ of the parameter vector $\mathbf{B}$ is obtained, and the same Cholesky decomposition as shown previously to the covariance matrix of least-squares residuals is used to obtain estimates $\hat{\alpha}$ and $\hat{\sigma}$ of the parameter vectors $\alpha$ and $\sigma$.

Then, normal priors for the initial values of the coefficients are given by:

$\mathbf{B}_0 \sim \mathcal{N}(\hat{\mathbf{B}}, 4\hat{V}_{\mathbf{B}})$

$\alpha_0 \sim \mathcal{N}(\hat{\alpha}, 4\hat{V}_{\alpha})$

and

$log\ \sigma_0 \sim \mathcal{N}(log\ \hat{\sigma}, I)$

based on those used by Primiceri (2005).

For the block elements of the variance-covariance matrix of innovations $\mathbf{V}$, inverse Wishart priors are defined as follows:

$\mathbf{Q} \sim \mathcal{IW}(22k_{\mathbf{Q}}^2 \hat{V}_{\mathbf{B}}, 22)$

$\mathbf{S}_1 \sim \mathcal{IW}(2k_{\mathbf{S}}^2 \hat{V}_{\alpha,1}, 2)$

$\mathbf{S}_2 \sim \mathcal{IW}(3k_{\mathbf{S}}^2 \hat{V}_{\alpha,2}, 3)$

and

$w_{i,i} \sim \mathcal{IW}(2k_w^2, 2)$

for $i = 1, 2, 3$, where $\hat{V}_{\alpha,1}$ and $\hat{V}_{\alpha,2}$ are diagonal blocks of $\hat{V}_\alpha$. Also, the settings are given taken from Belongia and Ireland (2016), where $k_{\mathbf{Q}}^2 = 0.00035$, $k_{\mathbf{S}}^2 = 0.01$ and $k_{\mathbf{W}}^2 = 0.0001$. Then, a Metropolis-within-Gibbs sampling algorithm is used on the remaining sample period starting from the priors given previously to compute blocks of parameters from their conditional posterior distribution. Again, the subsequent steps to obtain estimations for each parameter are well-described in Belongia and Ireland (2016) and in Appendix A. Draws for the parameters in $\mathbf{Q}$, $\mathbf{S}$ and $\mathbf{W}$ are taken from their inverse Wishart conditional posterior distribution.

This procedure is repeated 10,000 times in a burn-in period. The model is estimated with 5,000 draws of each parameter for the Gibbs sampling. To assess the convergence of the Markov Chain, draws' inefficiency factors are computed across the four blocks of parameters in the sequences $\mathbf{B}^T$, $\mathbf{A}^T$, $\mathbf{\Sigma}^T$, and in the elements from $\mathbf{V}$. For each individual parameter $\theta$, the ineffciency stastistic is defined as the inverse of the measure of relative numerical efficiency (Geweke, 1992):

$$IF(\theta) = 2\pi \frac{1}{\int_{-\pi}^{\pi} S_\theta(\omega) d\omega} S_\theta(0)$$

where $S_\theta(\omega)$ is the spectral density of $\theta$ at frequency $\omega$. According to Primiceri (2005) and Benati (2011), inefficiency factors are said acceptable at or below 20. The statistics for hyperparameters in $\mathbf{V}$ are slightly higher than that upper bound, but those for the parameters and shock covariances and volatilities are largely below it. Table D.1 and table D.2 containing the results are given in Appendix D.

**Structural shocks identification.** An approach based on sign restrictions on impulse responses is applied to identify structural disturbances. The technique is based on Rubio-Ramirez et al. (2010), Arias et al. (2018) and Arias et al. (2019), and has been applied to VAR models with time-varying coefficients in Benati (2011). Sign restrictions on the impact of structural disturbances are directly given in Table 1. Sign restrictions are imposed on the impulse response of variables to each structural shock: an aggregate supply shock, an aggregate demand shock, and a monetary policy shock. Aggregate supply shock is assumed to be contractionary: inflation increases but output decreases, and thus left the response of monetary policy unconstrained. Aggregate demand shock is expansionary, and is associated to an increase in output, inflation and interest rate. Finally, monetary policy (or interest rate) shock is assumed to be contractionary: it decreases inflation and output.

Table 1: Sign restrictions on the impact effects of structural shocks

| Impact effect on | Structural shocks | | |
|---|---|---|---|
| | Aggregate supply | Aggregate demand | Monetary policy |
| Inflation | + | + | - |
| Output gap | - | + | - |
| Shadow rate | ? | + | + |

*Note:* The symbol ? indicates that the response is left unconstrained.

As a result, the reduced form covariance matrix is factored as :

$\mathbf{\Omega}_t = \mathbf{C}_t^{-1}\mathbf{D}_t\mathbf{D}_t'(\mathbf{C}_t')^{-1}$

where the $3 \times 3$ matrix is no more lower triangular, but still with ones along its diagonal

$$\mathbf{C}_t = \begin{bmatrix} 1 & -c_{\pi g,t} & -c_{\pi r,t} \\ -c_{g\pi,t} & 1 & -c_{gr,t} \\ -c_{r\pi,t} & -c_{rg,t} & 1 \end{bmatrix}$$

and the $3 \times 3$ matrix is still diagonal

$$\mathbf{D}_t = \begin{bmatrix} \delta_{\pi,t} & 0 & 0 \\ 0 & \delta_{g,t} & 0 \\ 0 & 0 & \delta_{r,t} \end{bmatrix}$$

the three structural shocks now have an effect on inflation, output gap and the shadow rate.
Consequently, the structural model can be written is as:

$$\mathbf{C}_t\mathbf{y}_t = \boldsymbol{\gamma}_t + \mathbf{\Gamma}_{1,t}\mathbf{y}_{t-1} + \mathbf{\Gamma}_{2,t}\mathbf{y}_{t-2} + \mathbf{D}_t\xi_t$$

where $\boldsymbol{\gamma}_t = \mathbf{C}_t\mathbf{b}_t$, $\mathbf{\Gamma}_{i,t} = \mathbf{C}_t\mathbf{B}_{i,t}$, for $i = 1, 2$, and $\xi_t = \begin{bmatrix} \xi_t^{as} & \xi_t^{ad} & \xi_t^{mp} \end{bmatrix}'$ is a $3 \times 1$ vector of structural disturbances to aggregate supply, aggregate demand and monetary policy, with $\mathbb{E}\{\xi_t\xi_t'\} = \mathbf{I}_3$, and $\mathbf{I}_3$ is a $3 \times 3$ identity matrix.

**Time-varying monetary policy rule.** With estimation strategy and sign restrictions based on Belongia and Ireland (2016), the third row of the above-mentioned structural model is presented as a Taylor-type monetary policy rule:

$$\begin{aligned} R_t^s = {} & \gamma_{r,t} + c_{r\pi,t}\Pi_t + \gamma_{1,r\pi,t}\Pi_{t-1} + \gamma_{2,r\pi,t}\Pi_{t-2} \\ & + c_{rg,t}G_t + \gamma_{1,rg,t}G_{t-1} + \gamma_{2,rg,t}G_{t-2} + \gamma_{1,rr,t}R_{t-1}^s + \gamma_{2,rg,t}R_{t-2}^s + \delta_{r,t}\xi_t^{mp} \end{aligned} \tag{3}$$

This Taylor-type rule prescribes a setting for the policy rate regarding to changes in current and lagged inflation and output gap variables. It also includes lagged values of interest rate terms to capture central banks' tendency

to smooth short-term interest rates movements over time. The time-varying estimation of the intercept $\gamma_{r,t}$ and of the coefficients from matrices $\mathbf{\Gamma}_{1,t}$ and $\mathbf{\Gamma}_{2,t}$ allows to assess changes to monetary policy that might have occured on the sample period. $\xi_t^{mp}$ represents identified monetary policy shocks that capture deviations in the actual policy rate from the value dictated by the estimated monetary policy rule. Importantly, equation (3) allows for time-variation in all of the response coefficients but also in the standard deviation $\delta_{r,t}$ of the monetary policy shocks. Hence, this estimation permits disentangling changes in central bank's responses to inflation versus output gap stabilization and the extent to which the central bank departs from its rule-based behavior. As a whole, the estimated monetary policy rule given in equation (3) may be decomposed into central banks' response to macroeconomic conditions and smoothing behavior – i.e. the *systematic* component of monetary policy – and monetary policy shocks – i.e. the *non-systematic* component of monetary policy. The model is estimated with data described in the following section.

# 4 Data

**Monetary policy rules in normal times.** Using the TVP-VAR model, the present paper tracks the evolution of US and euro area monetary policies based on results derived from historical data. US data are extracted from the Federal Reserve Economic Data (FRED) database, and run from 1960:1 to 2018:4. The nominal interest rate is the federal funds rate. Core PCE price index is taken as a relevant measure of inflation in the estimation[10], and is given as a percentage annual change. The output gap is computed following the Congressional Budget Office (CBO).[11] Prior distribution of the coefficients is obtained from the training sample period from 1960:1 to 1969:4. Then, the Taylor rule is estimated by the TVP-VAR model with stochastic volatility from 1970:1 to 2018:4.

Concerning euro area data, interest rate, inflation and output gap series are from two major sources. The first one is the Area-Wide Model database (AWM, Fagan et al., 2005) that contains historical data from 1970:1 to 2017:4. Then, the data are updated to 2018:4 with Eurostat. The main policy rate is the Euribor 3-month. Inflation is the Harmonized Index of Consumer Prices (HICP), and the real potential GDP is estimated with the HP filter (Hodrick and Prescott, 1997) to compute the output gap following the basic formula mentioned above.[12] The period 1971:1 to 1980:4 is used as the training sample. The model is estimated from 1981:1 to 2018:4.

[10] John B. Taylor claims that the Fed has not followed the prescription of the Taylor rule by keeping the interest rate too low from 2003 to 2005 and hence generated the housing bubble in the US. Ben S. Bernanke disagreed with that by justifying that the Fed set the interest rate according to the Taylor rule by targeting core PCE inflation, and not GDP deflator as in Taylor's estimations. For more details, see Bernanke's Brookings post of April 28, 2015 titled "The Taylor Rule: A benchmark for monetary policy?". See also Janet L. Yellen's speech of March 27, 2015 on "Normalizing Monetary Policy: Prospects and Perspectives", or Tchatoka et al. (2017) for additional evidence for Taylor-type policy rule estimations including core PCE inflation.

[11] The output gap is constructed following the basic formula $y_t^{gap} = \frac{Y_t - Y_t^*}{Y_t^*}$ that can be approximated by $y_t^{gap} = log(Y_t) - log(Y_t^*)$, where $Y_t$ is the real output and $Y_t^*$ is the real potential output at time $t$. In accordance with the original Taylor rule (Taylor, 1993), including the output gap rather than real GDP growth in the estimates may help the TVP-VAR control for the effects of technology shocks affecting both real and potential GDP, as discussed in Giordani (2004).

[12] Following Hamilton's (2018) recent criticism of the use of Hodrick-Prescott filter, real potential GDP in the euro area is estimated with alternative filters to check the robustness of the results in Appendix F.

Figure 2: Inflation, output gap and policy rate

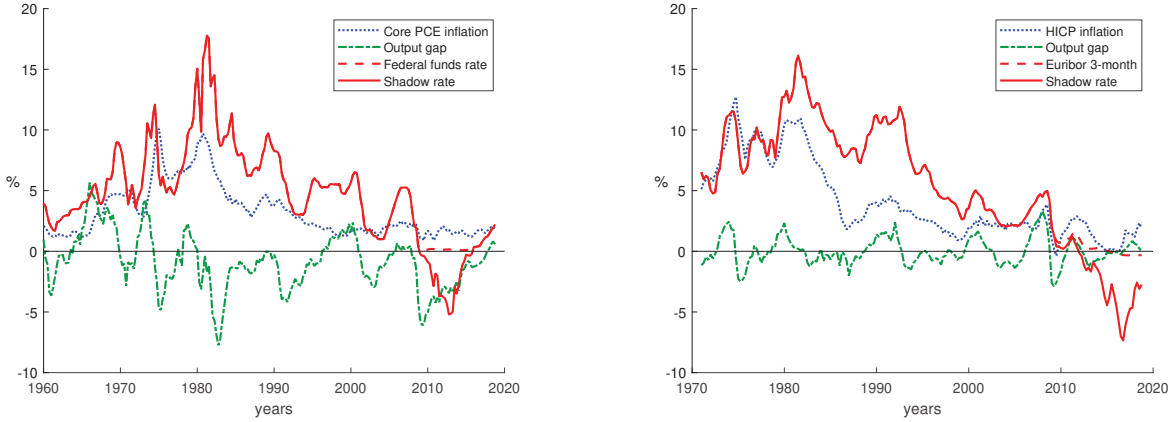


(a) US

(b) Euro area

Figure 2 shows the evolution of inflation, output gap and policy rates since 1960:1 in the US and 1971:1 in the euro area. Both interest rate and inflation have been lastingly decreasing over the sample period in the US and in the euro area. From a two-digit rate level around the 1970s, US core PCE inflation rate has substantially decreased to stabilize before the 2000s. The federal funds rate has been evolving along a similar path over the sample period, before hitting the ZLB at the end of 2008. The interpretation of the data is quite the same for the euro area, where both the HICP and Euribor 3-month have been trending down since the 1980s. However, Figure 2 also shows that, unlike the US, the euro area has struggled to recover from the 2008 crisis, suffering another recession induced by the sovereign debt crisis in 2011 and successive deflationary periods in 2015 and 2016.

**Unconventional monetary policies and shadow rates.** Since the data cover the period up to 2018:4, the estimation results capture both conventional and unconventional aspects of monetary policy. Therefore, a major concern is the constrained policy rate at the zero level during periods of unconventional measures. Because of flat interest rates at the ZLB, and along with the launch of non-standard measures, traditional data on policy rate do not entirely reflect central banks' actions during unconventional times and may lead to biased monetary policy rule estimation. Unconventional measures have been characterized by the use of 'non-standard' instruments – i.e. other than the policy rate – consisting mainly in LSAP or FG, to fulfill the main objectives stated in central banks' mandate. Consequently, and to be able to estimate the Taylor-type rule up to 2018:4, the policy rate instrument is proxied by the shadow short rate from Krippner (2013, 2019)[13], constructed as an extrapolation of the yield curve in the negative territory, and hence taking into account unconventional measures that are likely to have affected interest rates at different maturities.

Table 2 gives the outlines of US and euro area monetary policies since the 2008 crisis. It shows periods when the Fed and the ECB have launched their main non-standard measures, and periods during which they decided to reduce the magnitude of these measures. The Fed has reacted quickly to the financial crisis by implementing its first assets purchases programme (QE1, for 'Quantitative easing 1') of $600 billion. In the euro area, the ECB

[13]Shadow short rates data are available on Leo Krippner's webpage.

Table 2: Outlines of monetary policy since the Great Recession

| | United States | Euro area |
|---|---|---|
| First LSAP after the financial crisis | Nov. 2008 | July 2009 |
| Tapering | Dec. 2013 | Dec. 2016 |
| Period of ZLB | Dec. 2008 - Dec. 2015 | July 2012 - — |

*Source:* The symbol — means that the euro area is still stuck at the ZLB in 2018:4. *Source:* Federal Reserve, European Central Bank, Chen et al. (2017).

has enhanced credit support in October 2008 and lengthened the maturity of its LTROs in June 2009. However, the ECB has only implemented its first assets purchases programme in July 2009 (CBPP1, for 'Covered-bond purchase programme 1'). As of 2012, the ECB has gradually lowered interest rates to their lowest level, while the Fed was about to start tapering at this time. Indeed, the Fed announced slowing down assets purchases in December 2013, before raising its policy rate in December 2015. On the other hand, the ECB announced tapering in end-2016. In late 2018, monetary policy in the euro area was still at the ZLB.

Figure 3: Policy and shadow rates

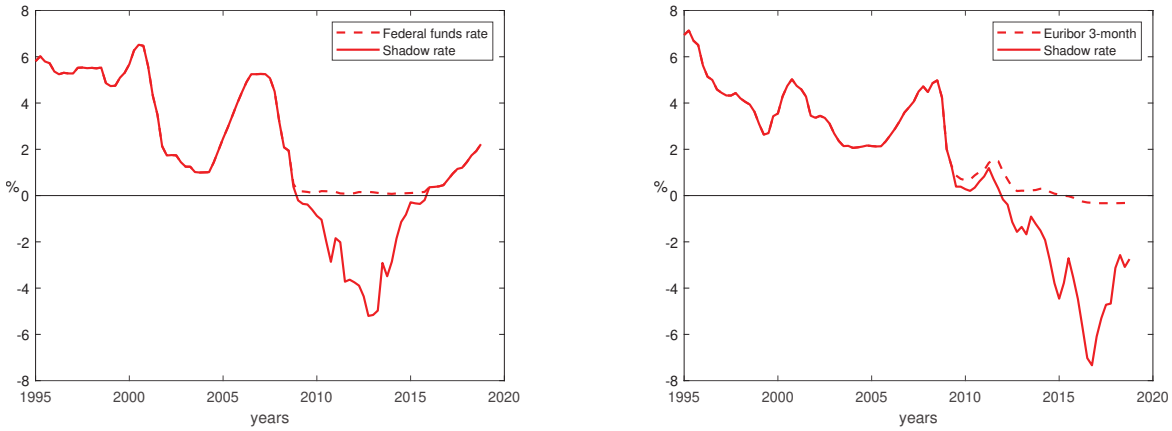


(a) US (b) Euro area

The shadow short rate (SSR) from Krippner (2013, 2019) is used as a proxy for unconventional measures of monetary policy in the TVP-VAR specification (Figure 2 and Figure 3).[14] Nominal interest rates used as policy rates in the model are replaced by shadow rates at the ZLB to get a consistent measure of the stance of monetary policy over the full sample period. In the US, the federal funds rate is replaced by the shadow rate from November 2008 to November 2015. In the euro area, the Euribor 3-month is replaced by the shadow rate

[14]Several papers highlight the plausibility to use the shadow rate in a VAR model as a measure of the stance of monetary policy under the ZLB. For instance, Wu and Xia (2016), Lombardi and Zhu (2018), Krippner (2019) and Francis et al. (2020) show how estimated monetary policy shocks provide a realistic picture of the post-crisis macroeconomic situation. Basu and Bundick (2017) and Caggiano et al. (2017) investigate the macroeconomic effect of uncertainty at the ZLB. Forbes et al. (2018), Rogers et al. (2018) and Pasricha et al. (2018) find empirical evidence of monetary policy effects at the international level. Georgiadis (2016), Horvath and Voslarova (2016), Potjagailo (2017) focus on global spillovers of unconventional monetary policies in the US and in the euro area. Plante et al. (2017), Caraiani and Călin (2018) and Crespo Cuaresma et al. (2019) incorporate shadow rates in a TVP-VAR model. Similarly, shadow rates can also be used in estimated DSGE models, as in Mouabbi and Sahuc (2019).

in July 2009. These dates closely correspond to information reported in Table 2. To fit the frequency of the rest of the data, quarterly rates are constructed as a three-month average.

As discussed in Christensen and Rudebusch (2015), Halberstadt and Krippner (2016), Bauer and Rudebusch (2016) and Krippner (2019), shadow rate estimations are very sensitive to several factors, such as the calibration of the lower bound or the range of rates included in the dataset. The robustness of estimates using Wu and Xia's (2016) shadow rate is checked in Appendix F.

# 5 Results

**Response coefficients of the time-varying reaction function.** The baseline model is estimated with the data mentioned previously. Figure 4 compares the evolution of contemporaneous responses of the policy rate to macroeconomic fluctuations in the United States and the euro area. Figure 4a shows the evolution of contemporaneous coefficients on inflation from 1995:1 to 2018:4. The estimated coefficient in the US has peaked during the ZLB period. The median coefficient on inflation rose from 0.81 in 2009:1 to 1.33 in 2013:1, before falling to 0.40 in 2017:1. In the euro area, the contemporaneous coefficient on inflation has been stable since 1995:1 and has slightly increased once the euro area was stuck at the ZLB. Indeed, the short-run response coefficient on inflation increased from 0.58 in 2009:1 to 0.72 in 2013:1 before reaching 0.92 in 2017:1. However, 68% credible intervals show no significant changes in the short-run coefficient on inflation within and between the US and the euro area.

Figure 4b tracks changes in the contemporaneous response to output gap over time. The interpretation of the path of the median coefficient is the same as that of the evolution of response coefficients on inflation: a peak in the middle of the ZLB era in the US (0.50 in 2009:1, 0.78 in 2013:1 and 0.30 in 2017:1) and a continuous and sharp increase in the euro area at the ZLB (0.51 in 2009:1, 0.88 in 2013:1, and 1.50 in 2017:1). Depicted 68% credible intervals show however significant difference between contemporaneous coefficients on output gap in the US and in the euro area at the end of the sample period. Nevertheless, there is no evidence of significant shifts in the contemporaneous response coefficient on output gap within the US and the euro area.

On the basis of these results, coefficients on inflation and output gap appear to be correlated both in the US and in the euro area. But the path of short-run coefficients in the US tends to be more volatile than in the euro area: the Fed seems to react more aggressively to inflation and output gap fluctuations than the ECB, or at least behaves with more discretion.[15] Also, lagged unconventional monetary policy implementation in the euro area compared to the US may have led to a gap between the timing of ECB's and Fed's response coefficients. Contemporaneous coefficients from the ECB monetary policy rule reached an all-time high at the end of the period of estimation, whereas they came back to a pre-crisis level in the US. This result may be interpreted as the difference in the timing of policy normalization in the US and in the euro area: the Fed began normalizing the stance of monetary policy at a time when the ECB had not yet reached the ZLB.

[15] This may be interpreted as the 'constrained discretion' raised by Bernanke (2003): the Fed has adopted a flexible behavior such as the inflation targeting objective may be de-emphasized in an output stabilization purpose under some circumstances. As Bernanke mentioned in his speech, "under constrained discretion, the central bank is free to do its best to stabilize output and employment in the face of short-run disturbances, with the appropriate caution born of our imperfect knowledge of the economy and of the effects of policy".

Figure 4: Contemporaneous coefficients from the estimated monetary policy rule

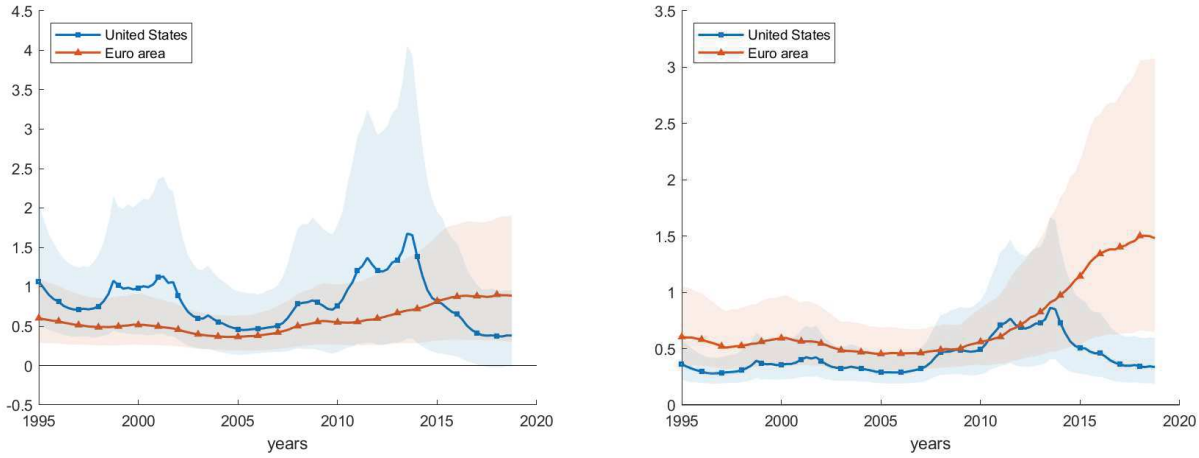


(a) Contemporaneous coefficient on inflation

(b) Contemporaneous coefficient on output gap

*Note:* Contemporaneous coefficients on inflation and output gap are respectively given by $c_{r\pi,t}$ and $c_{rg,t}$ in equation (3). Median (solid lines) and 68% credible interval (shaded areas) of the posterior distribution of coefficients are plotted for each indicated variable.

Figure 5 plots the time-varying standard deviations of structural monetary policy disturbances in the US and in the euro area. Monetary policy shock volatility follows a path similar to short-run coefficients. In the US, it has peaked during the ZLB. In the euro area, it has increased continuously since ECB's early reaction to the 2008 crisis. But interestingly, 68% Bayesian credible sets associated to $\delta_{r,t}$ coefficients highlight strong significant changes in the volatility of monetary policy shocks over the sample period.

Figure 5: Monetary policy shock volatility from the estimated monetary policy rule

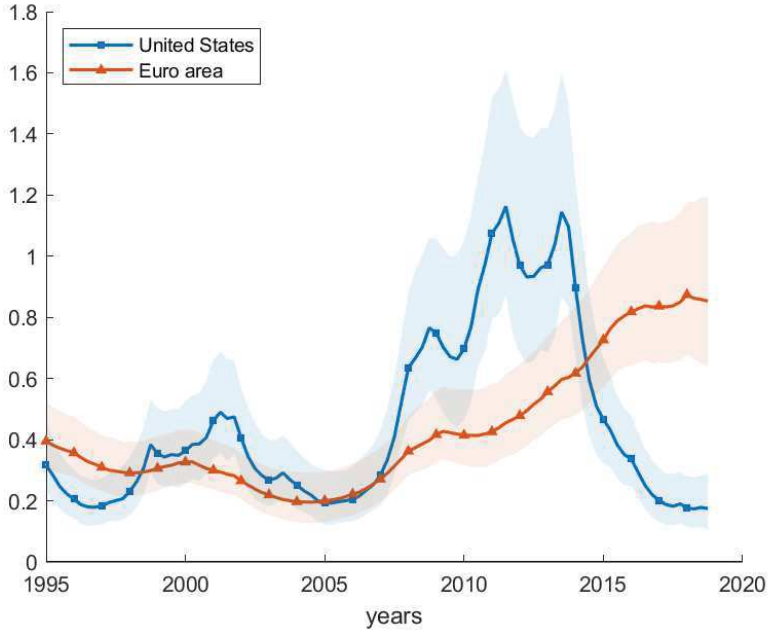


*Note:* The volatility of monetary policy shocks is captured by $\delta_{r,t}$ in equation (3). Median (solid lines) and 68% credible interval (shaded areas) of the posterior distribution of coefficients are plotted for the indicated variable.

The evolution of monetary policy shocks volatility shows that unconventional monetary policy decisions at the ZLB have been characterized by large departures of the Fed and the ECB from the policy rate prescribed by the Taylor rule. QE has largely contributed to lower expected future short-term rates through the signaling channel, that can be interpreted as an additional monetary policy discretion, whereas FG is commonly defined as the commitment to deviate from the monetary policy rule in the future, resulting in more policy discretion.[16] Based on these results and on the whole influential related literature, Fed's and ECB's unconventional monetary policy tools such as QE and FG may have undoubtedly led to statistically different and persistent deviations from the baseline Taylor-type policy rule at the ZLB in the US and in the euro area. By definition, these departures from rule-like behavior are interpreted as more policy discretion at the ZLB.[17]

**Non-systematic monetary policy.** Figure 6 shows the evolution of realized monetary policy shocks since 1995. It reveals that the Fed and the ECB have departed a lot from the behavior prescribed by their estimated policy rule at the ZLB, and that these monetary policy shocks have been considerably negative when the 2008 crisis occurred. A negative monetary policy shock means that the central bank sets interest rate at a level below the rate prescribed by the estimated monetary policy rule. In that case, monetary policy is perceived as expansionary. However, it can be graphically deduced that US and euro area monetary policies have been mostly expansionary after the 2008 crisis, describing potentially important deviations from estimated policy rules that also occurred with the launch of unconventional measures at the ZLB.

Figure 6: Realized monetary policy shocks

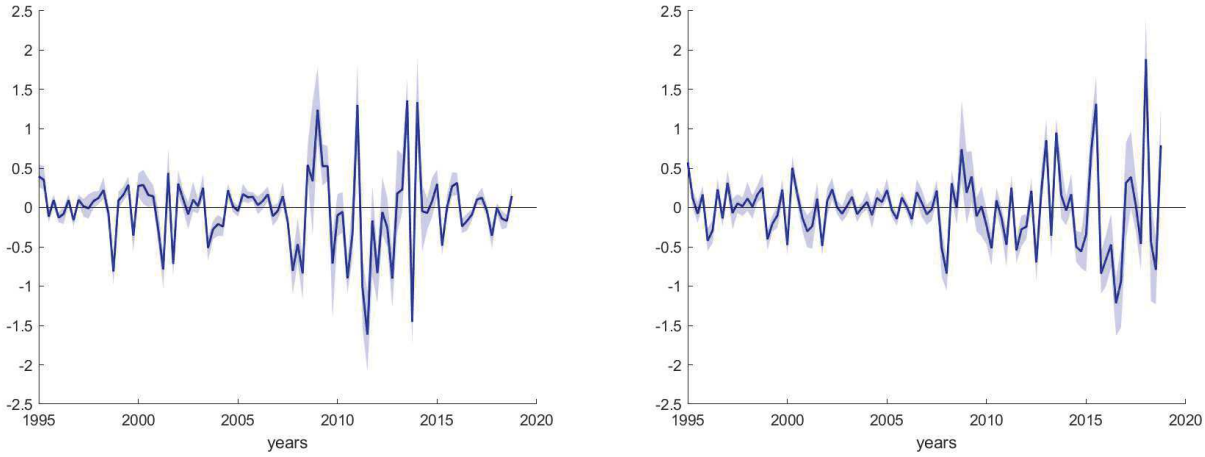


(a) US

(b) Euro area

*Note:* Median (solid lines) and 68% credible interval (shaded areas) of the posterior distribution of the realized monetary policy shock are plotted. A negative monetary policy shock is equivalent to an interest rate setting below the rate prescribed by the estimated monetary policy rule (i.e. expansionary monetary policy).

Then, the purpose is to investigate changes in the macroeconomic impact of monetary policy shocks. Figure 7 and Figure 8 plot impulse responses of inflation and output gap to monetary policy shocks over a 40 quarter

[16] See Vissing Jorgensen and Krishnamurthy (2011) and Bauer and Rudebusch (2014) for evidence of the signaling role of QE, and Campbell et al. (2012) and Woodford et al. (2012) for the effects of FG.

[17] Further measures of inflation and real economic activity are employed in the model to check the robustness of the results. Dynamic response coefficients of these alternative specifications are shown in Appendix F.

horizon at different dates between 2007:4 and 2015:1. The responses are computed based on draws from the posterior distributions of the parameters estimated for each indicated period. They show how the economy responded to a monetary policy shock at a given point in time. Overall, the signs of the impulse response functions of the TVP-VAR variables to a monetary policy shock do not change at the ZLB. In the US, inflation has significantly reacted to monetary policy shocks as long as the Fed was easing monetary policy at the ZLB. The response of output gap to policy shocks is however not as strong and significant as the median response of inflation. Meanwhile in the euro area, the response of both inflation and output gap to monetary policy shocks have been strong and significant at the ZLB. Furthermore, compared to the US, impulse responses are less persistent in the euro area. Also, and importantly, the evolution of impulse responses in the US shows that the impact of monetary policy shocks on inflation and output gap has been getting larger up to 2011:1. Since then, those responses have simultaneously and continuously decreased with the magnitude of US monetary policy shocks. In the euro area, impulse responses of inflation and output gap to monetary policy shocks have only increased up to 2009:1, whereas the magnitude of policy shocks has been growing throughout the entire post-crisis period.

Figure 7: Impulse responses to monetary policy shocks in the US

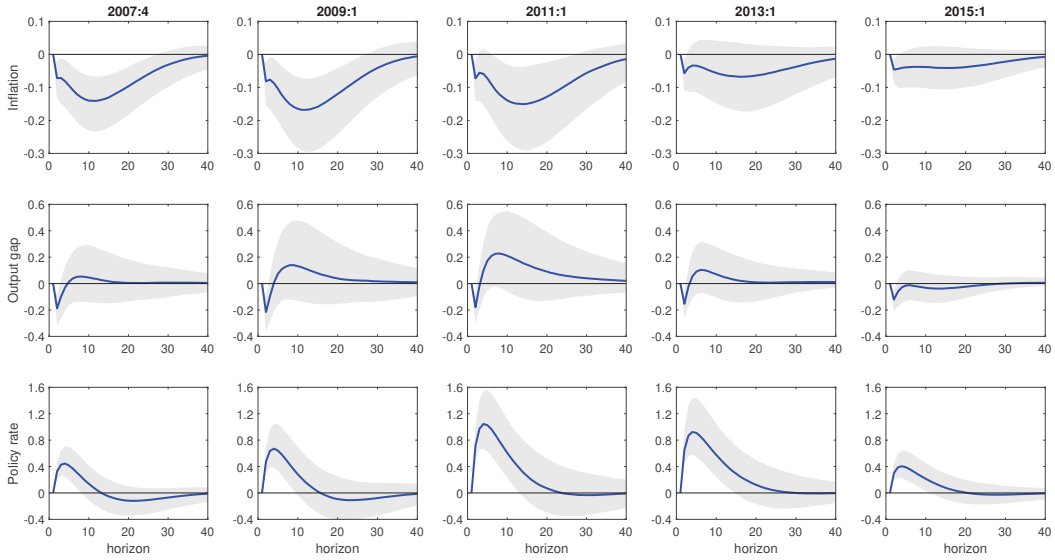


*Note:* Impulse response of the indicated variable to a contractionary monetary policy shock at the indicated date. Blue lines represent the median and grey shaded areas represent 68% credible intervals of the posterior distribution of each impulse response.

Table 3 reports the percentage share of forecast error variances in inflation and output gap attributable to monetary policy shocks for horizons up to 40 quarters. Variance decompositions are based on draws of the model's parameters from their posterior distributions for 2007:4, 2011:1 and 2015:1. As with impulse response functions, the dates are chosen such that the analysis covers both pre-crisis and ZLB periods. The model estimated using US data attributes large fractions of inflation and output gap volatility to monetary policy shocks. This fraction is sizeable in 2011:1, and then decreases in 2015:1. Hence, monetary policy shocks contribute to the variance of inflation and output more importantly during the ZLB period, and particularly in the easing phase of US monetary policy when short-term interest rates were constrained by the lower bound. In

Figure 8: Impulse responses to monetary policy shocks in the euro area

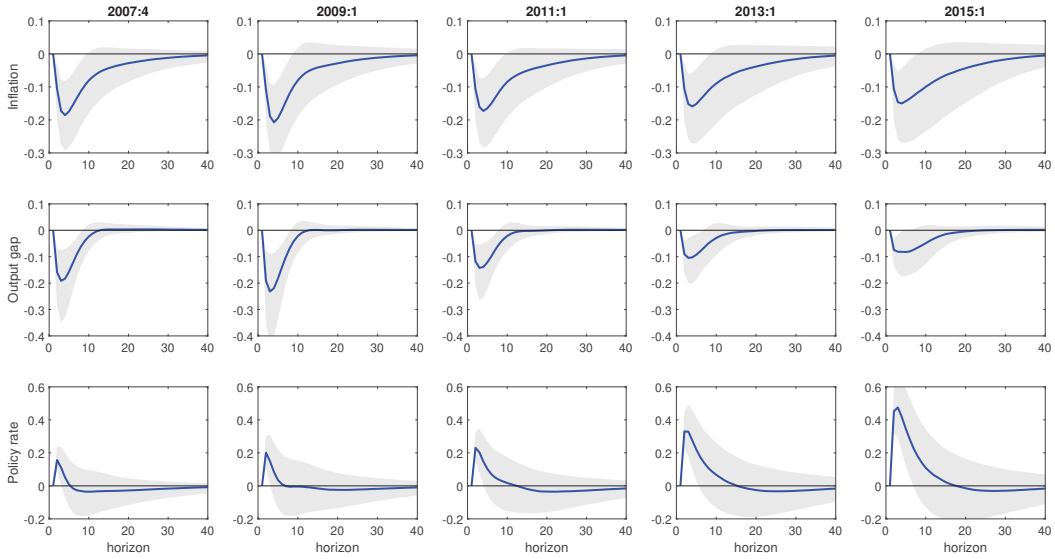


*Note:* Impulse response of the indicated variable to a contractionary monetary policy shock at the indicated date. Blue lines represent the median and grey shaded areas represent 68% credible intervals of the posterior distribution of each impulse response.

the euro area, monetary policy shocks explain a smaller part of macroeconomic volatility than in the US. Also, and as shown with impulse responses, the effects of monetary policy shocks are less persistent in the euro area. Paying attention to shorter horizons, the contribution of monetary policy shocks to the variance of inflation and output in the euro area is nearly stable when the economy moves from normal times to the ZLB. But 16th and 84th percentiles based on draws from the posterior distributions for each date bring little evidence of significant changes in forecast error variances due to monetary policy shocks. Only median coefficients are reported here.

As a whole, the results presented above show that the Fed and the ECB shifted their behavior during the post-2008 decade, when their respective policy rate hit the effective lower bound and when a novel set of unconventional measure was launched. Response coefficients of the time-varying reaction function have increased with expansionary monetary policy at the ZLB. In the US, they peaked when the Fed started tapering in end-2013 and went back to pre-crisis levels around the time of the federal funds rate lift-off. In the euro area, they went up around 2009 and are still large due to ongoing massive expansionary ECB's monetary policy. These dynamics are interpreted as the reflection of the implementation of respective unconventional measures at the ZLB.

Although they do not indicate clear evidence of significant changes in emphasis between the two objectives in the standard Taylor rule, estimated response coefficients suggest dramatic shifts in monetary policy shocks during and after the Great Recession. Larger and more volatile realized policy shocks both in the US and in the euro area imply statistical difference from pre-recession periods, and support striking evidence of a change in monetary policy after the 2008 crisis. Impulse response functions and variance decompositions highlight the increasing macroeconomic impact of unconventional monetary policy shocks in the easing phase of US monetary policy at the ZLB. However, rising euro area monetary policy shocks at the ZLB do not transmit to the real economy as efficiently as in normal times, and do not explain a larger part of the variance of inflation and

Table 3: Variance decompositions

| Horizon | % of forecast error variance due to monetary policy shocks | | | | | |
|---|---|---|---|---|---|---|
| | US | | | Euro area | | |
| | 2007:4 | 2011:1 | 2015:1 | 2007:4 | 2011:1 | 2015:1 |
| *Inflation* | | | | | | |
| 4 | 8.71 | 6.81 | 5.86 | 15.36 | 14.85 | 12.83 |
| 8 | 15.09 | 13.06 | 6.82 | 14.92 | 14.59 | 13.76 |
| 12 | 20.93 | 20.53 | 8.30 | 14.28 | 14.18 | 15.13 |
| 16 | 25.12 | 26.12 | 10.00 | 13.98 | 14.25 | 15.95 |
| 20 | 27.54 | 30.30 | 11.47 | 13.78 | 14.47 | 16.43 |
| 40 | 29.34 | 35.73 | 14.67 | 13.37 | 14.41 | 17.18 |
| *Output gap* | | | | | | |
| 4 | 5.94 | 8.81 | 6.29 | 9.66 | 10.13 | 9.96 |
| 8 | 7.61 | 13.18 | 7.42 | 10.42 | 11.80 | 16.85 |
| 12 | 8.82 | 16.29 | 9.81 | 10.76 | 12.33 | 19.67 |
| 16 | 9.91 | 18.29 | 11.72 | 10.79 | 12.48 | 20.16 |
| 20 | 10.69 | 19.89 | 12.68 | 10.79 | 12.56 | 20.28 |
| 40 | 13.07 | 22.97 | 14.01 | 10.93 | 12.70 | 20.32 |

*Note:* Horizon is the number of quarters ahead. Variance decompositions are based on draws of the median coefficients from their posterior distributions for 2007:4, 2011:1 and 2015:1.

output when short-term movements are constrained by the effective lower bound.

# 6 Counterfactual analysis

The estimated VAR model with time-varying coefficients is used to propose different counterfactual scenarios. The aim is to investigate how changes in the conduct of monetary policy may have affected macroeconomic performances. This experiment gives the path that would have followed inflation, output gap and the policy rate in the US and in the euro area under some circumstances. Counterfactuals for the US are presented in Figure 9 and in Figure 10 for the euro area.

The first scenario consists in drawing the coefficients of the policy rule from the posterior distribution from 2007:4. Focusing on inflation rate, there is no significant difference in the path according to the different scenarios in the US. Core PCE inflation would have been slightly lower than that has been observed after the crisis if the Fed would have kept monetary policy rule unchanged since 2007:4. Although they are not statistically significant, the results are more striking in the euro area. Changes in ECB's monetary policy had a huge impact on HICP, especially during the Great Recession: unconventional monetary policy has strongly reduced the deflationary risk in the euro area. Concerning the output gap, aggressive monetary policies implemented at the ZLB by the Fed and the ECB have led to positive output gap at the end of the period of estimation, whereas the euro area would have suffered negative output gap if the ECB would have kept the 2007:4 monetary policy

rule unchanged.

In the second scenario, the Taylor rule parameters are also drawn from their 2007:4 posterior distribution, and monetary policy shocks are assumed to be muted from 2007:4 forward. In that case, counterfactuals also induced a shift in the non-systematic component of monetary policy. The interpretation of the results is similar to that has been observed in the first scenario. However, changes in ECB's systematic and non-systematic components of monetary policy led to a significant gap between actual and counterfactual inflation path: without any change in ECB's behavior at the ZLB, the euro area would have suffered a prolonged period of deflation from 2014:1 to 2018:1. In the US, this gap widened from 2007:4 onward, more than that observed in the first scenario. But the results still do not suggest significant evidence of the efficiency of Fed's policy shifts on economic performances in the US.

The third counterfactual scenario reports results when monetary policy shocks are turned off from 2007:4 onward. There is no noticeable difference between the actual and counterfactual paths. However, and importantly, it appears that monetary policy shocks matter as much as changes in the systematic component of monetary policy in the US. But the latter is substantial in the euro area compared to the role of monetary policy shocks in explaining macroeconomic performances.

Figure 9: Counterfactual simulations (US)

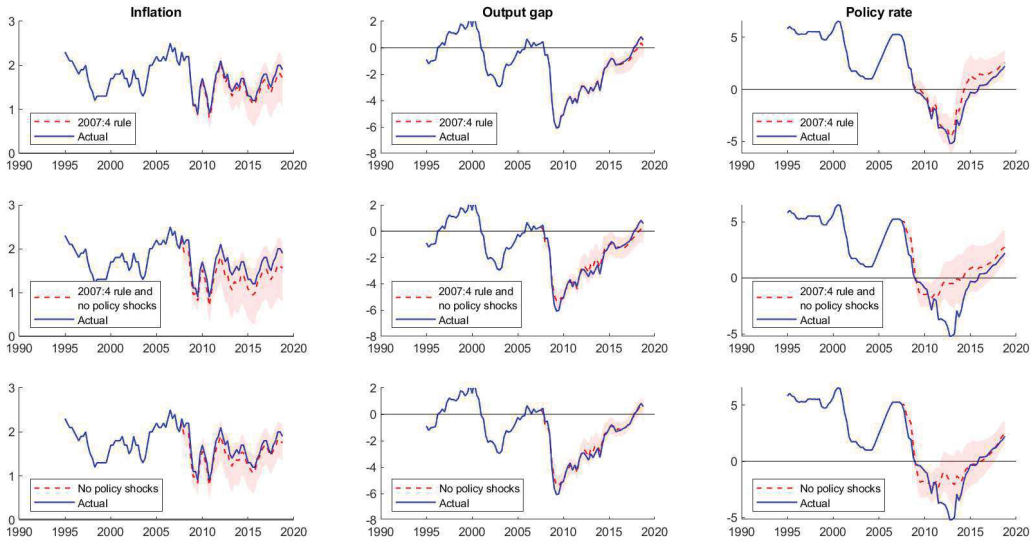


*Note:* Median counterfactual path (red dashed lines) and 68% credible interval (red shaded areas) are plotted for each indicated variable.

Other counterfactuals are shown on Figure E.4 and Figure E.5 (see Appendix E), and gives further insights on the macroeconomic implications of changes in the non-systematic component of monetary policy. The focus is now on the volatility of monetary policy shocks. Three different counterfactual scenarios are proposed. The first scenario has been previously described and consists in drawing the coefficients of the policy rule from the posterior distribution from 2007:4. In the second, however, all the coefficients are drawn from the 2007:4 posterior distribution, including the volatility of monetary policy shocks. The third scenario gives counterfactuals only in the case where the volatility coefficient is drawn from its 2007:4 posterior distribution, allowing the rest of policy rule parameters to be time-varying from 2007:4 forward. The results do not suggest

Figure 10: Counterfactual simulations (Euro area)

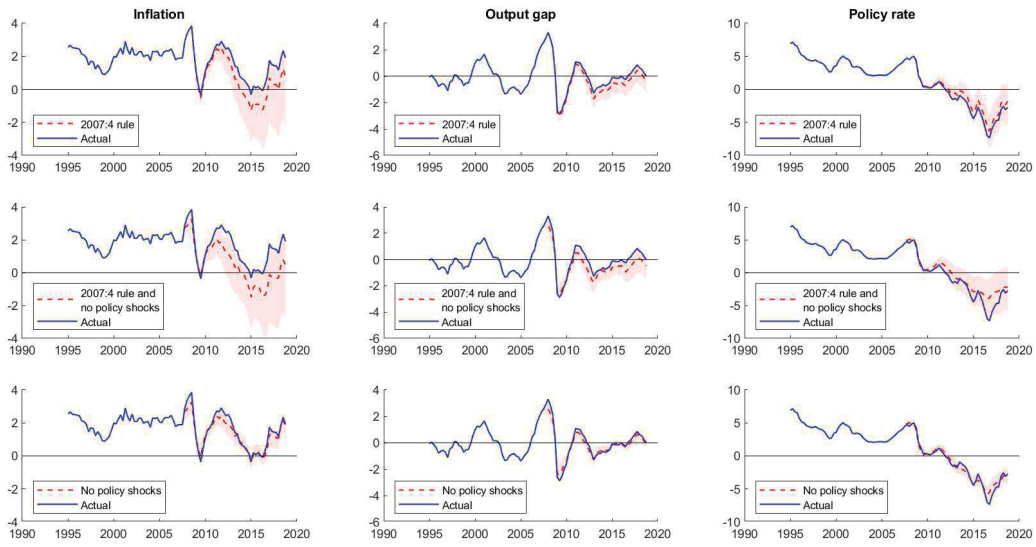


*Note:* Median counterfactual path (red dashed lines) and 68% credible interval (red shaded areas) are plotted for each indicated variable.

any role for monetary policy shocks volatility in macroeconomic performances in the US and in the euro area.

# 7 Conclusion

The question of changes in central banks behavior can be explored by assuming that central banks follow a standard Taylor-type rule to guide monetary policy decisions. According to this framework, the central bank focuses attention on the evolution of macroeconomic fundamentals, such as inflation and output, to determine its target value for the interest rate. The time-varying parameters vector autoregressive model used in this paper gives some empirical assessments of time-variations in the simple Taylor rule in the US and in the euro area during the post-2008 decade. It allows a better understanding of monetary policy implementations by assessing changes in Fed's and ECB's behavior over the post-crisis period. Using a shadow rate to capture the stance of monetary policy at the ZLB, the empirical analysis shows that both the Fed and the ECB changed their behavior in the aftermath of the Great Recession. Furthermore, the results indicate that the Fed has behaved differently than the ECB since the Great Recession. Although the Fed announced starting tapering in end-2013, the ECB had not even reached the ZLB at this time. This shift in the timing of monetary policy normalization between the US and the euro area led to a different path in the contemporaneous coefficients of the monetary policy rules: since the level of Fed's response coefficients went back to their pre-crisis level, the ECB is still in high-coefficients phase due to a massive expansionary monetary policy. These results do not indicate clear evidence of significant changes in Fed's and ECB's responses to inflation and output, but they suggest strong and significant shifts in monetary policy shocks after the Global Financial Crisis. The path of realized policy shocks volatility both in the US and in the euro area is statistically different from the pre-recession period, and support striking evidence of a change in monetary policy after the 2008 crisis. These large and significant departures from rule-based behavior are perceived as additional monetary policy discretion

and evolve in line with the implementation of unconventional measures. Monetary policy shocks are shown to strongly affect the US macroeconomy and to contribute to the variance of inflation and output even more importantly when the Fed launched unconventional measures at the ZLB. This is however not the case in the euro area, despite increasing monetary policy shocks at the ZLB, that do not explain a large part of the variance of inflation and output. A counterfactual analysis shows how macroeconomic performances have benefited from changes in Fed's and ECB's behavior during and after the Great Recession in the US, and especially in the euro area.

Estimation results concerning changes in Fed's and ECB's behavior since the Great Recession raise some potential policy implications. Among them, it challenges the idea of a monetary policy coordination (Cœuré, 2014). A cooperation between Fed and ECB monetary policies should rely on strong assumptions, such as similar objectives, common aspects in the transmission mechanisms or synchronized business cycles. All these points could explain estimation results presented in this paper, and could also be considered as a possible explanation for the gap in the timing of monetary policy decisions between the Fed and the ECB. From this point of view, a two-country structural model allowing for international spillovers would be welcomed to investigate the relationship between Fed's and ECB's behavior and macroeconomic fluctuations at the ZLB, and to suggest a theoretical framework consistent with the empirical findings. Such implications for the conduct of monetary policy are left for future research.

# Appendix

# A TVP-VAR methodology

## A.1 The model

The model is from Primiceri (2005), with the MCMC algorithm corrected as described by Del Negro and Primiceri (2015). This section is a step-by-step guide to use the TVP-VAR methodology, as described in details by Belongia and Ireland (2016). The present section is mostly based on Primiceri's (2005) and Belongia and Ireland's (2016) corresponding appendices.

The baseline model is applied to quarterly data on the inflation rate (measured using the core PCE inflation rate in the US, and the HICP in the euro area), $\Pi_t$, output gap (estimated using CBO formula in the US, and HP filter in the euro area), $G_t$, and the short-term shadow rate (federal funds rate in the US, 3-month Euribor in the euro area in normal times, shadow short rates at the ZLB), $R_t^s$. US data run from 1960:1 to 2018:4, and euro area data run from 1971:1 to 2018:4.

These observable endogenous series are combined into the $3 \times 1$ vector

$$\mathbf{y}_t = \begin{bmatrix} \Pi_t & G_t & R_t^s \end{bmatrix}', \tag{A.1}$$

which is assumed to follow a second-order vector autoregression with time-varying coefficients and a time-varying covariance matrix for the innovations. Thus, the model's reduced form is

$$\mathbf{y}_t = \mathbf{b}_t + \mathbf{B}_{1,t}\mathbf{y}_{t-1} + \mathbf{B}_{2,t}\mathbf{y}_{t-2} + \mathbf{u}_t \tag{A.2}$$

where

$$\mathbf{b}_t = \begin{bmatrix} b_{\pi,t} & b_{g,t} & b_{r,t} \end{bmatrix}'$$

is a $3 \times 1$ vector of time-varying constant terms,

$$\mathbf{B}_{i,t} = \begin{bmatrix} b_{i,\pi\pi,t} & b_{i,\pi g,t} & b_{i,\pi r,t} \\ b_{i,g\pi,t} & b_{i,gg,t} & b_{i,gr,t} \\ b_{i,r\pi,t} & b_{i,rg,t} & b_{i,rr,t} \end{bmatrix},$$

with $i = 1, 2$, are $3 \times 3$ matrices of time-varying coefficients, and

$$\mathbf{u}_t = \begin{bmatrix} u_{\pi,t} & u_{g,t} & u_{r,t} \end{bmatrix}'$$

is a $3 \times 1$ vector of heteroskedastic shocks with covariance matrix $\mathbf{\Omega}_t$, such that $\mathbb{E}\{\mathbf{u}_t\mathbf{u}_t'\} = \mathbf{\Omega}_t$.

Without loss of generality, $\mathbf{\Omega}_t$ can be decomposed as

$$\mathbf{\Omega}_t = \mathbf{A}_t^{-1}\mathbf{\Sigma}_t\mathbf{\Sigma}_t'(\mathbf{A}_t')^{-1} \tag{A.3}$$

where $\mathbf{A}_t$ is the lower triangular matrix

$$\mathbf{A}_t = \begin{bmatrix} 1 & 0 & 0 \\ \alpha_{g\pi,t} & 1 & 0 \\ \alpha_{r\pi,t} & \alpha_{rg,t} & 1 \end{bmatrix} \tag{A.4}$$

and $\mathbf{\Sigma}_t$ is the diagonal matrix

$$\mathbf{\Sigma}_t = \begin{bmatrix} \sigma_{\pi,t} & 0 & 0 \\ 0 & \sigma_{g,t} & 0 \\ 0 & 0 & \sigma_{r,t} \end{bmatrix}. \tag{A.5}$$

The reduced form (A.2) can therefore be represented equivalently as

$$\mathbf{y}_t = \mathbf{b}_t + \mathbf{B}_{1,t}\mathbf{y}_{t-1} + \mathbf{B}_{2,t}\mathbf{y}_{t-2} + \mathbf{A}_t^{-1}\mathbf{\Sigma}_t\varepsilon_t, \tag{A.6}$$

where $E\{\varepsilon_t\varepsilon_t'\} = \mathbf{I}_3$. Stacking all the coefficients into the $21 \times 1$ vector

$$\mathbf{B}_t = \text{vec}\left(\begin{bmatrix} \mathbf{b}_t' \\ \mathbf{B}_{1,t}' \\ \mathbf{B}_{2,t}' \end{bmatrix}\right),$$

(A.6) can be rewritten as

$$\mathbf{y}_t = \mathbf{X}_t'\mathbf{B}_t + \mathbf{A}_t^{-1}\mathbf{\Sigma}_t\varepsilon_t, \tag{A.7}$$

where

$$\mathbf{X}_t = \mathbf{I}_3 \otimes \begin{bmatrix} 1 & \Pi_{t-1} & G_{t-1} & R^s_{t-1} & \Pi_{t-2} & G_{t-2} & R^s_{t-2} \end{bmatrix}$$

Let

$$\alpha_t = \begin{bmatrix} \alpha_{g\pi,t} & \alpha_{r\pi,t} & \alpha_{rg,t} \end{bmatrix}'$$

be the vector of non-zero and non-one elements of $\mathbf{A}_t$ and

$$\sigma_t = \begin{bmatrix} \sigma_{\pi,t} & \sigma_{g,t} & \sigma_{r,t} \end{bmatrix}'$$

be the vector of diagonal elements of $\mathbf{\Sigma}_t$. The dynamics of the time-varying parameters are specified as

$$\mathbf{B}_t = \mathbf{B}_{t-1} + \nu_t, \tag{A.8}$$

$$\alpha_t = \alpha_{t-1} + \zeta_t, \tag{A.9}$$

and

$$\log\sigma_t = \log\sigma_{t-1} + \eta_t. \tag{A.10}$$

In (A.7)-(A.10), all of the innovations are assumed to be jointly normally distributed with

$$\mathbf{V} = \mathbb{V}\text{ar}\left(\begin{bmatrix} \varepsilon_t \\ \nu_t \\ \zeta_t \\ \eta_t \end{bmatrix}\right) = \mathbb{E}\left(\begin{bmatrix} \varepsilon_t \\ \nu_t \\ \zeta_t \\ \eta_t \end{bmatrix}\begin{bmatrix} \varepsilon_t & \nu_t & \zeta_t & \eta_t \end{bmatrix}\right) = \begin{bmatrix} \mathbf{I}_3 & \mathbf{0}_{3,21} & \mathbf{0}_{3,3} & \mathbf{0}_{3,3} \\ \mathbf{0}_{21,3} & \mathbf{Q} & \mathbf{0}_{21,3} & \mathbf{0}_{21,3} \\ \mathbf{0}_{3,3} & \mathbf{0}_{3,21} & \mathbf{S} & \mathbf{0}_{3,3} \\ \mathbf{0}_{3,3} & \mathbf{0}_{3,21} & \mathbf{0}_{3,3} & \mathbf{W} \end{bmatrix}, \tag{A.11}$$

where $\mathbf{Q}$ is $21 \times 21$, $\mathbf{S}$ is $3 \times 3$, and $\mathbf{W}$ is $3 \times 3$ and diagonal, so that the standard deviations in $\sigma_t$ evolve as independent geometric random walks. Following Primiceri (2005), it will be assumed that $\mathbf{S}$ is block-diagonal, with one non-zero element in the first column of the first row and three distinct non-zero elements in the second and third columns of the second and third rows. Hence, $\mathbf{Q}$ has 231 distinct elements, $\mathbf{S}$ has 4 distinct elements and is block-diagonal in the following form:

$$\mathbf{S} = \begin{bmatrix} s_{1,1} & 0 & 0 \\ 0 & s_{2,2} & s_{2,3} \\ 0 & s_{3,2} & s_{3,3} \end{bmatrix}$$

where $s_{i,j}$ are non-zero elements on line-i and row-j of matrix $\mathbf{S}$. Hence, the two diagonal blocks are given by the following matrices:

$$\mathbf{S}_1 = s_{1,1} \text{ and } \mathbf{S}_2 = \begin{bmatrix} s_{2,2} & s_{2,3} \\ s_{3,2} & s_{3,3} \end{bmatrix}, \text{ where } s_{2,3} = s_{3,2}$$

Moreover, $\mathbf{W}$ is diagonal with elements $w_{i,i}$ for $i = 1, 2, 3$, and has three distinct elements.

In all that follows, let

$$\omega^{\tau} = \begin{bmatrix} \omega_1' & \dots & \omega_{\tau}' \end{bmatrix}'$$

denote the history of a generic vector of variables $\omega_t$ up to a generic time $\tau$. And for a generic matrix of variables and constant terms $\mathbf{M}_t$, let

$$\mathbf{M}^{\tau} = \begin{bmatrix} m_1' & \dots & m_{\tau}' \end{bmatrix}'$$

where $m_t$ is a column vector constructed from the time varying elements of $\mathbf{M}_t$.

## A.2 Prior Distributions

Following Cogley and Sargent (2005) and Primiceri (2005), classical estimates of the parameters obtained by applying a training sample consisting of the first ten years of data to a constant-parameter version of the model are used to calibrate the prior means and standard deviations for the time-varying parameters when estimated with the rest of the sample. The constant-parameter version of the reduced form (A.2) is written as

$$\mathbf{y}_t = \mathbf{b} + \mathbf{B}_1 \mathbf{y}_{t-1} + \mathbf{B}_2 \mathbf{y}_{t-2} + \mathbf{u}_t,$$

Hamilton (1994) and Lütkepohl (2005) show that estimates of the constant and slope coefficients in $\mathbf{b}$, $\mathbf{B}_1$, and $\mathbf{B}_2$ can be obtained by applying OLS separately to each equation. Stacking these estimated coefficients into the $21 \times 1$ vector

$$\hat{\mathbf{B}} = \text{vec}\left( \begin{bmatrix} \hat{\mathbf{b}}' \\ \hat{\mathbf{B}}_1' \\ \hat{\mathbf{B}}_2' \end{bmatrix} \right),$$

and defining

$$\mathbf{x}_t = \begin{bmatrix} 1 & \Pi_{t-1} & G_{t-1} & R_{t-1}^s & \Pi_{t-2} & G_{t-2} & R_{t-2}^s \end{bmatrix},$$

standard errors can be computed using the formulas from Hamilton's (1994) proposition on maximum likelihood estimation of vector autoregressions:

$$\mathbb{V}\mathrm{ar}(\hat{\mathbf{B}}) = \hat{\mathbf{\Omega}} \otimes \left( \sum_{t=1}^{T} \mathbf{x}_t \mathbf{x}_t' \right)^{-1},$$

where

$$\hat{\mathbf{\Omega}} = \frac{1}{T} \sum_{t=1}^{T} \hat{\mathbf{u}}_t \hat{\mathbf{u}}_t'$$

is the estimated covariance matrix for the least squares residuals

$$\hat{\mathbf{u}}_t = \mathbf{y}_t - \hat{\mathbf{b}} - \hat{\mathbf{B}}_1 \mathbf{y}_{t-1} - \hat{\mathbf{B}}_2 \mathbf{y}_{t-2}$$

The initial states for the coefficients, covariances, and log volatilities as well as the hyperparameters in $\mathbf{V}$ are assumed to be all independent of each other. The priors for $\mathbf{B}_0$, $\alpha_0$, and $\log \sigma_0$ are assumed to be normal and the priors for $\mathbf{Q}$, $\mathbf{W}$, and the blocks of $\mathbf{S}$ are assumed to be distributed as independent inverse-Wishart. These assumptions together with (A.6)-(A.8) imply normal priors on the entire sequences $\mathbf{B}^T$, $\alpha^T$, and $\mathbf{\Sigma}^T$.

Estimates $\hat{\mathbf{A}}$ and $\hat{\mathbf{\Sigma}}$ of $\mathbf{A}$ and $\mathbf{\Sigma}$ can then be obtained by decomposing $\hat{\mathbf{\Omega}}$ as in (A.3):

$$\hat{\mathbf{\Omega}} = \hat{\mathbf{A}}^{-1} \hat{\mathbf{\Sigma}} \hat{\mathbf{\Sigma}}' (\hat{\mathbf{A}}')^{-1}.$$

Standard errors for the non-zero, non-one elements $\hat{\alpha}$ and $\hat{\sigma}$ of $\hat{\mathbf{A}}$ and $\hat{\mathbf{\Sigma}}$ can be computed using the formulas in Lütkepohl's (2005) proposition on the properties of the structural VAR maximum likelihood estimators. Start by rewriting

$$\mathrm{vec}(\mathbf{A}) = R_{\mathbf{A}} \alpha + r_{\mathbf{A}}$$

and

$$\mathrm{vec}(\mathbf{\Sigma}) = R_{\mathbf{\Sigma}} \sigma$$

with $R_{\mathbf{A}}$ and $R_{\mathbf{\Sigma}}$ are $9 \times 3$ suitable fixed matrices of zeros and ones, where

$$R_{\mathbf{A}} = \begin{bmatrix} 0 & 1 & 0 & 0 & 0 & 0 & 0 & 0 & 0 \\ 0 & 0 & 1 & 0 & 0 & 0 & 0 & 0 & 0 \\ 0 & 0 & 0 & 0 & 0 & 1 & 0 & 0 & 0 \end{bmatrix}'$$

and

$$R_{\mathbf{\Sigma}} = \begin{bmatrix} 1 & 0 & 0 & 0 & 0 & 0 & 0 & 0 & 0 \\ 0 & 0 & 0 & 0 & 1 & 0 & 0 & 0 & 0 \\ 0 & 0 & 0 & 0 & 0 & 0 & 0 & 0 & 1 \end{bmatrix}'$$

and $r_{\mathbf{A}}$ is a $9 \times 1$ vector of fixed parameters allowing for the normalization of diagonal elements of matrix $A$.

$$r_{\mathbf{A}} = \begin{bmatrix} 1 & 0 & 0 & 0 & 1 & 0 & 0 & 0 & 1 \end{bmatrix}'$$

Next, let $\mathbf{K}_{9,9}$ be the commutation matrix that, for any $3 \times 3$ matrix $\mathbf{D}$, is such that

$$\mathrm{vec}(\mathbf{D}) = \mathbf{K}_{9,9} \mathrm{vec}(\mathbf{D}').$$

Then, in particular, $\mathbf{K}_{9,9}$ is a $9 \times 9$ matrix of zeros and ones such that

$$\mathbf{K}_{9,9} = \begin{bmatrix} 1 & 0 & 0 & 0 & 0 & 0 & 0 & 0 & 0 \\ 0 & 0 & 0 & 1 & 0 & 0 & 0 & 0 & 0 \\ 0 & 0 & 0 & 0 & 0 & 0 & 1 & 0 & 0 \\ 0 & 1 & 0 & 0 & 0 & 0 & 0 & 0 & 0 \\ 0 & 0 & 0 & 0 & 1 & 0 & 0 & 0 & 0 \\ 0 & 0 & 0 & 0 & 0 & 0 & 0 & 1 & 0 \\ 0 & 0 & 1 & 0 & 0 & 0 & 0 & 0 & 0 \\ 0 & 0 & 0 & 0 & 0 & 1 & 0 & 0 & 0 \\ 0 & 0 & 0 & 0 & 0 & 0 & 0 & 0 & 1 \end{bmatrix}$$

Following Lütkepohl's (2005) proposition

$$\sqrt{T}\left(\begin{bmatrix}\hat{\alpha}\\ \hat{\sigma}\end{bmatrix} - \begin{bmatrix}\alpha\\ \sigma\end{bmatrix}\right) \rightarrow \mathcal{N}\left(0, \mathcal{I}_a\left(\begin{bmatrix}\alpha\\ \sigma\end{bmatrix}\right)^{-1}\right)$$

and hence

$$\mathbb{V}\text{ar}\left(\begin{bmatrix}\hat{\alpha}\\ \hat{\sigma}\end{bmatrix}\right) = \frac{1}{T}\left[\mathcal{I}_a\left(\begin{bmatrix}\alpha\\ \sigma\end{bmatrix}\right)\right]^{-1}$$

where $\mathcal{I}_a(.)$ is the is the asymptotic information matrix that has the form

$$\mathcal{I}_a\left(\begin{bmatrix}\alpha\\ \sigma\end{bmatrix}\right) = \begin{bmatrix} R'_{\mathbf{A}} & \mathbf{0}_{3,9} \\ \mathbf{0}_{3,9} & R'_{\mathbf{\Sigma}} \end{bmatrix} \mathcal{I}_a\left(\begin{bmatrix}\text{vec}(\mathbf{A})\\ \text{vec}(\mathbf{\Sigma})\end{bmatrix}\right) \begin{bmatrix} R_{\mathbf{A}} & \mathbf{0}_{9,3} \\ \mathbf{0}_{9,3} & R_{\mathbf{\Sigma}} \end{bmatrix},$$

and

$$\mathcal{I}_a\left(\begin{bmatrix}\text{vec}(\mathbf{A})\\ \text{vec}(\mathbf{\Sigma})\end{bmatrix}\right) = \begin{bmatrix} \mathbf{A}^{-1}\mathbf{\Sigma} \otimes \mathbf{\Sigma}'^{-1} \\ -(\mathbf{I}_3 \otimes \mathbf{\Sigma}'^{-1}) \end{bmatrix} (\mathbf{I}_9 + \mathbf{K}_{9,9}) \begin{bmatrix} [\mathbf{\Sigma}'\mathbf{A}'^{-1}] \otimes \mathbf{\Sigma}^{-1} & -(\mathbf{I}_3 \otimes \mathbf{\Sigma}^{-1}) \end{bmatrix},$$

Priors can now be selected along the same lines proposed by Cogley and Sargent (2005), Primiceri (2005) and Benati (2011). Specifically, for $\mathbf{B}_0$, $\alpha_0$, and $\log \sigma_0$, it is assumed that

$$\mathbf{B}_0 \sim \mathcal{N}(\hat{\mathbf{B}}, k^2_{\mathbf{B}} V_{\mathbf{B}}),$$

$$\alpha_0 \sim \mathcal{N}(\hat{\alpha}, k^2_{\alpha} V_{\alpha}),$$

and

$$\log \sigma_0 \sim \mathcal{N}(\log \hat{\sigma}, k^2_{\sigma} \mathbf{I}_3),$$

where choices for the hyperparameters are tabulated below.

Training Sample Prior Hyperparameters

| | $k^2_{\mathbf{B}}$ | $V_{\mathbf{B}}$ | $k_{\alpha}$ | $V_{\alpha}$ | $k^2_{\sigma}$ |
|---|---|---|---|---|---|
| Cogley and Sargent (2005) | 1 | $\mathbb{V}\text{ar}(\hat{\mathbf{B}})$ | 10000 | $\mathbf{I}_3$ | 10 |
| Primiceri (2005) | 4 | $\mathbb{V}\text{ar}(\hat{\mathbf{B}})$ | 4 | $\mathbb{V}\text{ar}(\hat{\mathbf{A}})$ | 1 |
| Benati (2011) | 4 | $\mathbb{V}\text{ar}(\hat{\mathbf{B}})$ | $\sqrt{10}$ | $\text{diag}(\hat{\alpha})$ | 10 |

Training sample prior hyperparameters used in the TVP-VAR are calibrated according to Primiceri (2005). Note that (A.8)-(A.10) imply that

$$\mathbf{B}_t|\mathbf{B}_{t-1}, \mathbf{Q} \sim \mathcal{N}(\mathbf{B}_{t-1}, \mathbf{Q}),$$

$$\alpha_t|\alpha_{t-1}, \mathbf{S} \sim \mathcal{N}(\alpha_{t-1}, \mathbf{S}),$$

and

$$\log \sigma_t|\sigma_{t-1}, \mathbf{W} \sim \mathcal{N}(\log \sigma_{t-1}, \mathbf{W}).$$

Hence, priors for the entire sequences $\mathbf{B}^T$, $\alpha^T$, and $\mathbf{\Sigma}^T$ are

$$p(\mathbf{B}^T|\mathbf{B}_0, \mathbf{Q}) = \prod_{t=1}^{T} p(\mathbf{B}_t|\mathbf{B}_{t-1}, \mathbf{Q}),$$

$$p(\alpha^T|\alpha_0, \mathbf{S}) = \prod_{t=1}^{T} p(\alpha_t|\alpha_{t-1}, \mathbf{S}),$$

and

$$p(\mathbf{\Sigma}^T|\mathbf{\Sigma}_0, \mathbf{W}) = \prod_{t=1}^{T} p(\log \sigma_t| \log \sigma_{t-1}, \mathbf{W}).$$

For $\mathbf{Q}$ and the two blocks of $\mathbf{S}$, the inverse Wishart priors are calibrated as

$$\mathbf{Q} \sim \mathcal{IW}(d_{\mathbf{Q}} k_{\mathbf{Q}}^2 V_{\mathbf{Q}}, d_{\mathbf{Q}}),$$

$$\mathbf{S}_1 \sim \mathcal{IW}(d_{\mathbf{S}1} k_{\mathbf{S}}^2 V_{\mathbf{S}1}, d_{\mathbf{S}1}),$$

and

$$\mathbf{S}_2 \sim \mathcal{IW}(d_{\mathbf{S}2} k_{\mathbf{S}}^2 V_{\mathbf{S}2}, d_{\mathbf{S}2}).$$

Finally, for each diagonal element $w_{i,i}$, $i = 1, 2, 3$, of $\mathbf{W}$, the inverse Gamma prior used by Cogley and Sargent (2005) and Benati (2011) can also be expressed as an inverse Wishart:

$$w_{i,i} \sim \mathcal{IG}\left(\frac{d_{\mathbf{W}}}{2}, \frac{d_{\mathbf{W}} k_{\mathbf{W}}^2}{2}\right) = \mathcal{IW}(d_{\mathbf{W}} k_{\mathbf{W}}^2, d_{\mathbf{W}}).$$

Choices for the hyperparameters are tabulated below. Cogley and Sargent (2005) do not allow for time-variation in the elements of $\mathbf{A}$.

Time-Varying Parameter Prior Hyperparameters

| | $k_{\mathbf{Q}}^2$ | $V_{\mathbf{Q}}$ | $d_{\mathbf{Q}}$ | $k_{\mathbf{S}}^2$ | $V_{\mathbf{S}1}$ | $d_{\mathbf{S}1}$ | $V_{\mathbf{S}2}$ | $d_{\mathbf{S}2}$ | $k_{\mathbf{W}}^2$ | $d_{\mathbf{W}}$ |
|---|---|---|---|---|---|---|---|---|---|---|
| Cogley and Sargent (2005) | 0.00035 | $\mathbb{V}\text{ar}(\hat{\mathbf{B}})$ | 22 | – | – | – | – | – | 0.0001 | 1 |
| Primiceri (2005) | 0.0001 | $\mathbb{V}\text{ar}(\hat{\mathbf{B}})$ | 40 | 0.01 | $V_{\alpha}^{1,1}$ | 2 | $V_{\alpha}^{2:3,2:3}$ | 3 | 0.0001 | 2 |
| Benati (2011) | 0.00035 | $\mathbb{V}\text{ar}(\hat{\mathbf{B}})$ | 22 | 0.001 | $\hat{\alpha}^1$ | 2 | $\text{diag}(\hat{\alpha}^{2:3})$ | 3 | 0.0001 | 1 |

where $V_{\alpha}^{1,1}$ is the element from the first row and first column of $V_{\alpha}$, $V_{\alpha}^{2:3,2:3}$ is the matrix formed from the last two rows and columns of $V_{\alpha}$, and $\hat{\alpha}^1$ and $\hat{\alpha}^{2:3}$ correspond to the first and the second through third elements of the vector $\hat{\alpha}$. Time-varying parameter model's prior hyperparameters are calibrated according to Cogley and Sargent (2005) and Benati (2011) for matrix $Q$. Cogley and Sargent (2005) suggest to set out the degree of freedom of inverse Wishart as $d_{\mathbf{Q}} = \dim(\mathbf{B}_t) + 1$. Otherwise, model's prior hyperparameters are calibrated according to Primiceri (2005).

## A.3 The Markov Chain Monte Carlo Algorithm

The algorithm gets initialized by choosing initial draws for $\alpha^T$, $\sigma^T$, and $\mathbf{V}$ from the prior distributions described above. The Gibbs sampling algorithm then loops through the following steps.

### A.3.1 Drawing the Coefficient States

Conditional on $(\alpha^T, \sigma^T, \mathbf{V})$, the observation equation (A.5) in linear and has Gaussian innovations with known variance. As shown in Carter and Kohn (1994) and Frühwirth-Schnatter (1994), the density can be factored as

$$p(\mathbf{B}^T|\mathbf{y}^T, \alpha^T, \sigma^T, \mathbf{V}) = p(\mathbf{B}_T|\mathbf{y}^T, \alpha^T, \sigma^T, \mathbf{V}) \prod_{t=1}^{T-1} p(\mathbf{B}_t|\mathbf{B}_{t+1}, \mathbf{y}^t, \alpha^T, \sigma^T, \mathbf{V}),$$

where

$$\mathbf{B}_t|\mathbf{B}_{t+1}, \mathbf{y}^t, \alpha^T, \sigma^T, \mathbf{V} \sim \mathcal{N}(\mathbf{B}_{t|t+1}, \mathbf{P}_{t|t+1}),$$

$$\mathbf{B}_{t|t+1} = \mathbb{E}(\mathbf{B}_t|\mathbf{B}_{t+1}, \mathbf{y}^t, \alpha^T, \sigma^T, \mathbf{V}),$$

and

$$\mathbf{P}_{t|t+1} = \mathbb{V}\mathbb{a}\mathbb{r}(\mathbf{B}_t|\mathbf{B}_{t+1}, \mathbf{y}^t, \alpha^T, \sigma^T, \mathbf{V}).$$

The vector of $\mathbf{B}$s can be drawn easily because $\mathbf{B}_{t|t+1}$ and $\mathbf{P}_{t|t+1}$ can be computed using forward and backward recursions on the Kalman filter as follows.

The measurement equation for this step is (A.7), rewritten as

$$\mathbf{y}_t = \mathbf{X}_t'\mathbf{B}_t + \mathbf{u}_t \tag{A.12}$$

where $\mathbf{u}_t = \mathbf{A}_t^{-1}\mathbf{\Sigma}_t\varepsilon_t$, $\mathbb{E}\{\mathbf{u}_t\mathbf{u}_t'\} = \mathbf{\Omega}_t$ and $\mathbf{\Omega}_t = \mathbf{A}_t^{-1}\mathbf{\Sigma}_t\mathbf{\Sigma}_t'(\mathbf{A}_t^{-1})'$, and the state transition equation is given by (A.8) as

$$\mathbf{B}_t = \mathbf{B}_{t-1} + \nu_t$$

where $\mathbb{E}\{\nu_t\nu_t'\} = \mathbf{Q}$. Let

$$\mathbf{B}_{t|s} = \mathbb{E}(\mathbf{B}_t|\mathbf{y}^s, \mathbf{X}^s, \mathbf{\Omega}^s, \mathbf{Q})$$

and

$$\mathbf{P}_{t|s} = \mathbb{V}\mathbb{a}\mathbb{r}(\mathbf{B}_t|\mathbf{y}^s, \mathbf{X}^s, \mathbf{\Omega}^s, \mathbf{Q}).$$

Then, given $\mathbf{B}_{0|0} = \hat{\mathbf{B}}$ and $\mathbf{P}_{0|0} = k_{\mathbf{B}}^2 V_{\mathbf{B}}$, the Kalman filter implies

$$\mathbf{B}_{t|t-1} = \mathbf{B}_{t-1|t-1},$$

$$\mathbf{P}_{t|t-1} = \mathbf{P}_{t-1|t-1} + \mathbf{Q},$$

$$\mathbf{K}_t = \mathbf{P}_{t|t-1}\mathbf{X}_t(\mathbf{X}_t'\mathbf{P}_{t|t-1}\mathbf{X}_t + \mathbf{\Omega}_t)^{-1},$$

$$\mathbf{B}_{t|t} = \mathbf{B}_{t|t-1} + \mathbf{K}_t(\mathbf{y}_t - \mathbf{X}_t'\mathbf{B}_{t|t-1}),$$

and

$$\mathbf{P}_{t|t} = \mathbf{P}_{t|t-1} - \mathbf{K}_t\mathbf{X}_t'\mathbf{P}_{t|t-1}.$$

The last elements from these recursions are $\mathbf{B}_{T|T}$ and $\mathbf{P}_{T|T}$, which are the mean and variance of the normal distribution used to make a draw for $\mathbf{B}_t$. The draw for $\mathbf{B}_t$ and the output of the filter can now be used for the first step of the backward recursions

$$\mathbf{B}_{t|t+1} = \mathbf{B}_{t|t} + \mathbf{P}_{t|t}\mathbf{P}_{t+1|t}^{-1}(\mathbf{B}_{t+1} - \mathbf{B}_{t|t}) = \mathbf{B}_{t|t} + \mathbf{P}_{t|t}(\mathbf{P}_{t|t} + \mathbf{Q})^{-1}(\mathbf{B}_{t+1} - \mathbf{B}_{t|t})$$

and

$$\mathbf{P}_{t|t+1} = \mathbf{P}_{t|t} - \mathbf{P}_{t|t}\mathbf{P}_{t+1|t}^{-1}\mathbf{P}_{t|t} = \mathbf{P}_{t|t} - \mathbf{P}_{t|t}(\mathbf{P}_{t|t} + \mathbf{Q})^{-1}\mathbf{P}_{t|t},$$

which are the means and variances used to make the draws for $\mathbf{B}_t$, $t = T-1, T-2, \ldots, 1$.

### A.3.2 Drawing Covariance States

The system of equations in (A.7) can be rewritten as

$$\mathbf{A}_t(\mathbf{y}_t - \mathbf{X}_t'\mathbf{B}_t) = \mathbf{A}_t\mathbf{u}_t = \mathbf{\Sigma}_t\varepsilon_t, \tag{A.13}$$

where, taking $\mathbf{B}^T$ as given, $\mathbf{u}_t$ is observable from (A.12). Since $\mathbf{A}_t$ is a lower triangular matrix with ones on the main diagonal, (A.13) can be rewritten as

$$\mathbf{u}_t = \mathbf{Z}_t\alpha_t + \mathbf{\Sigma}_t\varepsilon_t, \tag{A.14}$$

where $\alpha_t$ is defined in (A.9) and $\mathbf{Z}_t$ is the following $3 \times 3$ matrix:

$$\mathbf{Z}_t = \begin{bmatrix} 0 & 0 & 0 \\ -u_{\pi,t} & 0 & 0 \\ 0 & -u_{\pi,t} & -u_{g,t} \end{bmatrix}$$

The model given by (A.14) and (A.9) has a Gaussian but nonlinear state space representation. The problem is that the dependent variable of the observation equation, $\mathbf{u}_t$, also appears on the right-hand side in $\mathbf{Z}_t$. Therefore, the vector $\begin{bmatrix} \mathbf{u}_t & \alpha_t \end{bmatrix}$ is not jointly normal and, as a consequence, the conditional distributions cannot be computed using the standard Kalman filter recursions. However, under the additional maintained assumption that $\mathbf{S}$ is block diagonal, this problem can be solved by applying the Kalman filter and the backward recursion equation by equation.

Thus, consider the second equation from (A.14), which can be written

$$u_{g,t} = \mathbf{Z}_{1t}\alpha_{g\pi,t} + \sigma_{g,t}\varepsilon_{g,t}, \tag{A.15}$$

where $\mathbf{Z}_{1t} = -u_{\pi,t}$ and $\varepsilon_{g,t} \sim iid\mathcal{N}(0,1)$. Taking $\mathbf{B}^T$ and $\sigma^T$ as given, $u_{gt}$ and $\mathbf{Z}_{1t}$ are observable and $\sigma_{g,t}$ is given as well. Equation (A.15) can serve as the observation equation and the first equation from (A.9),

$$\alpha_{g\pi,t} = \alpha_{g\pi,t-1} + \zeta_{1,t} \tag{A.16}$$

as the state transition equation, where $\xi_{1,t} \sim \mathcal{N}(0, \mathbf{S}_1)$, with $\mathbf{S}_1$ given as well.

Thus, given $\alpha_{g\pi,0|0} = \hat{\alpha}_{g\pi}$ and $\mathbf{P}_{0|0} = k_\alpha^2 V_\alpha^{1,1}$, the Kalman filter implies

$$\alpha_{g\pi,t|t-1} = \alpha_{g\pi,t-1|t-1},$$

$$\mathbf{P}_{t|t-1} = \mathbf{P}_{t-1|t-1} + \mathbf{S}_1,$$

$$\mathbf{K}_t = \mathbf{P}_{t|t-1}\mathbf{Z}_{1t}'(\mathbf{Z}_{1t}\mathbf{P}_{t|t-1}\mathbf{Z}_{1t}' + \sigma_{g,t}^2)^{-1},$$

$$\alpha_{g\pi,t|t} = \alpha_{g\pi,t|t-1} + \mathbf{K}_t(u_{g,t} - \mathbf{Z}_{1t}\alpha_{g\pi,t|t-1}),$$

and

$$\mathbf{P}_{t|t} = \mathbf{P}_{t|t-1} - \mathbf{K}_t\mathbf{Z}_{1t}\mathbf{P}_{t|t-1}.$$

The last elements from these recursions are $\alpha_{g\pi,T|T}$ and $\mathbf{P}_{t|t}$, which are the mean and variance of the normal distribution used to make a draw for $\alpha_{g\pi,T}$. The draw for $\alpha_{g\pi,T}$ and the output of the filter can now be used for the first step of the backward recursions

$$\alpha_{g\pi,t|t+1} = \alpha_{g\pi,t|t} + \mathbf{P}_{t|t}\mathbf{P}_{t+1|t}^{-1}(\alpha_{g\pi,t+1} - \alpha_{g\pi,t|t}) = \alpha_{g\pi,t|t} + \mathbf{P}_{t|t}(\mathbf{P}_{t|t} + \mathbf{S}_1)^{-1}(\alpha_{g\pi,t+1} - \alpha_{g\pi,t|t})$$

and

$$\mathbf{P}_{t|t+1} = \mathbf{P}_{t|t} - \mathbf{P}_{t|t}\mathbf{P}_{t+1|t}^{-1}\mathbf{P}_{t|t} + \mathbf{P}_{t|t} - \mathbf{P}_{t|t}(\mathbf{P}_{t|t} + \mathbf{S}_1)^{-1}\mathbf{P}_{t|t},$$

which are the means and variances used to make the draws for $\alpha_{u\pi,t}$, $t = T-1, T-2, \ldots, 1$.

Now consider the third equation from (A.14), which can be written

$$u_{r,t} = \mathbf{Z}_{2t}\alpha_{2,t} + \sigma_{r,t}\varepsilon_{r,t}, \tag{A.17}$$

where $\mathbf{Z}_{2t} = \begin{bmatrix} -u_{\pi,t} & -u_{g,t} \end{bmatrix}$, $\alpha_{2,t} = \begin{bmatrix} \alpha_{r\pi,t} & \alpha_{rg,t} \end{bmatrix}'$, and $\varepsilon_{r,t} \sim iid\mathcal{N}(0,1)$. Taking $\mathbf{B}^T$ and $\sigma^T$ as given, $u_{rt}$ and $\mathbf{Z}_{2t}$ are observable and $\sigma_{r,t}$ is given as well. Equation (A.17) can serve as the observation equation and last two equations from (A.9),

$$\alpha_{2,t} = \alpha_{2,t-1} + \xi_{2,t} \tag{A.18}$$

as the state transition equation, where $\xi_{2,t} \sim \mathcal{N}(0, \mathbf{S}_2)$, with $\mathbf{S}_2$ given as well.

Thus, given $\alpha_{2,0|0} = \begin{bmatrix} \hat{\alpha}_{r\pi} & \hat{\alpha}_{rg,t} \end{bmatrix}'$ and $\mathbf{P}_{0|0} = k_\alpha^2 V_\alpha^{2:3,2:3}$, the Kalman filter implies

$$\alpha_{2,t|t-1} = \alpha_{2,t-1|t-1},$$

$$\mathbf{P}_{t|t-1} = \mathbf{P}_{t-1|t-1} + \mathbf{S}_2,$$

$$\mathbf{K}_t = \mathbf{P}_{t|t-1}\mathbf{Z}_{2t}'(\mathbf{Z}_{2t}\mathbf{P}_{t|t-1}\mathbf{Z}_{2t}' + \sigma_{r,t}^2)^{-1},$$

$$\alpha_{2,t|t} = \alpha_{2,t|t-1} + \mathbf{K}_t(u_{r,t} - \mathbf{Z}_{2t}\alpha_{2,t|t-1}),$$

and

$$\mathbf{P}_{t|t} = \mathbf{P}_{t|t-1} - \mathbf{K}_t\mathbf{Z}_{2t}\mathbf{P}_{t|t-1}.$$

The last elements from these recursions are $\alpha_{2,T|T}$ and $\mathbf{P}_{t|t}$, which are the mean and variance of the normal distribution used to make draws for $\alpha_{r\pi,T}$ and $\alpha_{rg,T}$. The draw for $\alpha_{2,T}$ and the output of the filter can now be used for the first step of the backward recursions

$$\alpha_{2,t|t+1} = \alpha_{2,t|t} + \mathbf{P}_{t|t}P_{t+1|t}^{-1}(\alpha_{2,t+1} - \alpha_{2,t|t}) = \alpha_{2,t|t} + \mathbf{P}_{t|t}(\mathbf{P}_{t|t} + \mathbf{S}_2)^{-1}(\alpha_{2,t+1} - \alpha_{2,t|t})$$

and

$$\mathbf{P}_{t|t+1} = \mathbf{P}_{t|t} - \mathbf{P}_{t|t}\mathbf{P}_{t+1|t}^{-1}\mathbf{P}_{t|t} = \mathbf{P}_{t|t} - \mathbf{P}_{t|t}(\mathbf{P}_{t|t} + \mathbf{S}_2)^{-1}\mathbf{P}_{t|t},$$

which are the means and variances used to make the draws for $\alpha_{u\pi,t}$, $t = T-1, T-2, \ldots, 1$.

### A.3.3 Drawing Volatility States

Consider next the system of equations

$$\mathbf{A}_t(\mathbf{y}_t - \mathbf{X}_t'\mathbf{B}_t) = \mathbf{y}_t^* = \mathbf{\Sigma}_t\varepsilon_t, \tag{A.19}$$

where, taking $\mathbf{B}^T$ and $\alpha^T$ as given, $\mathbf{y}_t^*$ is observable. This is a system of nonlinear measurement equations, but can be converted into a linear one by squaring and taking logs of every element of (A.19). Due to the fact that $\mathbf{y}_{i,t}^2$ can be very small, an offset constant can be used to make the estimation procedure more robust. This leads to the following approximating state space form:

$$\mathbf{y}_t^{**} = 2h_t + e_t \tag{A.20}$$

and

$$h_t = h_{t-1} + \eta_t, \tag{A.21}$$

where $\mathbf{y}_{i,t}^{**} = \log[(\mathbf{y}_{i,t}^*)^2 + \bar{c}]$, $\bar{c}$ is the offset constant, set equal to 0.001, $e_{i,t} = \log(\varepsilon_{i,t}^2)$, and $h_{i,t} = \log\sigma_{i,t}$. Observe $e$ and $\eta$ are not correlated, since $\varepsilon$ and $\eta$ are independant.

This system has a linear, but non-Gaussian, state space form because the innovations in the measurement equations are distributed as $\log\chi^2(1)$. In order to further transform the system into a Gaussian one, a mixture of normal approximations of the $\log\chi^2$ distribution is used, as described by Kim et al. (1998). This involves selecting a mixture of seven normal densities with component probabilities $q_j$, means $m_j - 1.2704$ and variances $v_j^2$, where the constants are chosen to match a number of moments of the $\log\chi^2(1)$ distribution as reported in Kim et al.'s (1998) paper:

Selection of the mixing distribution to be $\log\chi^2(1)$

| $\omega$ | $q_j = Pr(\omega = j)$ | $m_j$ | $v_j^2$ |
|---|---|---|---|
| 1 | 0.00730 | -10.12999 | 5.79596 |
| 2 | 0.10556 | -3.97281 | 2.61369 |
| 3 | 0.00002 | -8.56686 | 5.17950 |
| 4 | 0.04395 | 2.77786 | 0.16735 |
| 5 | 0.34001 | 0.61942 | 0.64009 |
| 6 | 0.24566 | 1.79518 | 0.34023 |
| 7 | 0.25750 | -1.08819 | 1.26261 |

Define $s^T = \begin{bmatrix} s_1 & \dots & s_T \end{bmatrix}'$, the matrix of indicator variables selecting at every point in time which member of the mixture of the normal approximation will be used for each element of $e$. Given $(\mathbf{y}^{**})^T$ and $h^T$, each $s_{i,t}$ is sampled from the discrete density defined by

$$Pr(s_{i,t} = j|\mathbf{y}_{i,t}^{**}, h_{i,t}) \propto q_j f_N(\mathbf{y}_{i,t}^{**}|2h_{i,t} + m_j - 1.2704, v_j^2), \qquad i = 1, 2, ..., n \quad j = 1, 2, ..., 7.$$

$j = 1, 2, \dots, 7$, where $f_N(\cdot|\mu, v^2)$ denotes the probability density function for a normal random variable with mean $\mu$ and variance $v^2$. Conditional on $\mathbf{B}^T$, $\mathbf{A}^T$, $\mathbf{V}$ and $s^T$, the system has an approximate linear and Gaussian state space form, where each element $e_{i,t}$ of $e_t$ in (A.18) can now be viewed as being distributed as normal with mean $m_j - 1.2704$ and variance $v_j^2$ if $s_{i,t} = j$.

For each $t = 1, 2, \ldots, T$, let $m_t$ denote the $3 \times 1$ vector consisting of the means $m_j - 1.2704$ of each element of $e_t$ as determined above and let $\mathbf{V}_t$ denote the $3 \times 3$ matrix with the corresponding variances $v_j^2$ along its diagonal. Finally, define $\mathbf{X}_t = \mathbf{y}_t^{**} - m_t + 1.2704$. Now (A.20) can be rewritten as the observation equation

$$\mathbf{X}_t = 2h_t + e_t, \tag{A.22}$$

where $e_t \sim \mathcal{N}(0, \mathbf{V}_t)$ and

$$h_t = h_{t-1} + \eta_t$$

remains as the state transition equation given in (A.21), with $\eta_t \sim \mathcal{N}(0, \mathbf{W})$.

Given $h_{0|0} = \log \hat{\sigma}$ and $\mathbf{P}_{0|0} = k_\sigma^2 \mathbf{I}_3$, the Kalman filter implies

$$h_{t|t-1} = h_{t-1|t-1},$$

$$\mathbf{P}_{t|t-1} = \mathbf{P}_{t-1|t-1} + \mathbf{W},$$

$$\mathbf{K}_t = 2\mathbf{P}_{t|t-1}(4\mathbf{P}_{t|t-1} + \mathbf{V}_t)^{-1},$$

$$h_{t|t} = h_{t|t-1} + \mathbf{K}_t(\mathbf{X}_t - 2h_{t|t-1}),$$

and

$$\mathbf{P}_{t|t} = \mathbf{P}_{t|t-1} - 2\mathbf{K}_t\mathbf{P}_{t|t-1}.$$

The last elements from these recursions are $h_{T|T}$ and $\mathbf{P}_{T|T}$, which are the mean and variance of the normal distribution used to make a draw for $h_T$. The draw for $h_T$ and the output of the filter can now be used for the first step of the backward recursions

$$h_{t|t+1} = h_{t|t} + \mathbf{P}_{t|t}\mathbf{P}_{t+1|t}^{-1}(h_{t+1} - h_{t|t}) = h_{t|t} + \mathbf{P}_{t|t}(\mathbf{P}_{t|t} + \mathbf{W})^{-1}(h_{t+1} - h_{t|t})$$

and

$$\mathbf{P}_{t|t+1} = \mathbf{P}_{t|t} - \mathbf{P}_{t|t}\mathbf{P}_{t+1|t}^{-1}\mathbf{P}_{t|t} = \mathbf{P}_{t|t} - \mathbf{P}_{t|t}(\mathbf{P}_{t|t} + \mathbf{W})^{-1}\mathbf{P}_{t|t},$$

which are the means and variances used to make the draws for $h_t$, $t = T-1, T-2, \ldots, 1$.

Del Negro and Primiceri (2015) note that, strictly speaking, because the mixture of normal distributions used in the Kim-Shephard-Chib algorithm is only an approximation to the true distribution of the innovations in the measurement equation (A.20), each draw selected using this algorithm should be used as a proposal in a Metropolis-Hastings step, following the general analysis in Stroud et al. (2003). With $\mathbf{y}_t^*$ and $\mathbf{y}_{i,t}^{**}$ defined as above, let $\tilde{\mathbf{\Sigma}}_t$ and $\mathbf{\Sigma}_t^{old}$ be the latest and previous draws for the volatility state for period $t = 1, 2, \ldots, T$, and let $\tilde{\sigma}_{i,t}$ and $\sigma_{i,t}^{old}$ be the $i$th diagonal elements of $\tilde{\mathbf{\Sigma}}_t$ and $\mathbf{\Sigma}_t^{old}$. Del Negro and Primiceri (2015) show that in the Metropolis step, the new draw should be accepted with probability $\alpha$, where

$$\alpha = \frac{\left[\prod_{t=1}^{T} F_N(\mathbf{y}_t^* | \mathbf{0}_{3,1}, \tilde{\mathbf{\Sigma}}_t \tilde{\mathbf{\Sigma}}_t')\right] \left[\prod_{t=1}^{T}\prod_{i=1}^{3}\prod_{j=1}^{7} q_j f_N(\mathbf{y}_{i,t}^{**} | 2\sigma_{i,t}^{old} + m_j - 1.2704, v_j^2)\right]}{\left[\prod_{t=1}^{T} F_N(\mathbf{y}_t^* | \mathbf{0}_{3,1}, \mathbf{\Sigma}_t^{old}(\mathbf{\Sigma}_t^{old})')\right] \left[\prod_{t=1}^{T}\prod_{i=1}^{3}\prod_{j=1}^{7} q_j f_N(\mathbf{y}_{i,t}^{**} | 2\tilde{\sigma}_{i,t} + m_j - 1.2704, v_j^2)\right]},$$

and $F_N(\cdot | \mu, \mathbf{V})$ is the probability density function for the multivariate normal distribution with mean $\mu$ and covariance matrix $\mathbf{V}$.

### A.3.4 Drawing Hyperparameters

The hyperparameters are the diagonal blocks of $\mathbf{V}$, each of which has an inverse-Wishart posterior distribution. Conditional on $\mathbf{B}^T$, $\alpha^T$, $\sigma^T$, and $\mathbf{y}^T$, it is easy to draw from these posteriors because the innovations are observable. Use (A.8) to compute

$$\nu_t = \mathbf{B}_t - \mathbf{B}_{t-1},$$

use (A.16) to compute

$$\zeta_{1,t} = \alpha_{u\pi,t} - \alpha_{u\pi,t-1},$$

use (A.18) to compute

$$\zeta_{2,t} = \alpha_{2,t} - \alpha_{2,t-1},$$

and use (A.10) to compute

$$\eta_t = \log \sigma_t - \log \sigma_{t-1}.$$

Then a new draw for $\mathbf{Q}$ can be taken from the inverse-Wishart posterior distribution with scale matrix

$$d_{\mathbf{Q}} k_{\mathbf{Q}}^2 V_{\mathbf{Q}} + \sum_{t=1}^{T} \nu_t \nu_t',$$

and degrees of freedom $d_{\mathbf{Q}} + T$, a new draw for $\mathbf{S}_1$ can be taken from the inverse-Wishart posterior distribution with scale matrix

$$d_{\mathbf{S}1} k_{\mathbf{S}}^2 V_{\mathbf{S}1} + \sum_{t=1}^{T} \zeta_{1,t} \zeta_{1,t}',$$

and degrees of freedom $d_{\mathbf{S}1} + T$, a new draw for $\mathbf{S}_2$ can be taken from the inverse-Wishart posterior distribution with scale matrix

$$d_{\mathbf{S}2} k_{\mathbf{S}}^2 V_{\mathbf{S}2} + \sum_{t=1}^{T} \zeta_{2,t} \zeta_{2,t}',$$

and degrees of freedom $d_{\mathbf{S}2} + T$, and new draws for each diagonal element of $\mathbf{W}$ can be taken from the inverse-Wishart posterior distributions with scale matrix

$$d_{\mathbf{W}} k_{\mathbf{W}}^2 + \sum_{t=1}^{T} \eta_t \eta_t',$$

which in this case is a scalar, and degrees of freedom $d_{\mathbf{W}} + T$.

### A.3.5 Assessing Convergence

To assess the convergence of the MCMC algorithm, Primiceri (2005) recommends initializing the chain from different, randomly selected starting points, to verify that none of the results is affected. A related but slightly more formal approach is suggested by Geweke (1992). For any model statistic $\theta$, which may be an element of $\mathbf{B}^T$, $\mathbf{A}^T$, $\mathbf{\Sigma}^T$, $\mathbf{V}$, or any function of these parameters, calculate the means $\bar{\theta}_A$ and $\bar{\theta}_B$ from two disjoint subsamples of the Gibbs sampling output: Geweke (1992) suggests letting subsample $A$ be formed from the first 10 percent of the draws and subsample $B$ from the last 50 percent of the draws. The numerical standard errors of the means $\bar{\theta}_A$ and $\bar{\theta}_B$ are given by

$$\left(\frac{1}{N_A}\right)[2\pi S_{\theta,A}(0)] \text{ and } \left(\frac{1}{N_B}\right)[2\pi S_{\theta,B}(0)],$$

where $S_{\theta,A}(0)$ and $S_{\theta,B}(0)$ denote the spectral densities of $\hat{\theta}_A$ and $\hat{\theta}_B$ at frequency zero, which can be estimated using Newey and West's (1987) Bartlett weighting scheme as

$$S_{\theta,A}(0) = \frac{1}{2\pi}\left[\upsilon_{\theta,A,0} + 2\sum_{j=1}^{m}\left(1 - \frac{j}{m+1}\right)\upsilon_{\theta,A,j}\right]$$

and

$$S_{\theta,B}(0) = \frac{1}{2\pi}\left[\upsilon_{\theta,B,0} + 2\sum_{j=1}^{m}\left(1 - \frac{j}{m+1}\right)\upsilon_{\theta,B,j}\right],$$

where $\upsilon_{\theta,A,j}$ and $\upsilon_{\theta,B,j}$ are the $j$-th autocovariances of the draws for $\theta$ in subsamples $A$ and $B$. Geweke's (1992) convergence diagnostic

$$CD(\theta) = \frac{\bar{\theta}_A - \bar{\theta}_B}{\{N_A^{-1}[2\pi S_{\theta,A}(0)] + N_B^{-1}[2\pi S_{\theta,B}(0)]\}^{1/2}} \to \mathcal{N}(0,1),$$

which, as shown, has the standard normal distribution as $N_A \to \infty$ and $N_B \to \infty$.

To gauge the extent to which the chain mixes, Primiceri (2005) and Benati (2011) compute inefficiency factors. The inefficiency factor for any individual statistic $\theta$, which may again be an element of $\mathbf{B}^T$, $\mathbf{A}^T$, $\mathbf{\Sigma}^T$, $\mathbf{V}$, or any function of these parameters, is defined as the inverse of Geweke's (1992) measure of relative numerical efficiency:

$$IF(\theta) = \frac{2\pi S_\theta(0)}{\mathbb{V}\mathbb{a}\mathbb{r}(\theta)} = \frac{2\pi S_\theta(0)}{\int_{-\pi}^{\pi} S_\theta(\omega)\mathrm{d}\omega},$$

where $S_\theta(\omega)$ is the spectral density of $\theta$ at frequency $\omega$ so that, in particular, $S_\theta(0)$ is the spectral density of $\theta$ at frequency zero. Primiceri (2005) notes that

$$IF(\theta) = 1 + 2\sum_{j=1}^{\infty}\rho_{\theta,j},$$

where $\rho_{\theta,j}$ is the $j$-th autocorrelations of the draws for $\theta$. Hence, $IF(\theta)$ will generally be larger than one, and lower values of $IF(\theta)$ reflect less autocorrelation in the draws. In computing $IF(\theta)$, Newey and West (1987) estimator

$$S_\theta(0) = \frac{1}{2\pi}\left[\upsilon_{\theta,0} + 2\sum_{j=1}^{m}\left(1 - \frac{j}{m+1}\right)\upsilon_{\theta,j}\right]$$

can be used for the numerator, while the denominator is simply the variance $\upsilon_{\theta,0}$ across all draws for $\theta$.

## A.4 Identification of Monetary Policy Shocks

### A.4.1 The Identification Problem

Two approaches can be taken to identify monetary policy shocks from the estimated reduced form. The first uses assumptions about the timing with which monetary policy disturbances affect inflation and the gap variable to re-interpret the triangular factorization of the reduced-form covariance matrix shown in (A.3) as a mapping between the reduced-form and structural models – an approach that dates back to Sims (1980). The second uses sign restrictions to identify monetary policy shocks based on their implied impulse responses. Faust (1998), Canova and De Nicolo (2002), and Uhlig (2005) propose and develop the idea that sign restrictions can serve a source of identifying assumptions in VARs, and Benati (2011) implements the particular scheme used here in a similar VAR framework with time-varying parameters.

Details on each of the two identification strategies follows, but each works to factor the reduced-form covariance matrix as

$$\mathbf{\Omega}_t = \mathbf{C}_t^{-1}\mathbf{D}_t\mathbf{D}_t'(\mathbf{C}_t')^{-1}, \tag{A.23}$$

where $\mathbf{C}_t$ and $\mathbf{D}_t$ are $3 \times 3$ matrices of the form

$$\mathbf{C}_t = \begin{bmatrix} 1 & -c_{\pi g,t} & -c_{\pi r,t} \\ -c_{g\pi,t} & 1 & -c_{gr,t} \\ -c_{r\pi,t} & -c_{rg,t} & 1 \end{bmatrix} \tag{A.24}$$

and

$$\mathbf{D}_t = \begin{bmatrix} \delta_{\pi,t} & 0 & 0 \\ 0 & \delta_{g,t} & 0 \\ 0 & 0 & \delta_{r,t} \end{bmatrix} \tag{A.25}$$

Equations (A.23)-(A.25) provide the general mapping between the reduced-form equation (A.2) and the structural model, which can now be written as

$$\mathbf{C}_t\mathbf{y}_t = \boldsymbol{\gamma}_t + \mathbf{\Gamma}_{1,t}\mathbf{y}_{t-1} + \mathbf{\Gamma}_{2,t}\mathbf{y}_{t-2} + \mathbf{D}_t\xi_t, \tag{A.26}$$

where $\boldsymbol{\gamma}_t = \mathbf{C}_t\mathbf{B}_t$, $\mathbf{\Gamma}_{i,t} = \mathbf{C}_t\mathbf{B}_{i,t}$ for $i = 1, 2$, and $\xi_t$ is a $3 \times 1$ vector of structural disturbances, normally distributed with zero mean and $\mathbb{E}\{\xi_t\xi_t'\} = \mathbf{I}_3$. The third row from (A.26) takes the form of a monetary policy rule

$$\begin{aligned} R_t^s = {} & \gamma_{r,t} + c_{r\pi,t}\Pi_t + \gamma_{1,r\pi,t}\Pi_{t-1} + \gamma_{2,r\pi,t}\Pi_{t-2} \\ & + c_{rg,t}G_t + \gamma_{1,rg,t}G_{t-1} + \gamma_{2,rg,t}G_{t-2} + \gamma_{1,rr,t}R_{t-1}^s + \gamma_{2,rg,t}R_{t-2}^s + \delta_{r,t}\xi_t^{mp} \end{aligned} \tag{A.27}$$

The Taylor-type monetary policy rule prescribes a setting for the policy rate regarding to changes in current and lagged inflation and output gap variables. It also includes lagged values of interest rate terms to capture central banks' tendency to smooth short-term interest rates movements over time. The time-varying estimation of the intercept $\gamma_{r,t}$ and of the coefficients from matrices $\mathbf{\Gamma}_{1,t}$ and $\mathbf{\Gamma}_{2,t}$ allows to assess changes to monetary policy that might have occured on the sample period. $\xi_t^{mp}$ represents identified monetary policy shocks that capture deviations in the actual policy rate from the value dictated by the estimated monetary policy rule. Importantly, equation (A.27) allows for time-variation in all of the response coefficients but also in the standard deviation $\delta_{r,t}$ of the monetary policy shocks. Hence, this estimation permits disentangling changes in central bank's responses to inflation versus output gap stabilization and the extent to which the central bank departs from its rule-based behavior. As a whole, the estimated monetary policy rule given in equation (A.27) may be decomposed into central banks' response to macroeconomic conditions and smoothing behavior – i.e. the *systematic* component of monetary policy – and monetary policy shocks – i.e. the *non-systematic* component of monetary policy.

Equation (A.27) can then be decomposed and interpreted as follows

$$R_t^s = \gamma_{r,t} + \overbrace{\underbrace{c_{r\pi,t}\Pi_t + \gamma_{1,r\pi,t}\Pi_{t-1} + \gamma_{2,r\pi,t}\Pi_{t-2}}_{\text{response to inflation}}}^{\text{systematic}}$$

$$\overbrace{+\underbrace{c_{rg,t}G_t + \gamma_{1,rg,t}G_{t-1} + \gamma_{2,rg,t}G_{t-2}}_{\text{response to output gap}} + \underbrace{\gamma_{1,rr,t}R_{t-1}^s + \gamma_{2,rg,t}R_{t-2}^s}_{\text{interest rate smoothing}}}^{\text{component of monetary policy}} + \overbrace{\delta_{r,t}\ \underbrace{\xi_t^{mp}}_{\substack{\text{MP}\\ \text{shocks}}}}^{\substack{\text{non-systematic comp.}\\ \text{of monetary policy}}}$$

Comparing (A.4) and (A.5) to (A.24) and (A.25) highlights the identification problem: together, the matrices $\mathbf{A}_t$ and $\mathbf{\Sigma}_t$ of reduced-form parameters contain 6 elements not equal to zero or one, whereas the matrices $\mathbf{C}_t$ and $\mathbf{D}_t$ of structural parameters have 9 such elements. Each of the two identification schemes described next imposes more structure on the matrix $\mathbf{C}_t$ to solve this problem.

### A.4.2 Triangular Identification Based on Timing Assumptions

The factorization of the symmetric, positive definite reduced-form covariance matrix $\mathbf{\Omega}_t$ shown in (A.3)-(A.5) always exists and is unique; hence, the model can be written in this form without any loss of generality. However, under the additional assumptions – made throughout much of the literature on VARs that builds on Sims (1980) – that inflation and the output gap respond to monetary policy shocks only after a one-period lag, the reduced-form parameters from the third rows of (A.3)-(A.5) are linked to structural parameters from the third rows on (A.23)-(A.25) via

$$c_{r\pi,t} = -\alpha_{r\pi,t},$$

$$c_{rg,t} = -\alpha_{rg,t},$$

and

$$\delta_{r,t} = \sigma_{r,t}$$

and the structural monetary policy shock $\xi_t^{mp}$ from (A.26) and (A.27) is identified as the third element of the vector $\varepsilon_t$ from (A.6).

### A.4.3 Sign Restrictions for the Variables that Respond to Monetary Policy

An alternative approach to identification builds on work by Faust (1998), Canova and De Nicolo (2002), and Uhlig (2005) by associating monetary policy shocks with the effects they have on observable variables. Following Benati (2011), suppose that the first element of $\xi_t$ corresponds to a supply shock that moves inflation and the output gap in opposite directions or inflation and the unemployment rate in the same direction. Suppose that the second element of $\xi_t$ is a non-monetary demand shock, that moves the short-term interest rate and inflation in the same direction and the interest rate and the output gap in the same direction or the interest rate and the unemployment rate in opposite directions. Finally, suppose that the third element of $\xi_t$ corresponds to a monetary policy shock that moves the short-term interest rate and inflation in opposite directions and the interest rate and the output gap in opposite directions or the interest rate and the unemployment rate in the same direction. Rubio-Ramirez et al. (2010) and Arias et al. (2018) emphasize that sign restrictions of this

form do not suffice to identify structural disturbances in the classical sense, but develop a Bayesian algorithm for characterizing the set of parameter values implying impulse responses that satisfy these restrictions.

Let the index $i = 1, 2, \ldots, N$ keep track of the number of desired draws. For $i = 1, 2, \ldots, N$, the algorithm loops through the following steps.

1. Draw $(\mathbf{A}^T, \mathbf{\Sigma}^T)$ from their posterior distribution during the Gibbs sampling stage.

2. For each $t = 1, 2, \ldots, T$, construct $\mathbf{A}_t$ and $\mathbf{\Sigma}_t$ based on the draw for $(\mathbf{A}^T, \mathbf{\Sigma}^T)$. Then let $\mathbf{L}_t = \mathbf{A}_t^{-1}\mathbf{\Sigma}_t$, so that the reduced-form error covariance matrix is given by $\mathbf{\Omega}_t = \mathbf{L}_t\mathbf{L}_t'$.

3. Draw $\tilde{\mathbf{X}}$, a $3 \times 3$ random matrix with each element having an independent standard normal distribution. Then factor $\tilde{\mathbf{X}} = \mathbf{Q}_\mathbf{X}\mathbf{R}_\mathbf{X}$, where $\mathbf{Q}_\mathbf{X}$ is an orthogonal matrix and $\mathbf{R}_\mathbf{X}$ is upper triangular with positive diagonal elements.

4. Let $\tilde{\mathbf{L}}_t = \mathbf{L}_t\mathbf{Q}_\mathbf{X}'$, and note that
$$\tilde{\mathbf{L}}_t\tilde{\mathbf{L}}_t' = \mathbf{L}_t\mathbf{Q}_\mathbf{X}'\mathbf{Q}_\mathbf{X}\mathbf{L}_t' = \mathbf{L}_t\mathbf{L}_t' = \mathbf{\Omega}_t,$$
by virtue of the fact that $\mathbf{Q}_\mathbf{X}$ is orthogonal. This highlights that multiplying the structural model (A.26) through by $\mathbf{D}_t^{-1}$ and then $\mathbf{Q}_\mathbf{X}$ results in an observationally-equivalent rotation of the model's three equations. Suppressing for convenience explicit reference to the constant and lagged terms in (A.26), the candidate structural model based on the specific draw for $\mathbf{Q}_\mathbf{X}$ can be written as
$$\mathbf{y}_t = \tilde{\mathbf{L}}_t\xi_t,$$
since
$$\mathbb{E}[(\tilde{\mathbf{L}}_t\xi_t)(\tilde{\mathbf{L}}_t\xi_t)'] = \mathbb{E}(\tilde{\mathbf{L}}_t\xi_t\xi_t'\tilde{\mathbf{L}}_t') = \tilde{\mathbf{L}}_t\mathbb{E}(\xi_t\xi_t')\tilde{\mathbf{L}}_t' = \tilde{\mathbf{L}}_t\tilde{\mathbf{L}}_t' = \mathbf{\Omega}_t.$$
Thus, the matrix $\tilde{\mathbf{L}}_t$ contains impact coefficients linking the structural shocks in $\xi_t$ to the observable variables in $\mathbf{y}_t$. The sign restriction used to identify the supply, demand, and monetary policy shocks as the first, second, and third elements of $\xi_t$ require the elements of $\tilde{\mathbf{L}}_t$ to have the sign patterns
$$\tilde{\mathbf{L}}_t = \begin{bmatrix} (+) & (+) & (-) \\ (-) & (+) & (-) \\ (?) & (+) & (+) \end{bmatrix}$$
if the gap variable is measured by the output gap or the real GDP growth and
$$\tilde{\mathbf{L}}_t = \begin{bmatrix} (+) & (-) & (-) \\ (+) & (+) & (+) \\ (?) & (-) & (+) \end{bmatrix}$$
if the gap variable is measured by the unemployment gap or unemployment rate. If these restrictions are not satisfied for any $t = 1, 2, \ldots, T$, the draws for $(\mathbf{A}^T, \mathbf{\Sigma}^T)$ and $\tilde{\mathbf{X}}$ are discarded and the algorithm returns to step one. If the restrictions are satisfied, then $\tilde{\mathbf{L}}_t$ is renormalized as $\tilde{\mathbf{L}}_t = \mathbf{C}_t^{-1}\mathbf{D}_t$, where $\mathbf{C}_t$ and $\mathbf{D}_t$ have the forms shown in (A.24) and (A.25), these draws are saved, and the Gibbs sampling algorithm moves on.

## A.5 Impulse Response and Forecast Error Variances Decomposition

Once draws are obtained for the structural parameters using one of three identification schemes, impulse responses can be generated from (A.26) after multiplying through by $\mathbf{C}_t^{-1}$. These computations can be simplified by writing the system in companion form as

$$\mathbf{Y}_t - \bar{\mu}_t = \mathbf{B}_{12,t}(\mathbf{Y}_{t-1} - \bar{\mu}_t) + \mathbf{F}_t \xi_t, \tag{A.28}$$

where

$$\mathbf{Y}_t = \begin{bmatrix} \mathbf{y}_t \\ \mathbf{y}_{t-1} \end{bmatrix},$$

$$\mathbf{B}_{12,t} = \begin{bmatrix} \mathbf{B}_{1,t} & \mathbf{B}_{2,t} \\ \mathbf{I}_3 & \mathbf{0}_{3,3} \end{bmatrix}, \tag{A.29}$$

$$\bar{\mu}_t = (\mathbf{I}_6 - \mathbf{B}_{12,t})^{-1} \begin{bmatrix} \mathbf{B}_t \\ \mathbf{0}_{3,1} \end{bmatrix}, \tag{A.30}$$

and

$$F_t = \begin{bmatrix} \mathbf{C}_t^{-1}\mathbf{D}_t \\ \mathbf{0}_{3,3} \end{bmatrix}. \tag{A.31}$$

Since (A.28) implies

$$\mathbf{Y}_{t+k} - \mathbb{E}_t\mathbf{Y}_{t+k} = \mathbf{F}_t\xi_{t+k} + \mathbf{B}_{12,t}\mathbf{F}_t\xi_{t+k-1} + \ldots + \mathbf{B}_{12,t}^{k-1}\mathbf{F}_t\xi_{t+1},$$

the $k$-step ahead forecast error variances for the elements of $\mathbf{Y}_t$ are

$$\mathbb{E}[(\mathbf{Y}_{t+k} - \mathbb{E}_t\mathbf{Y}_{t+k})(\mathbf{Y}_{t+k} - \mathbb{E}_t\mathbf{Y}_{t+k})'] = \mathbf{F}_t\mathbf{F}_t' + \mathbf{B}_{12,t}\mathbf{F}_t\mathbf{F}_t'\mathbf{B}_{12,t}' + \ldots + \mathbf{B}_{12,t}^{k-1}\mathbf{F}_t\mathbf{F}_t'(\mathbf{B}_{12,t}^{k-1})'. \tag{A.32}$$

Forecast error variances decompositions can be found by using (A.29), (A.31), and (A.32) to compute the total variances and then by using these same equations with the first two diagonal elements of $\mathbf{D}_t$ set equal to zero to find the variances attributable to monetary policy shocks alone.

## A.6 Counterfactual Monetary Policy Rules

The estimated VAR model with time-varying coefficients is used to propose different counterfactual scenarios. The aim is to investigate how changes in the conduct of monetary policy may have affected macroeconomic performances. Section 6 gives some counterfactuals based on empirical results. Counterfactual monetary policy rules $\tilde{R}_t^s$ are constructed according to different assumptions on parameters or policy shocks listed below, from 2007:4 onward. Otherwise, they follow the path of the estimated monetary policy rule given in equation (A.27). Running the TVP-VAR over the full sample period gives the path that would have followed inflation, output gap and the policy rate under these assumptions.

**2007:4 policy rule.** The first scenario consists in drawing the coefficients of the policy rule from the posterior distribution from 2007:4. Hence, both the time-varying intercept and policy parameters of the systematic

component of monetary policy are kept fixed from 2007:4 onward.

$$\tilde{R}_t^s = \begin{cases} \bar{\gamma}_{r,2007:4} + \bar{c}_{r\pi,2007:4}\Pi_t + \bar{\gamma}_{1,r\pi,2007:4}\Pi_{t-1} + \bar{\gamma}_{2,r\pi,2007:4}\Pi_{t-2} \\ \qquad +\bar{c}_{rg,2007:4}G_t + \bar{\gamma}_{1,rg,2007:4}G_{t-1} + \bar{\gamma}_{2,rg,2007:4}G_{t-2} & \text{if } t \geq 2007:4 \\ \qquad + \bar{\gamma}_{1,rr,2007:4}R_{t-1} + \bar{\gamma}_{2,rg,2007:4}R_{t-2} + \delta_{r,t}\xi_t^{mp} \\ R_t^s \text{ from equation (A.27)} & \text{otherwise} \end{cases}$$

**2007:4 policy rule and no policy shocks.** In the second scenario, the Taylor rule parameters are also drawn from their 2007:4 posterior distribution, and monetary policy shocks are assumed to be muted from 2007:4 forward. Hence, compared to the previous scenario, it is assumed that $\xi_t^{mp} = 0$.

$$\tilde{R}_t^s = \begin{cases} \bar{\gamma}_{r,2007:4} + \bar{c}_{r\pi,2007:4}\Pi_t + \bar{\gamma}_{1,r\pi,2007:4}\Pi_{t-1} + \bar{\gamma}_{2,r\pi,2007:4}\Pi_{t-2} \\ \qquad +\bar{c}_{rg,2007:4}G_t + \bar{\gamma}_{1,rg,2007:4}G_{t-1} + \bar{\gamma}_{2,rg,2007:4}G_{t-2} & \text{if } t \geq 2007:4 \\ \qquad + \bar{\gamma}_{1,rr,2007:4}R_{t-1} + \bar{\gamma}_{2,rg,2007:4}R_{t-2} \\ R_t^s \text{ from equation (A.27)} & \text{otherwise} \end{cases}$$

**No policy shocks.** The third counterfactual scenario reports results when monetary policy shocks are turned off from 2007:4 onward. Parameters are not kept fixed from 2007:4 in this case. However, policy shocks $\xi_t^{mp}$ are still set to 0.

$$\tilde{R}_t^s = \begin{cases} \gamma_{r,t} + c_{r\pi,t}\Pi_t + \gamma_{1,r\pi,t}\Pi_{t-1} + \gamma_{2,r\pi,t}\Pi_{t-2} \\ \qquad +c_{rg,t}G_t + \gamma_{1,rg,t}G_{t-1} + \gamma_{2,rg,t}G_{t-2} & \text{if } t \geq 2007:4 \\ \qquad + \gamma_{1,rr,t}R_{t-1}^s + \gamma_{2,rr,t}R_{t-2}^s \\ R_t^s \text{ from equation (A.27)} & \text{otherwise} \end{cases}$$

**2007:4 policy rule and volatility.** In a scenario presented in Appendix E, all the coefficients are drawn from the 2007:4 posterior distribution, including the volatility of monetary policy shocks $\delta_{r,t}$.

$$\tilde{R}_t^s = \begin{cases} \bar{\gamma}_{r,2007:4} + \bar{c}_{r\pi,2007:4}\Pi_t + \bar{\gamma}_{1,r\pi,2007:4}\Pi_{t-1} + \bar{\gamma}_{2,r\pi,2007:4}\Pi_{t-2} \\ \qquad +\bar{c}_{rg,2007:4}G_t + \bar{\gamma}_{1,rg,2007:4}G_{t-1} + \bar{\gamma}_{2,rg,2007:4}G_{t-2} & \text{if } t \geq 2007:4 \\ \qquad + \bar{\gamma}_{1,rr,2007:4}R_{t-1} + \bar{\gamma}_{2,rg,2007:4}R_{t-2} + \bar{\delta}_{r,2007:4}\xi_t^{mp} \\ R_t^s \text{ from equation (A.27)} & \text{otherwise} \end{cases}$$

**2007:4 volatility.** Another counterfactual scenario shown in Appendix E gives counterfactuals only in the case where the volatility coefficient $\delta_{r,t}$ is drawn from its 2007:4 posterior distribution, allowing the rest of policy rule parameters to be time-varying from 2007:4 forward.

$$\tilde{R}_t^s = \begin{cases} \gamma_{r,t} + c_{r\pi,t}\Pi_t + \gamma_{1,r\pi,t}\Pi_{t-1} + \gamma_{2,r\pi,t}\Pi_{t-2} \\ \qquad +c_{rg,t}G_t + \gamma_{1,rg,t}G_{t-1} + \gamma_{2,rg,t}G_{t-2} & \text{if } t \geq 2007:4 \\ \qquad + \gamma_{1,rr,t}R_{t-1}^s + \gamma_{2,rr,t}R_{t-2}^s + \bar{\delta}_{r,2007:4}\xi_t^{mp} \\ R_t^s \text{ from equation (A.27)} & \text{otherwise} \end{cases}$$

# B Shadow Taylor rules

Wu and Zhang (2019) argue that the shadow rate is a good proxy for monetary policy at the ZLB. For this purpose, they estimate a simple 'shadow Taylor rule' for the US using Wu and Xia's shadow rate (Wu and Xia, 2016).

This simple monetary policy rule takes the following form:

$$R_t^s = \alpha + \rho R_{t-1}^s + \beta_\Pi \Pi_t + \beta_G G_t + \varepsilon_t \tag{B.1}$$

where $\Pi_t$ is the inflation rate, $G_t$ is the output gap and $R_t^s$ is the shadow rate at period $t$, following the notation used in the TVP-VAR model. $\varepsilon_t$ is the error term, and can be interpreted as monetary policy shocks. $\alpha$ is an intercept. Also, and importantly, fixed parameters $\beta_\Pi$ and $\beta_G$ are the response coefficients on inflation and output gap, respectively. $\rho$ is the partial adjustment parameter that captures interest rate smoothing in central bank's behavior.

OLS estimation of equation (B.1) is used to construct shadow Taylor rates shown below.

Figure B.1: Shadow Taylor rules (Wu and Xia's shadow rate)

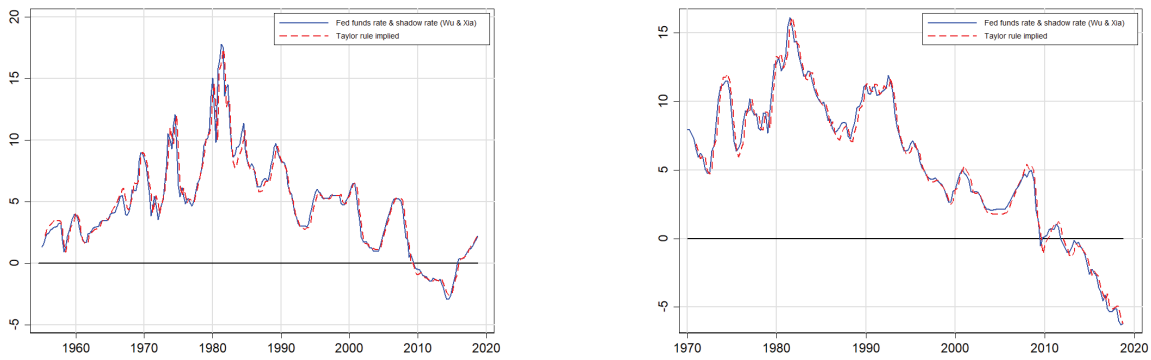


(a) US

(b) Euro area

*Note:* Based on "Wu, J. C., & Zhang, J. (2019). A shadow rate New Keynesian model. *Journal of Economic Dynamics and Control*, 107, 103728". US quarterly data from 1954:3 to 2018:4: Wu and Xia's shadow rate, GDP deflator, CBO output gap. Euro area quarterly data from 1971:1 to 2018:4 are Wu and Xia's shadow rate, HICP, estimated output gap.

As advocated by the authors, "the Taylor rule seems to be a good description of what actually happens, including the ZLB period". Using Wu and Xia's shadow rate (Figure B.1), the coefficient on inflation is 1.24 and the coefficient on output gap is 0.24 over the full US sample, consistent with the Taylor principle. For the euro area, the coefficient on inflation is 1.08 and the coefficient on output gap is 0.27.

Figure B.2: Shadow Taylor rules (Krippner's shadow rate)

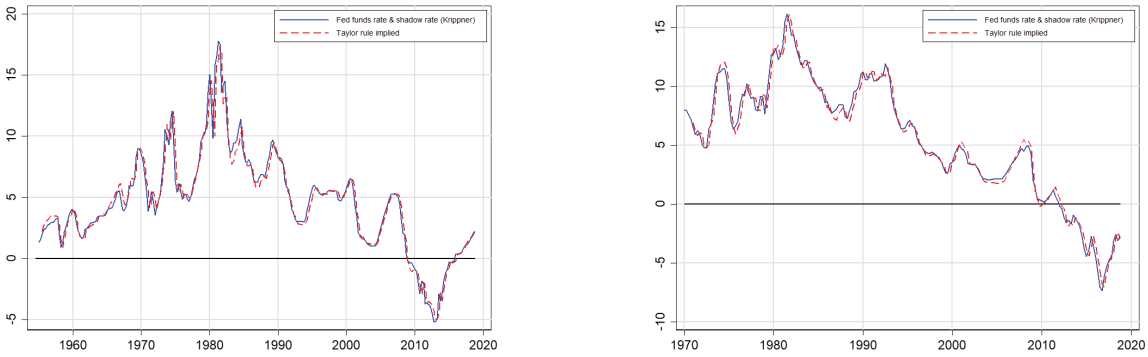


(a) US

(b) Euro area

*Note:* Based on "Wu, J. C., & Zhang, J. (2019). A shadow rate New Keynesian model. *Journal of Economic Dynamics and Control*, 107, 103728". US quarterly data from 1954:3 to 2018:4 are Krippner's shadow rate, GDP deflator, CBO output gap. Euro area quarterly data from 1971:1 to 2018:4 are Krippner's shadow rate, HICP, estimated output gap.

Using Krippner's shadow rate (Figure fig:shadowTR2), the coefficient on inflation is 1.27 and the coefficient on output gap is 0.31 over the full US sample. For the euro area, the coefficient on inflation is 1.10 and the coefficient on output gap is 0.30.

These results show that *(i)* the simple Taylor is a good description of the shadow rate dynamics, and that *(ii)* the response coefficients of the simple rule estimation seem to be robust to the choice of the shadow rate, as raised later in Appendix F.

# C Stability check for simple VAR analysis

## C.1 VAR stability

Times series models are usually assumed to be stable over time. Here, the stability of the simple VAR model is checked. First, let us consider a simple VAR(2) model in the form:

$$\mathbf{y}_t = \mathbf{b} + \mathbf{B}_1\mathbf{y}_{t-1} + \mathbf{B}_2\mathbf{y}_{t-2} + \mathbf{u}_t \tag{C.1}$$

where $\mathbf{y}_t = [\Pi_t \quad G_t \quad R_t^s]'$. Then, the companion form of the model can be given as:

$$\tilde{\mathbf{Y}}_t = \mathbf{B}_{12}\tilde{\mathbf{Y}}_{t-1} + \boldsymbol{\nu}_t \tag{C.2}$$

where

$$\tilde{\mathbf{Y}}_t = \begin{bmatrix} \tilde{\mathbf{y}}_t \\ \tilde{\mathbf{y}}_{t-1} \end{bmatrix} \tag{C.3}$$

with $\tilde{\mathbf{y}}_t$ the mean corrected element of $\mathbf{y}_t$,

$$\mathbf{B}_{12} = \begin{bmatrix} \mathbf{B}_1 & \mathbf{B}_2 \\ \mathbf{I}_3 & \mathbf{0}_{3,3} \end{bmatrix} \tag{C.4}$$

is the companion matrix, and

$$\boldsymbol{\nu}_t = \begin{bmatrix} \mathbf{u}_t \\ \mathbf{0}_{3,3} \end{bmatrix}. \tag{C.5}$$

The determinant defining the characteristic equation is defined as $\left|\mathbf{B}_{12} - \lambda\mathbf{I}\right| = \left|\lambda^2\mathbf{I} - \lambda\mathbf{B}_1 - \mathbf{B}_2\right| = 0$. Hence, the required condition for the stability of the system is that the roots of the previous equation must lie inside the unit circle. The figures showing the results are given below. The six roots lie inside the unit circle insuring the stability of the VAR.

Figure C.1: Roots of VAR(2) models

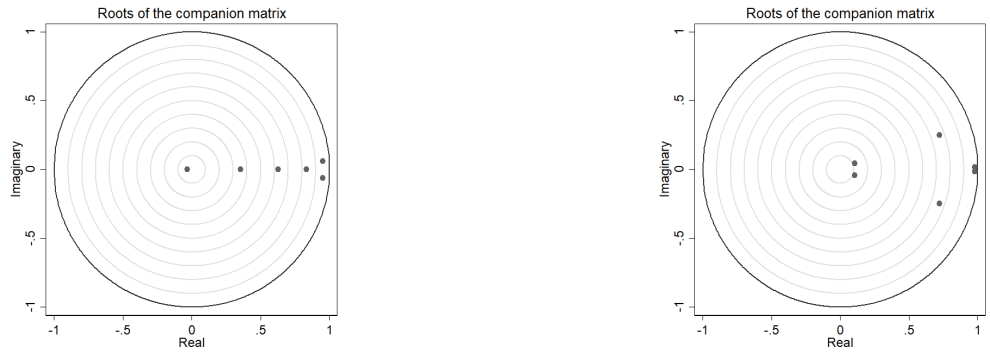


(a) US data

(b) Euro area data

## C.2 Rolling-window analysis for stability of parameters

A common assumption in time series analysis is that the coefficients are constant with respect to time. Checking for instability allows to assess whether the coefficients are time-invariant. A rolling-window analysis is used to check the stability of the VAR(2) model described above.

First, the size of the rolling window – the number of consecutive observations per rolling window – is set to $m = 40$, that is consistent with the size of the training sample used in the TVP-VAR (40 quarters, i.e. 10 years). Then, the number of increments between successive rolling windows is set to one quarter, in a way that the entire sample is divided into $N = T - m + 1$ subsamples, where $T$ is the sample size such that $t = 1, ..., T$.

Figure C.2 gives some insights on the path of coefficients running the VAR(2) with rolling-windows. The coefficients are subject to a high instability.

The use of the VAR model with time-varying parameters is justified by the instability of the coefficients from the VAR with rolling windows (i.e. fixed windows). More precisely, the first difference of each coefficient follows a random walk, validating the assumptions of the process that governs the dynamics of the time-varying coefficients in the TVP-VAR model. Moreover, it seems to be tricky to disentangle regime switches regarding the path of these coefficients on the estimation period. Hence, TVP-VAR estimation is an appropriate tool to investigate changes in the conduct of monetary policy over time. Note that the coefficients are also unstable when the monetary policy rule is estimated with OLS with rolling windows and sequential VAR estimation with recursive windows (i.e. increasing windows). The results are not reported here and are available upon request.

## C.3 Statistical tests for stability of parameters

Cogley and Sargent (2005) consider classical tests for variation in the parameters of their model. The purpose of this section is to apply some of those tests to US and euro area data used previously to give further insights on the stability of parameters.

Hence, one of the most prominent tests that can easily be implemented after fitting a VAR is the Wald test. It allows to compute the Wald lag-exclusion statistics to test the hypothesis that the endogenous variables at a given lag are jointly zero for each equation and for all equations jointly. Testing stability on an equation-by-equation basis, the hypothesis that all three endogenous variables have zero coefficients at the first lag can be rejected at the 1% level for the three equations. Similarly, we strongly reject the hypothesis that the coefficients on the first and second lags of the endogenous variables are zero in all three equations jointly. The results are not reported here and are available upon request.

Figure C.2: VAR(2) coefficients with rolling-windows

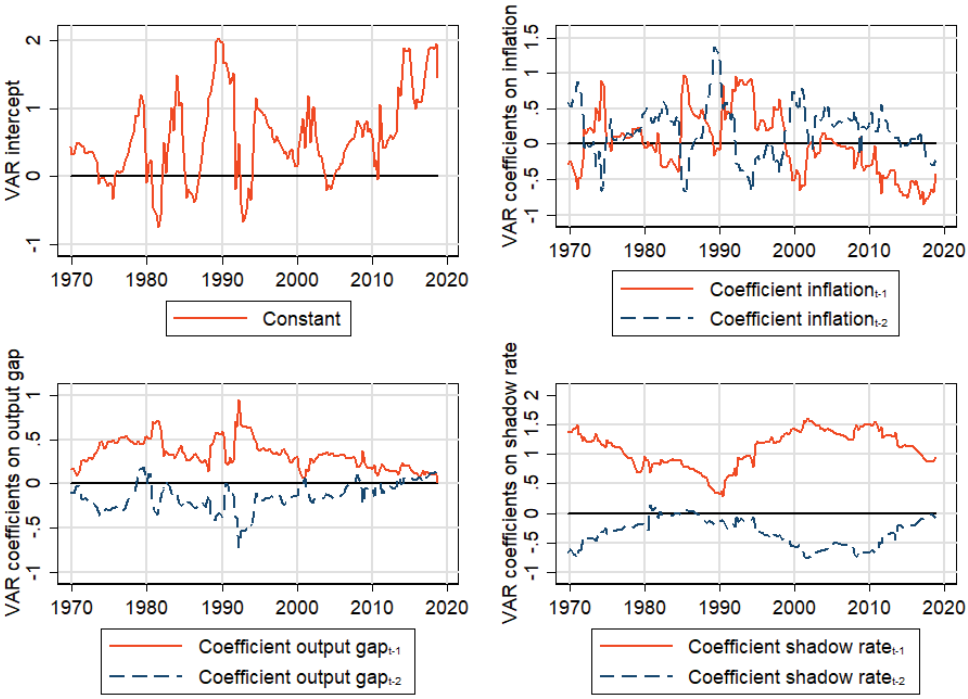


(a) US

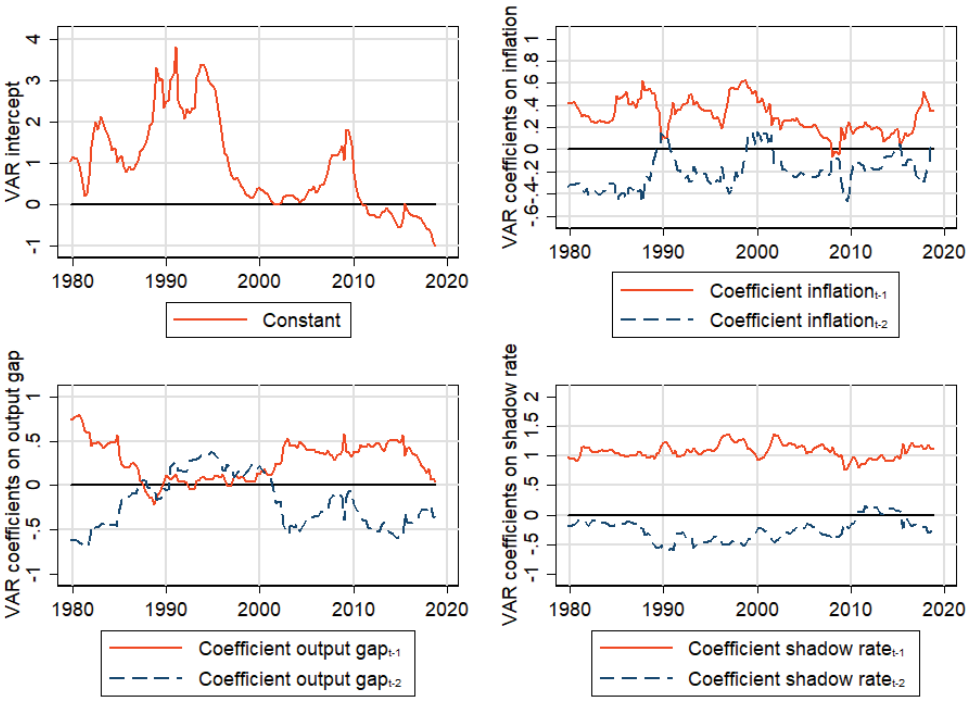


(b) Euro area

# D Tables

## D.1 Inefficiency factors

Table D.1: Inefficiency factors (US)

| | Median | Mean | Min. | Max. | 10th percentile | 90th percentile |
|---|---|---|---|---|---|---|
| 3150 Coefficients $\mathbf{B}^T$ | 5.00 | 5.36 | 1.92 | 6.75 | 2.81 | 6.20 |
| 450 Covariances $\mathbf{A}^T$ | 2.74 | 2.83 | 1.81 | 3.26 | 2.17 | 3.07 |
| 450 Volatilities $\mathbf{\Sigma}^T$ | 6.70 | 7.25 | 4.31 | 7.98 | 5.55 | 7.56 |
| 238 Hyperparameters $\mathbf{V}$ | 21.58 | 21.49 | 17.79 | 22.61 | 20.67 | 22.18 |

Table D.2: Inefficiency factors (Euro area)

| | Median | Mean | Min. | Max. | 10th percentile | 90th percentile |
|---|---|---|---|---|---|---|
| 3150 Coefficients $\mathbf{B}^T$ | 5.16 | 5.46 | 1.68 | 12.89 | 2.92 | 8.51 |
| 450 Covariances $\mathbf{A}^T$ | 2.64 | 2.91 | 1.81 | 6.70 | 2.08 | 4.05 |
| 450 Volatilities $\mathbf{\Sigma}^T$ | 7.08 | 7.64 | 4.83 | 16.18 | 5.68 | 9.88 |
| 238 Hyperparameters $\mathbf{V}$ | 20.51 | 20.45 | 17.84 | 22.48 | 19.45 | 21.42 |

## D.2 Descriptive statistics of the time-varying coefficients

Table D.3: Monetary policy rule parameters in the US (median coefficients)

| | 2009:1 | 2013:1 | 2017:1 |
|---|---|---|---|
| Impact coefficient on inflation | 0.81 | 1.33 | 0.40 |
| Impact coefficient on the output gap | 0.50 | 0.78 | 0.3 |
| Interest rate smoothing | 0.92 | 0.94 | 0.96 |
| Long-run coefficient on inflation | 1.86 | 2.52 | 2.05 |
| Long-run coefficient on output gap | 1.29 | 1.70 | 1.94 |
| Monetary policy shock volatility | 0.74 | 0.97 | 0.20 |

Table D.4: Monetary policy rule parameters in the US (mean of median coefficients)

| | 1970:1 - 2018:4 | | 1995:1 - 2018:4 | | |
|---|---|---|---|---|---|
| | Full sample | $< 2008{:}1$ | Full sample | $< 2008{:}1$ | $\geq 2008{:}1$ |
| Impact coefficient on inflation | 0.95 | 0.97 | 0.80 | 0.73 | 0.88 |
| Impact coefficient on the output gap | 0.50 | 0.47 | 0.45 | 0.35 | 0.58 |
| Interest rate smoothing | 0.95 | 0.95 | 0.93 | 0.93 | 0.94 |
| Long-run coefficient on inflation | 1.87 | 1.78 | 1.95 | 1.74 | 2.19 |
| Long-run coefficient on output gap | 1.28 | 1.16 | 1.40 | 1.18 | 1.66 |
| Monetary policy shock volatility | 0.73 | 0.75 | 0.45 | 0.29 | 0.64 |

Table D.5: Monetary policy rule parameters in the euro area (median coefficients)

| | 2009:1 | 2013:1 | 2017:1 |
|---|---|---|---|
| Impact coefficient on inflation | 0.58 | 0.72 | 0.92 |
| Impact coefficient on the output gap | 0.51 | 0.88 | 1.50 |
| Interest rate smoothing | 0.91 | 0.92 | 0.94 |
| Long-run coefficient on inflation | 1.65 | 2.11 | 2.52 |
| Long-run coefficient on output gap | 0.98 | 1.35 | 1.84 |
| Monetary policy shock volatility | 0.43 | 0.57 | 0.82 |

Table D.6: Monetary policy rule parameters in the euro area (mean of median coefficients)

| | 1981:1 - 2018:4 | | 1995:1 - 2018:4 | | |
|---|---|---|---|---|---|
| | Full sample | $< 2008{:}1$ | Full sample | $< 2008{:}1$ | $\geq 2008{:}1$ |
| Impact coefficient on inflation | 0.70 | 0.67 | 0.62 | 0.50 | 0.75 |
| Impact coefficient on the output gap | 0.68 | 0.54 | 0.77 | 0.56 | 1.02 |
| Interest rate smoothing | 0.90 | 0.89 | 0.91 | 0.90 | 0.92 |
| Long-run coefficient on inflation | 1.38 | 1.08 | 1.68 | 1.31 | 2.12 |
| Long-run coefficient on output gap | 1.56 | 1.60 | 1.37 | 1.30 | 1.46 |
| Monetary policy shock volatility | 0.47 | 0.41 | 0.45 | 0.30 | 0.62 |

# E Figures

## E.1 Long-run coefficients and full sample (baseline estimation)

Figure E.1: Interest rate smoothing and long-run coefficients from the estimated monetary policy rule

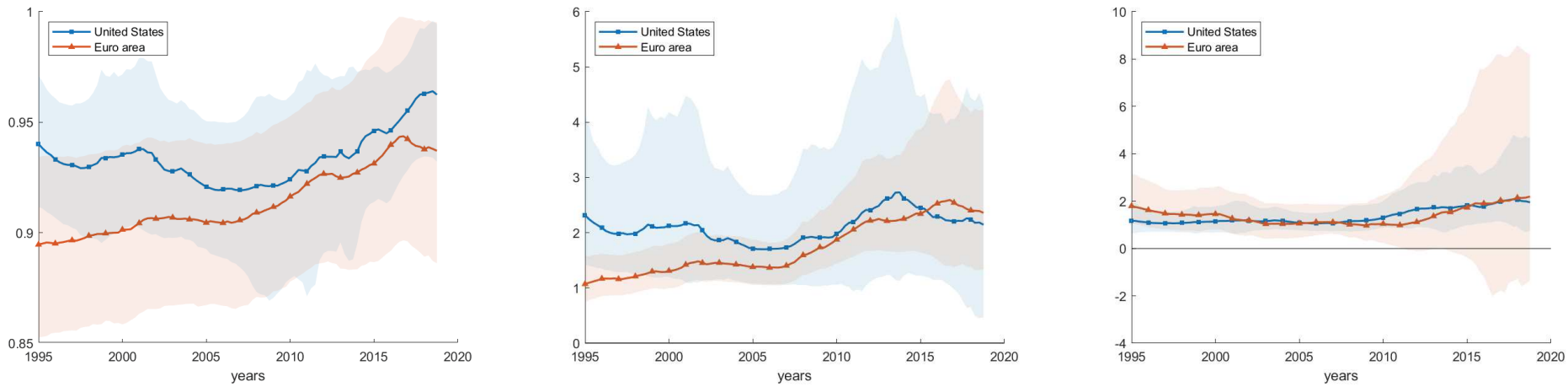


(a) Interest rate smoothing

(b) Long-run coefficient on inflation

(c) Long-run coefficient on output gap

*Note:* Interest rate smoothing is given by the sum $\gamma_{1,rr,t}+\gamma_{2,rr,t}$, and long-run coefficients on inflation and output gap are respectively given by $(c_{r\pi,t}+\gamma_{1,r\pi,t}+\gamma_{2,r\pi,t})/(1-\gamma_{1,rr,t}-\gamma_{2,rr,t})$ and $(c_{rg,t}+\gamma_{1,rg,t}+\gamma_{2,rg,t})/(1-\gamma_{1,rr,t}-\gamma_{2,rr,t})$ in equation (3). Median (solid lines) and 68% credible interval (shaded areas) of the posterior distribution of coefficients are plotted for each indicated variable.

Figure E.2: Contemporaneous coefficients from the estimated monetary policy rule and monetary policy shock volatility (full sample)

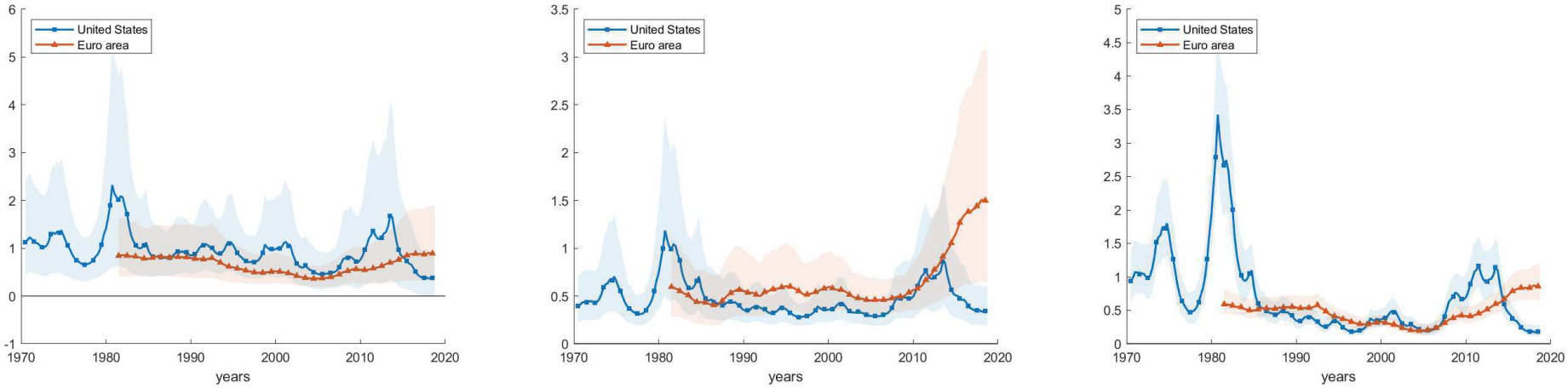


(a) Contemporaneous coefficient on inflation

(b) Contemporaneous coefficient on output gap

(c) Monetary policy shock volatility

*Note:* Contemporaneous coefficients on inflation and output gap are respectively given by $c_{r\pi,t}$ and $c_{rg,t}$, and the volatility of monetary policy shocks is captured by $\delta_{r,t}$ in equation (3). Median (solid lines) and 68% credible interval (shaded areas) of the posterior distribution of coefficients are plotted for each indicated variable.

Figure E.3: Interest rate smoothing and long-run coefficients from the estimated monetary policy rule (full sample)

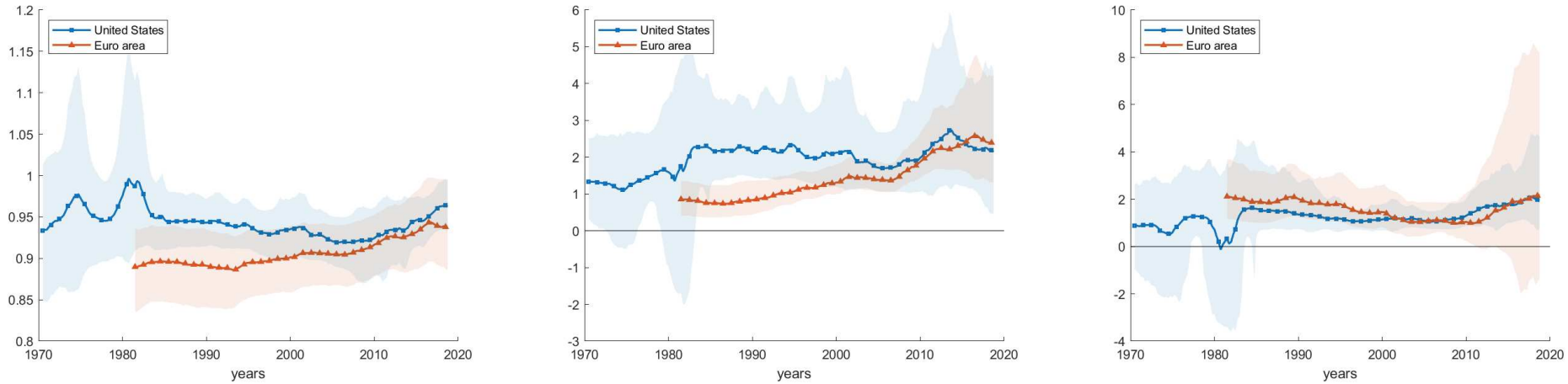


(a) Interest rate smoothing

(b) Long-run coefficient on inflation

(c) Long-run coefficient on output gap

*Note:* Interest rate smoothing is given by the sum $\gamma_{1,rr,t}+\gamma_{2,rr,t}$, and long-run coefficients on inflation and output gap are respectively given by $(c_{r\pi,t}+\gamma_{1,r\pi,t}+\gamma_{2,r\pi,t})/(1-\gamma_{1,rr,t}-\gamma_{2,rr,t})$ and $(c_{rg,t}+\gamma_{1,rg,t}+\gamma_{2,rg,t})/(1-\gamma_{1,rr,t}-\gamma_{2,rr,t})$ in equation (3). Median (solid lines) and 68% credible interval (shaded areas) of the posterior distribution of coefficients are plotted for each indicated variable.

## E.2 Counterfactual analysis (baseline estimation)

Figure E.4: Counterfactual simulations (US)

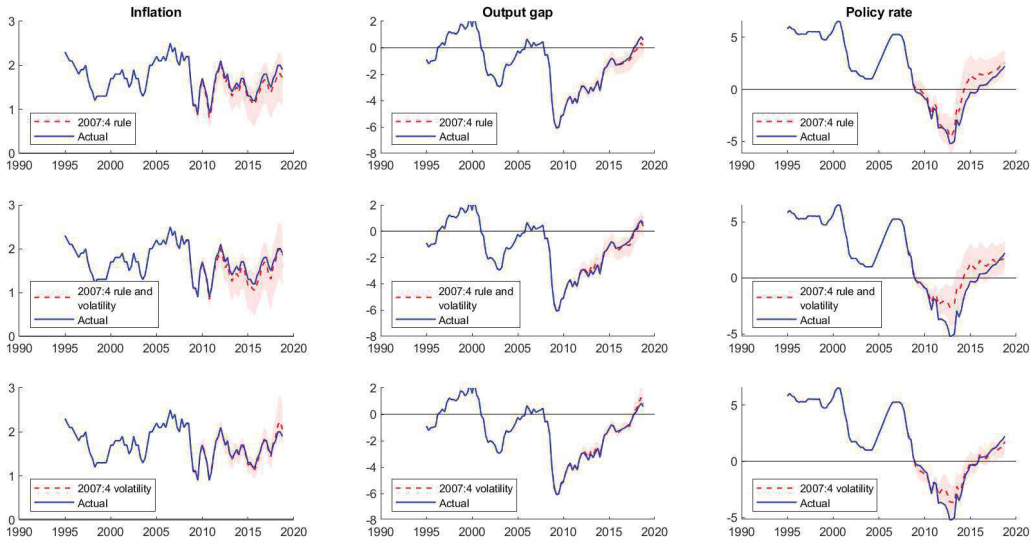


*Note:* Median counterfactual path (red dashed lines) and 68% credible interval (red shaded areas) are plotted for each indicated variable.

Figure E.5: Counterfactual simulations (Euro area)

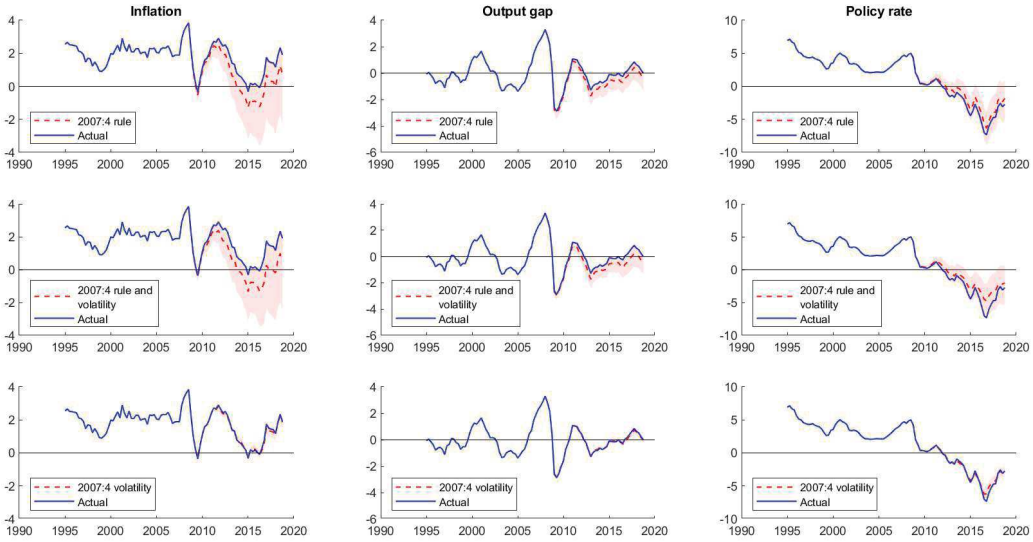


*Note:* Median counterfactual path (red dashed lines) and 68% credible interval (red shaded areas) are plotted for each indicated variable.

# F Robustness checks

## F.1 Shadow rate (Wu and Xia, 2016)

The model is re-estimated with the shadow rate extracted from Wu and Xia (2016).[18] As discussed previously in this paper, this shadow rate follows a different path than Krippner; Krippner's (2013; 2019) shadow short rate (Figure F.1)

Figure F.1: Shadow rates

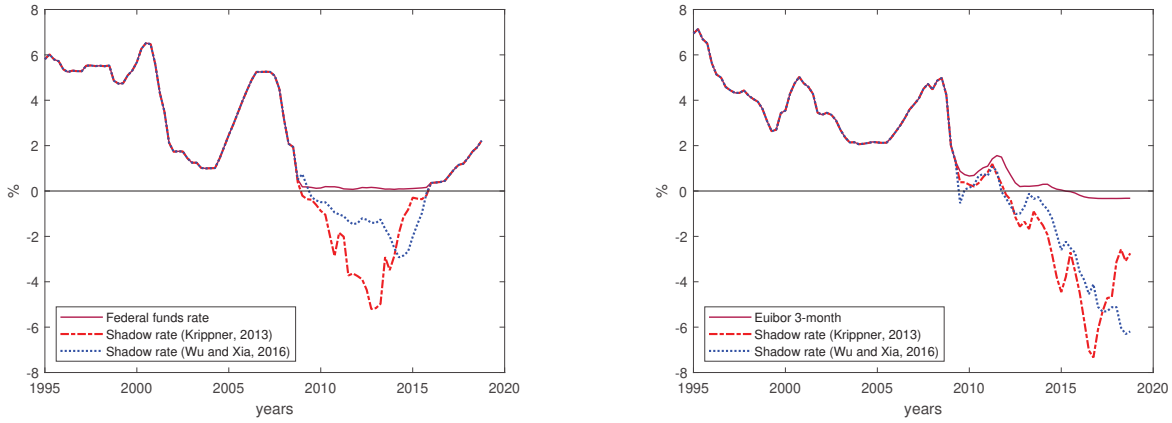


(a) US

(b) Euro area

Short and long-run coefficients are given by the following figures (Figure F.2 and Figure F.3). Although the tables containing median coefficients are not reported here, it can be graphically deduced that the path of the coefficients from the model estimated with Wu and Xia's shadow rate are quite the same than the model estimated with Krippner's shadow rate, except concerning the peak after the 2008 crisis. Whereas the estimation with Krippner's shadow short rate gives contemporaneous coefficients at a level similar to the one observed in the early 1980s, the estimation with Wu and Xia's shadow rate gives post-crisis short-run coefficients without any obvious significant change during this period. However, the results seem to be robust to the shadow rate specification when considering the volatility of monetary policy shocks, interest rate smoothing and long-term coefficients on inflation and output.

[18]The US shadow rate data are available on Jing Cynthia Wu's webpage. I am very grateful to her for providing euro area shadow rate data.

Figure F.2: Contemporaneous coefficients from the estimated monetary policy rule and monetary policy shock volatility (Wu and Xia's shadow rate)

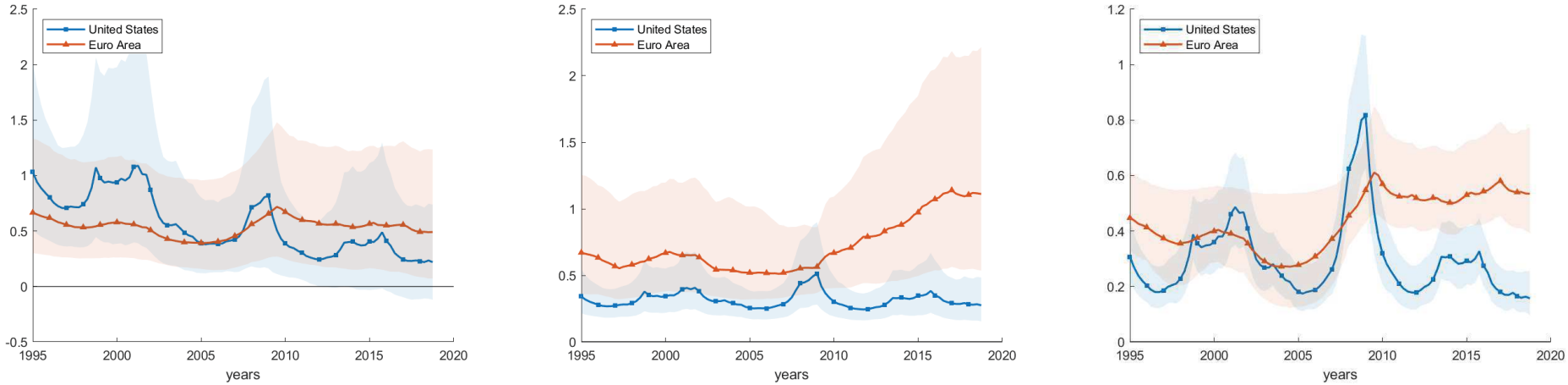


(a) Contemporaneous coefficient on inflation

(b) Contemporaneous coefficient on output gap

(c) Monetary policy shock volatility

*Note:* Contemporaneous coefficients on inflation and output gap are respectively given by $c_{r\pi,t}$ and $c_{rg,t}$, and the volatility of monetary policy shocks is captured by $\delta_{r,t}$ in equation (3). Median (solid lines) and 68% credible interval (shaded areas) of the posterior distribution of coefficients are plotted for each indicated variable.

Figure F.3: Interest rate smoothing and long-run coefficients from the estimated monetary policy rule (Wu and Xia's shadow rate)

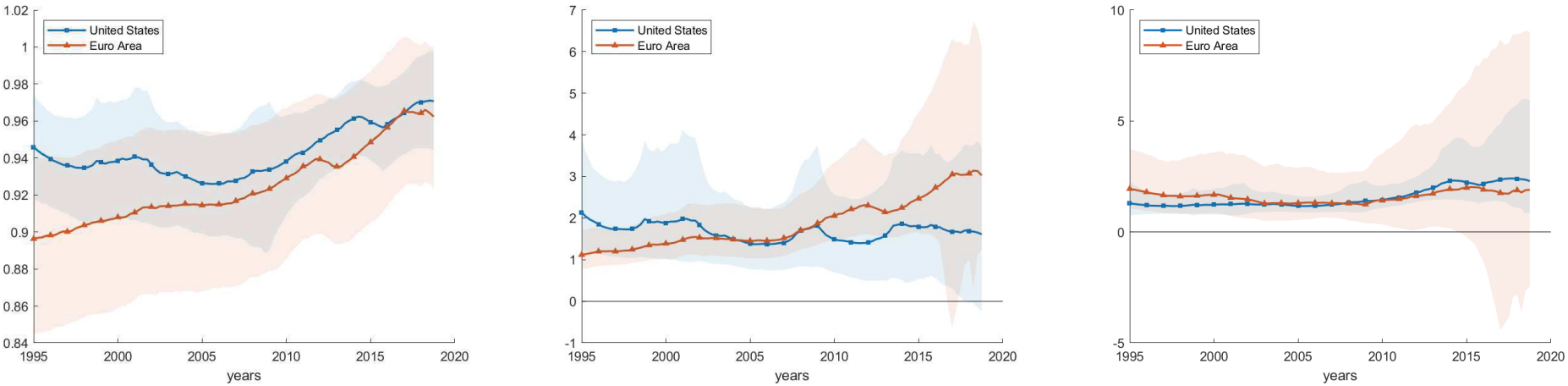


(a) Interest rate smoothing

(b) Long-run coefficient on inflation

(c) Long-run coefficient on output gap

*Note:* Interest rate smoothing is given by the sum $\gamma_{1,rr,t}+\gamma_{2,rr,t}$, and long-run coefficients on inflation and output gap are respectively given by $(c_{r\pi,t}+\gamma_{1,r\pi,t}+\gamma_{2,r\pi,t})/(1-\gamma_{1,rr,t}-\gamma_{2,rr,t})$ and $(c_{rg,t}+\gamma_{1,rg,t}+\gamma_{2,rg,t})/(1-\gamma_{1,rr,t}-\gamma_{2,rr,t})$ in equation (3). Median (solid lines) and 68% credible interval (shaded areas) of the posterior distribution of coefficients are plotted for each indicated variable.

## F.2 Alternative measures of inflation and business cycle proxies

Alternative specification of the estimated monetary policy rule are run over the sample. The robustness of the results are tested with different series of ex-post inflation (including GDP deflator for the US and for the euro area, CPI and headline PCE price index only for the US) and ex-post proxies for real activity (including real GDP growth and unemployment rate for the US and for the euro area, unemployment gap for the US and estimated output gap using Christiano and Fitzgerald (2003) bandpass filter for the euro area). The path of estimated response coefficients are robust to other inflation series and real activity proxies, especially for the volatility of monetary policy shocks.

As made clear by Orphanides (2001, 2003, 2004), real-time and forecast data should also be used in the estimates. Such data are available for the US over a long timespan.[19] However, estimates for the euro area with real-time and forecast data are hardly possible because of the lack of observation due to the need for at least 10 years of training sample to calibrate the prior distribution of the time-varying coefficients. This is incompatible with the relatively short period of time covered by those datasets.[20] Hence, to make the comparison between Fed and ECB monetary policy possible, only historical ex-post data are used in the TVP-VAR specification presented in this paper. Croushore and Evans (2006) show that the use of revised data is not a serious limitation for the analysis of monetary policy shocks in recursively identified VARs. However, note that Amir-Ahmadi et al. (2017) employ a TVP-VAR and show that impulse reponses to monetary policy shocks is stronger using final data instead of real-time data.

Following Okun's law (Okun, 1962), output gap or real GDP growth are replaced by unemployment gap[21] or simply unemployment rate in the estimate. As a consequence, the strategy based on sign restriction on impulse responses used to identify structural shocks has to be slightly modified as follows:

Table F.1: Sign restrictions on the impact effects of structural shocks

| Impact effect on | Structural shocks | | |
|---|---|---|---|
| | Aggregate supply | Aggregate demand | Monetary policy |
| Inflation | + | + | - |
| Unemployment rate/gap | + | - | + |
| Shadow rate | ? | + | + |

*Note:* The symbol ? indicates that the response is left unconstrained.

Proxied by unemployment rate or gap, real activity is assumed to react positively to aggregate supply shocks, negatively to aggregate demand shocks and positively to monetary policy shocks. Note also that sign restrictions on impulse responses are the same than those presented in Table 1 when considering real GDP growth instead of output gap in the empirical procedure.

[19] Real-time data in the US are reported by the Federal Reserve Bank of Philadelphia in the Real-Time Data Set for Macroeconomists, and forecast data are reported in the Survey of Professional Forecasters.

[20] The ECB real-time database (RTD) begins in 1995:1, and the ECB Survey of Professional Forecasters (SPF) only begins in 1999:1.

[21] Unemployment gap is constructed following the formula $u_t^{gap} = u_t - \bar{u}_t$ , where $u_t$ is the unemployment rate and $\bar{u}_t$ is the estimated non-accelerating inflation rate of unemployment (NAIRU) at time $t$.

Figure F.4: Contemporaneous coefficients from the estimated monetary policy rule and monetary policy shock volatility (GDP deflator and real GDP growth)

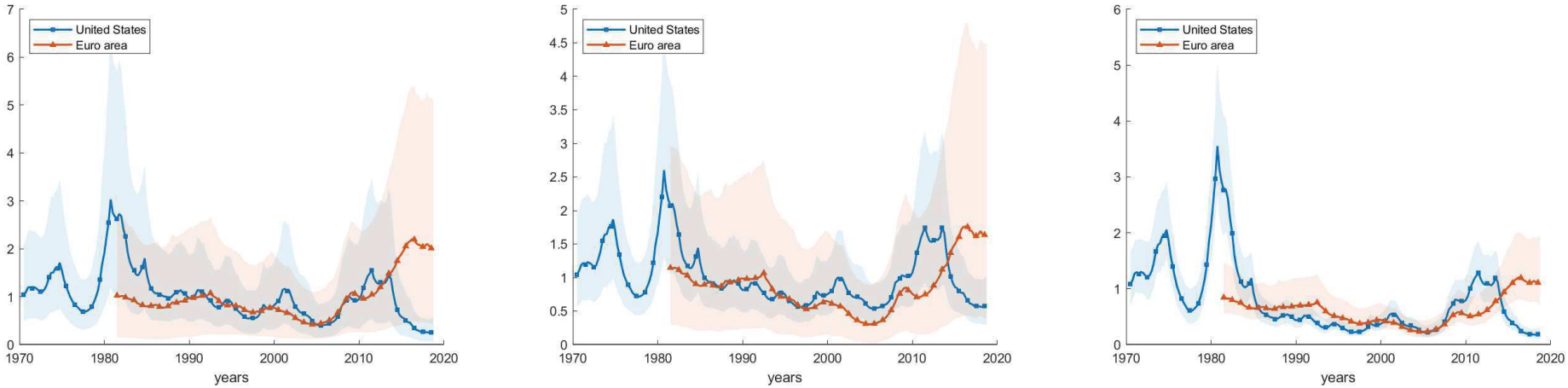


(a) Contemporaneous coefficient on inflation (GDP deflator) (b) Contemporaneous coefficient on real GDP growth (c) Monetary policy shock volatility

*Note:* Contemporaneous coefficients on inflation and real GDP growth are respectively given by $c_{r\pi,t}$ and $c_{rg,t}$, and the volatility of monetary policy shocks is captured by $\delta_{r,t}$ in equation (3). Median (solid lines) and 68% credible interval (shaded areas) of the posterior distribution of coefficients are plotted for each indicated variable.

Figure F.5: Interest rate smoothing and long-run coefficients from the estimated monetary policy rule (GDP deflator and real GDP growth)

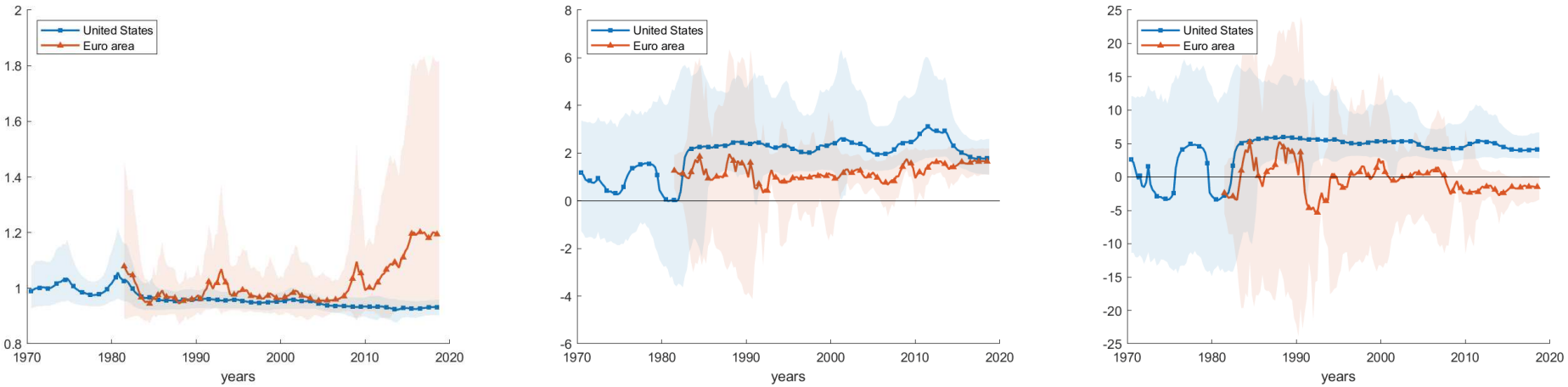


(a) Interest rate smoothing (b) Long-run coefficient on inflation (GDP deflator) (c) Long-run coefficient on real GDP growth

*Note:* Interest rate smoothing is given by the sum $\gamma_{1,rr,t}+\gamma_{2,rr,t}$, and long-run coefficients on inflation and real GDP growth are respectively given by $(c_{r\pi,t}+\gamma_{1,r\pi,t}+\gamma_{2,r\pi,t})/(1-\gamma_{1,rr,t}-\gamma_{2,rr,t})$ and $(c_{rg,t}+\gamma_{1,rg,t}+\gamma_{2,rg,t})/(1-\gamma_{1,rr,t}-\gamma_{2,rr,t})$ in equation (3). Median (solid lines) and 68% credible interval (shaded areas) of the posterior distribution of coefficients are plotted for each indicated variable.

Figure F.6: Contemporaneous coefficients from the estimated monetary policy rule and monetary policy shock volatility (CPI/HICP and unemployment rate)

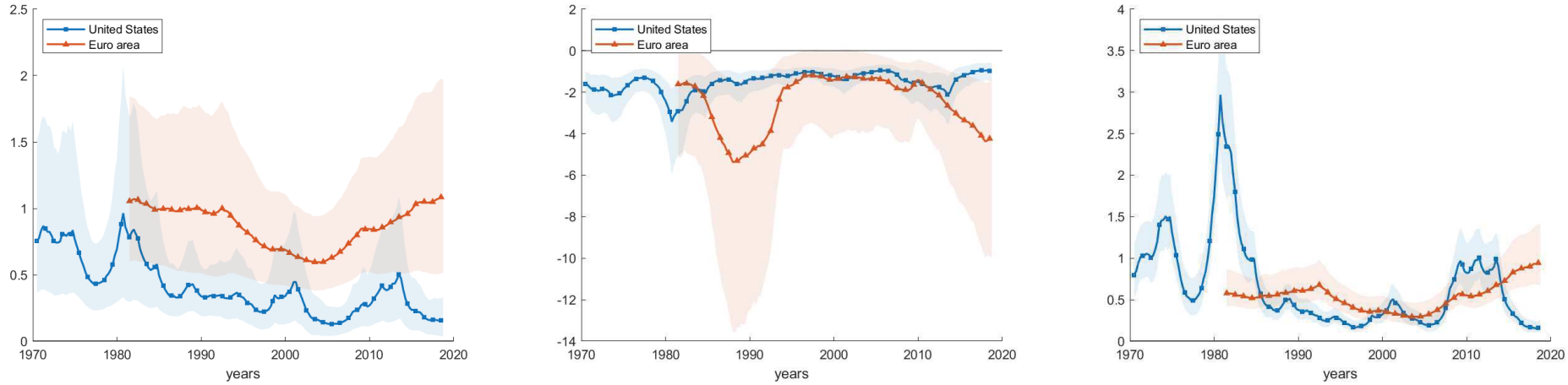


(a) Contemporaneous coefficient on inflation (b) Contemporaneous coefficient on unemployment rate (c) Monetary policy shock volatility

*Note:* Contemporaneous coefficients on inflation and unemployment rate are respectively given by $c_{r\pi,t}$ and $c_{rg,t}$, and the volatility of monetary policy shocks is captured by $\delta_{r,t}$ in equation (3). Median (solid lines) and 68% credible interval (shaded areas) of the posterior distribution of coefficients are plotted for each indicated variable.

Figure F.7: Interest rate smoothing and long-run coefficients from the estimated monetary policy rule (CPI/HICP and unemployment rate)

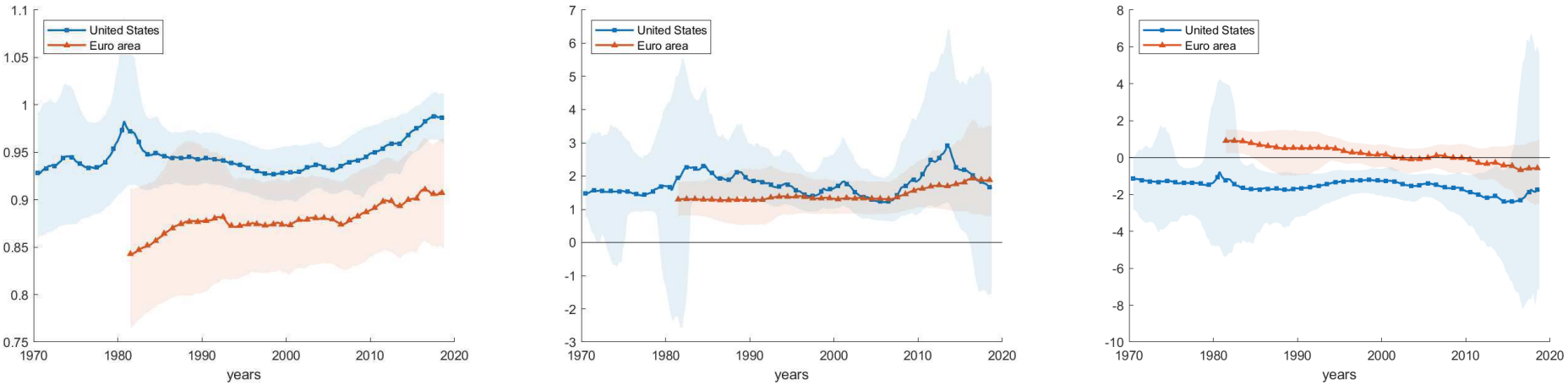


(a) Interest rate smoothing (b) Long-run coefficient on inflation (c) Long-run coefficient on unemployment rate

*Note:* Interest rate smoothing is given by the sum $\gamma_{1,rr,t}+\gamma_{2,rr,t}$, and long-run coefficients on inflation and unemployment rate are respectively given by $(c_{r\pi,t}+\gamma_{1,r\pi,t}+\gamma_{2,r\pi,t})/(1-\gamma_{1,rr,t}-\gamma_{2,rr,t})$ and $(c_{rg,t}+\gamma_{1,rg,t}+\gamma_{2,rg,t})/(1-\gamma_{1,rr,t}-\gamma_{2,rr,t})$ in equation (3). Median (solid lines) and 68% credible interval (shaded areas) of the posterior distribution of coefficients are plotted for each indicated variable.

Figure F.8: Contemporaneous coefficients from the estimated monetary policy rule and monetary policy shock volatility in the US (PCE and unemployment gap)

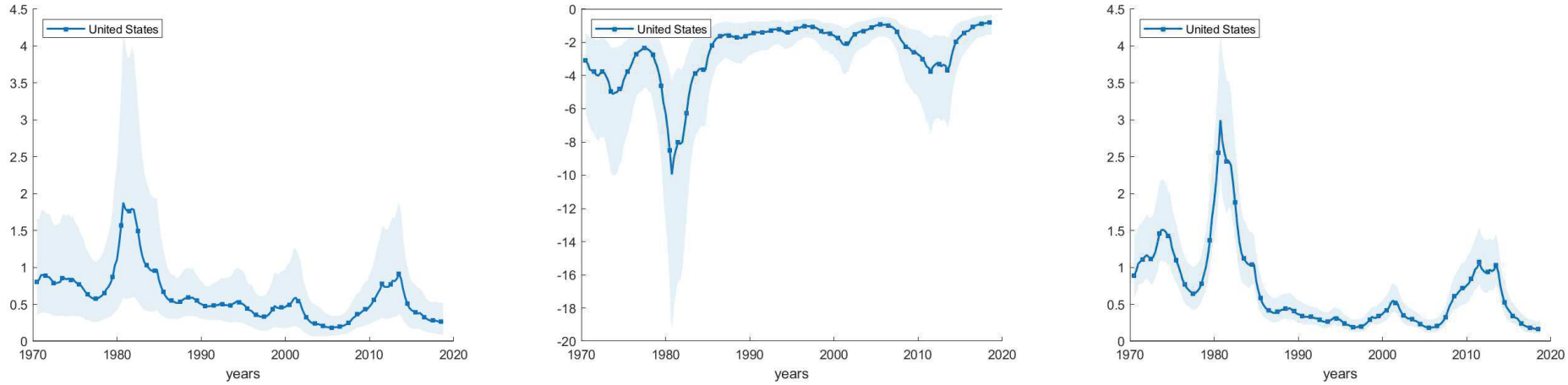


(a) Contemporaneous coefficient on inflation (PCE) (b) Contemporaneous coefficient on unemployment gap (c) Monetary policy shock volatility

*Note:* Contemporaneous coefficients on inflation and unemployment gap are respectively given by $c_{r\pi,t}$ and $c_{rg,t}$, and the volatility of monetary policy shocks is captured by $\delta_{r,t}$ in equation (3). Median (solid lines) and 68% credible interval (shaded areas) of the posterior distribution of coefficients are plotted for each indicated variable.

Figure F.9: Interest rate smoothing and long-run coefficients from the estimated monetary policy rule in the US (PCE and unemployment gap)

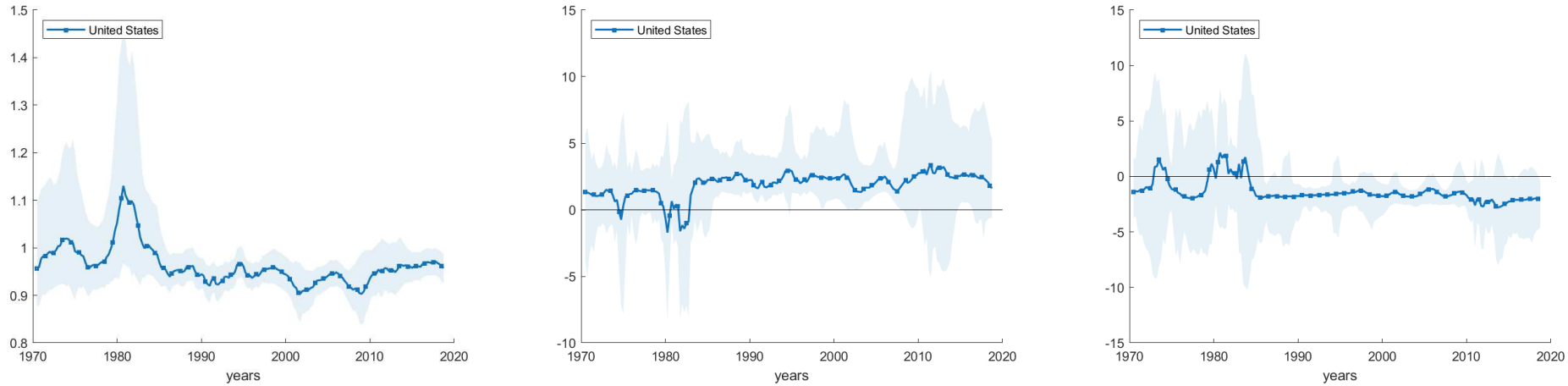


(a) Interest rate smoothing (b) Long-run coefficient on inflation (PCE) (c) Long-run coefficient on unemployment gap

*Note:* Interest rate smoothing is given by the sum $\gamma_{1,rr,t}+\gamma_{2,rr,t}$, and long-run coefficients on inflation and unemployment gap are respectively given by $(c_{r\pi,t}+\gamma_{1,r\pi,t}+\gamma_{2,r\pi,t})/(1-\gamma_{1,rr,t}-\gamma_{2,rr,t})$ and $(c_{rg,t}+\gamma_{1,rg,t}+\gamma_{2,rg,t})/(1-\gamma_{1,rr,t}-\gamma_{2,rr,t})$ in equation (3). Median (solid lines) and 68% credible interval (shaded areas) of the posterior distribution of coefficients are plotted for each indicated variable.

## Estimating real potential GDP in the euro area with filters

Although it has been universally used in macroeconomics, the Hodrick-Prescott filter may be subject to criticism. According to Hamilton (2018), the HP filter is not a reliable tool to decompose series into a trend and a cycle component, because it introduces spurious dynamic relations and have no basis in the true data-generating process. Therefore, I propose alternative filtering methods commonly used in macroeconomics to estimate euro area real potential GDP. For this purpose, real potential GDP in the euro area is estimated with filtering methods based on Christiano and Fitzgerald (2003), Baxter and King (1999), and following Hamilton (2018) more recently. As a reminder, I briefly give the conceptual framework of Hodrick and Prescott (1997), and raise potential issues implied by the use of the HP filter. Then, other filters are discussed and used to test the robustness of the results.

In accordance with Hodrick and Prescott's (1997) notations, a given time series $y_t$ may be decomposed into a growth (or trend) component $g_t$ and a cyclical component $c_t$ such that:

$y_t = g_t + c_t$

for $t = 1, \dots, T$. As for any filtering methods, the aim of the HP filter is to give a measure of smoothness of the $\{g_t\}$ path. In Hodrick and Prescott (1997), the growth component is determined by the resolution of the following optimization program:

$$\underset{\{g_t\}_{t=-1}^{T}}{\text{Min}} \left\{ \sum_{t=1}^{T} \underbrace{(y_t - g_t)}_{=c_t}^2 + \lambda \sum_{t=1}^{T} [(g_t - g_{t-1}) - (g_{t-1} - g_{t-2})]^2 \right\} \tag{F.1}$$

where $\lambda > 0$ is a 'smoothing parameter' which penalizes variations in the growth component. The larger the value of $\lambda$, the smoother is the trend. As a rule of thumb, it is commonly set to 1600 for quarterly data.

However, as highlighted by Hamilton (2018), the HP filter suffers from an end-point bias, and filtered values at the end of the sample are also characterized by spurious dynamics. Also, the author advocates that the value of $\lambda$ should be data-consistent instead of being calibrated to $\lambda = 1600$ for quarterly data. Hence, Hamilton (2018) suggests an alternative statistical procedure, and proposes running an OLS regression of $y_{t+h}$ on a constant and on the four more recent values as of date $t$ to offer a robust alternative to HP filter:

$$y_{t+h} = \underbrace{\beta_0 + \beta_1 y_t + \beta_2 y_{t-1} + \beta_3 y_{t-2} + \beta_4 y_{t-3}}_{\text{trend component}} + \underbrace{\upsilon_{t+h}}_{\substack{\text{cycle} \\ \text{component}}} \tag{F.2}$$

Hamilton (2018) advocates that for large samples, OLS estimates of equation (F.2) converge to $\beta_1 = 1$ and $\beta_i = 0$ for $i = 0, 2, 3, 4$, and can therefore be written:

$$y_{t+h} = \underbrace{y_t}_{\substack{\text{trend} \\ \text{component}}} + \underbrace{\upsilon_{t+h}}_{\substack{\text{cycle} \\ \text{component}}} \tag{F.3}$$

that gives how much the series $y_{t+h}$ change over a given $h$ horizon.

Euro area output gaps implied by filtered real GDP based on Hamilton's (2018) procedure are presented in the following Figure F.10.

Figure F.10: Regression and 8-quarter-change filters applied to euro area real GDP following Hamilton (2018)

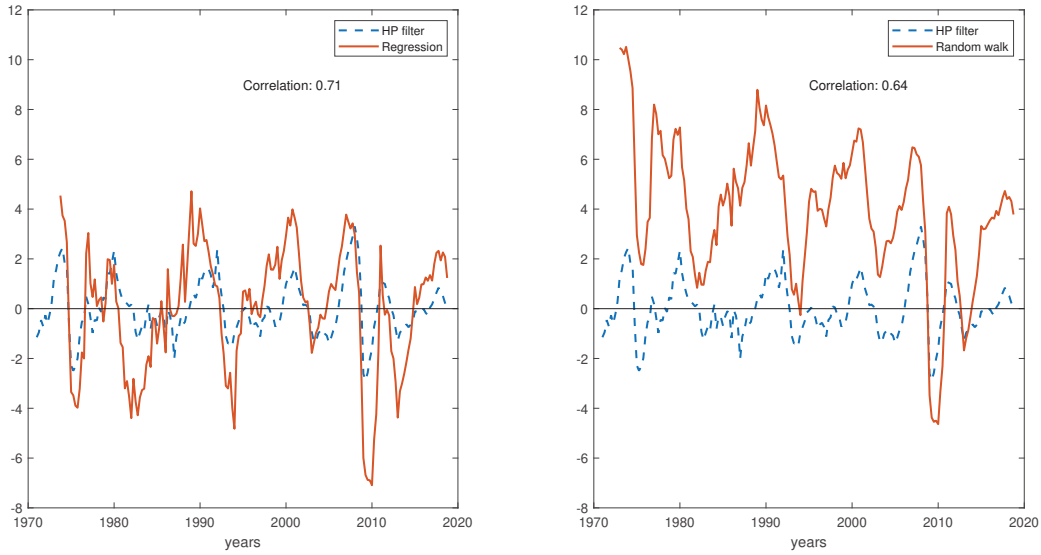


*Note:* Dashed line shows euro area output gap constructed with real potential GDP estimated by an Hodrick-Prescott filter. Left: solid line plots $v_t = y_t - \hat{\beta}_0 - \hat{\beta}_1 y_{t-8} - \hat{\beta}_2 y_{t-9} - \hat{\beta}_3 y_{t-10} - \hat{\beta}_4 y_{t-11}$, following equation (F.2). Right: solid line plots $v_t = y_t - y_{t-8}$, following equation (F.3).

Other filtering methods have been widely used in empirical macroeconomics, such as Baxter and King (1999) or Christiano and Fitzgerald (2003) (see Figure F.11).

Figure F.11: Band-pass filters applied to euro area real GDP

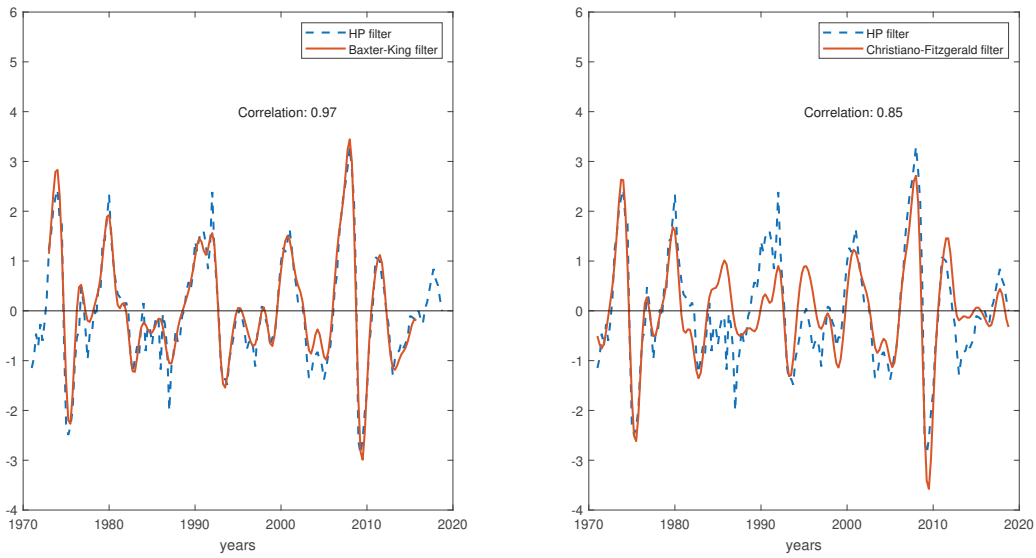


*Note:* Dashed line shows euro area output gap constructed with real potential GDP estimated by an Hodrick-Prescott filter. Left: solid line plots the cyclical component of euro area real GDP is obtained using a Baxter and King (1999) filter. Right: solid line plots the cyclical component of euro area real GDP is obtained using a Christiano and Fitzgerald (2003) filter.

Figure F.12: Contemporaneous coefficients from the estimated monetary policy rule and monetary policy shock volatility in the euro area (HICP and output gap)

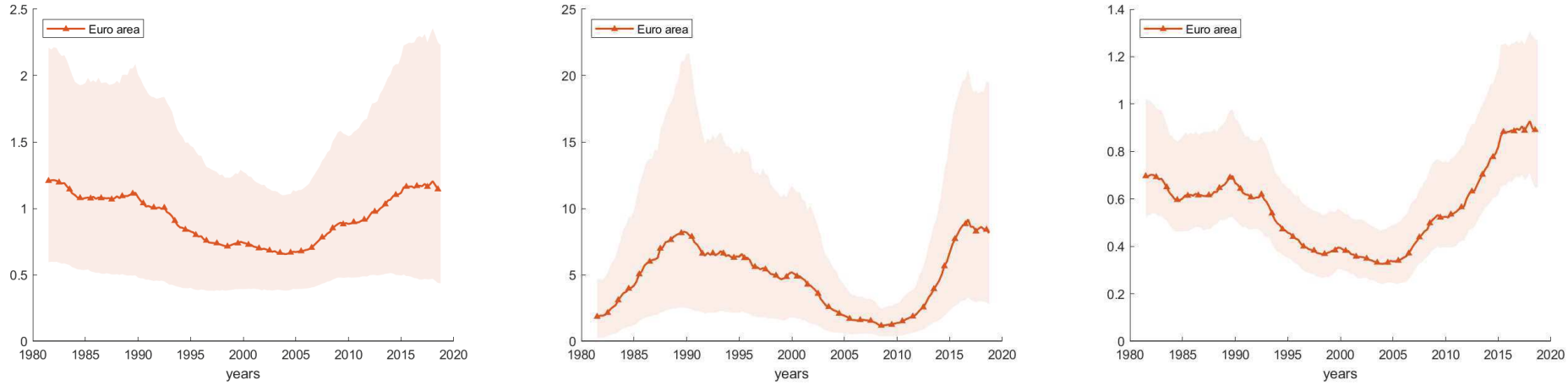


(a) Contemporaneous coefficient on inflation (HICP)

(b) Contemporaneous coefficient on output gap (bandpass filter)

(c) Monetary policy shock volatility

*Note:* Contemporaneous coefficients on inflation and output gap are respectively given by $c_{r\pi,t}$ and $c_{rg,t}$, and the volatility of monetary policy shocks is captured by $\delta_{r,t}$ in equation (3). Median (solid lines) and 68% credible interval (shaded areas) of the posterior distribution of coefficients are plotted for each indicated variable.

Figure F.13: Interest rate smoothing and long-run coefficients from the estimated monetary policy rule in the euro area (HICP and output gap)

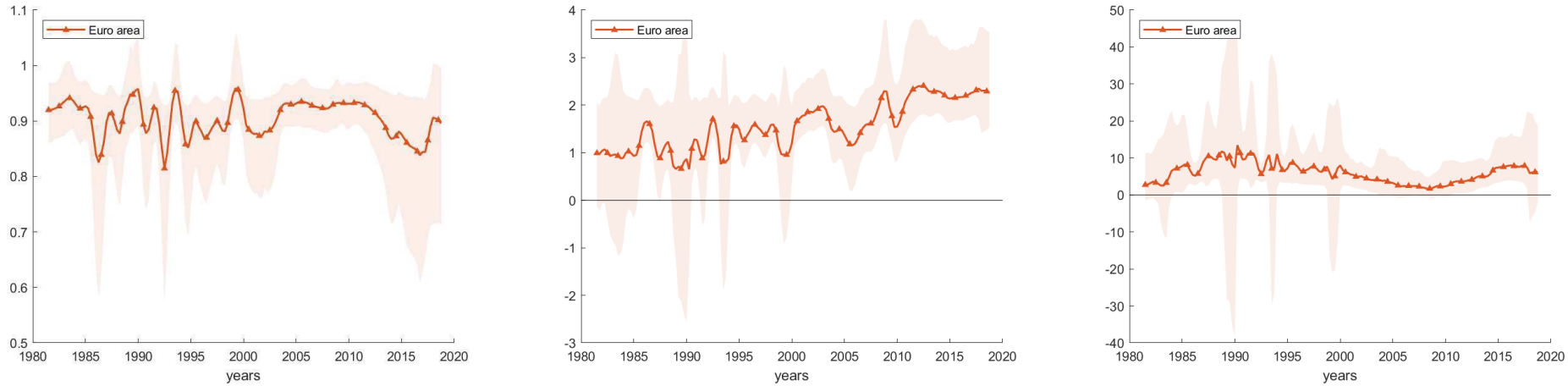


(a) Interest rate smoothing

(b) Long-run coefficient on inflation (HICP)

(c) Long-run coefficient on output gap (bandpass filter)

*Note:* Interest rate smoothing is given by the sum $\gamma_{1,rr,t}+\gamma_{2,rr,t}$, and long-run coefficients on inflation and output gap are respectively given by $(c_{r\pi,t}+\gamma_{1,r\pi,t}+\gamma_{2,r\pi,t})/(1-\gamma_{1,rr,t}-\gamma_{2,rr,t})$ and $(c_{rg,t}+\gamma_{1,rg,t}+\gamma_{2,rg,t})/(1-\gamma_{1,rr,t}-\gamma_{2,rr,t})$ in equation (3). Median (solid lines) and 68% credible interval (shaded areas) of the posterior distribution of coefficients are plotted for each indicated variable.

# References


Aastveit, K. A., Carriero, A., Clark, T. E., and Marcellino, M. (2017). Have standard vars remained stable since the crisis? *Journal of Applied Econometrics*, 32(5):931–951.

Ahmed, S., Levin, A., and Wilson, B. A. (2004). Recent us macroeconomic stability: good policies, good practices, or good luck? *Review of economics and statistics*, 86(3):824–832.

Amir-Ahmadi, P., Matthes, C., and Wang, M.-C. (2016). Drifts and volatilities under measurement error: Assessing monetary policy shocks over the last century. *Quantitative Economics*, 7(2):591–611.

Amir-Ahmadi, P., Matthes, C., and Wang, M.-C. (2017). Measurement errors and monetary policy: Then and now. *Journal of Economic Dynamics and Control*, 79:66–78.

Arias, J. E., Caldara, D., and Rubio-Ramirez, J. F. (2019). The systematic component of monetary policy in svars: An agnostic identification procedure. *Journal of Monetary Economics*, 101:1–13.

Arias, J. E., Rubio-Ramírez, J. F., and Waggoner, D. F. (2018). Inference based on structural vector autoregressions identified with sign and zero restrictions: Theory and applications. *Econometrica*, 86(2):685–720.

Basu, S. and Bundick, B. (2017). Uncertainty shocks in a model of effective demand. *Econometrica*, 85(3):937–958.

Bauer, M. D. and Rudebusch, G. D. (2014). The signaling channel for federal reserve bond purchases. *International Journal of Central Banking*, 10(3):233–289.

Bauer, M. D. and Rudebusch, G. D. (2016). Monetary policy expectations at the zero lower bound. *Journal of Money, Credit and Banking*, 48(7):1439–1465.

Baumeister, C. and Benati, L. (2013). Unconventional monetary policy and the great recession: Estimating the macroeconomic effects of a spread compression at the zero lower bound. *International Journal of Central Banking*.

Baxa, J., Horváth, R., and Vašíček, B. (2014). How does monetary policy change? evidence on inflation-targeting countries. *Macroeconomic Dynamics*, 18(3):593–630.

Baxter, M. and King, R. G. (1999). Measuring business cycles: approximate band-pass filters for economic time series. *Review of Economics and Statistics*, 81(4):575–593.

Belke, A. and Klose, J. (2013). Modifying taylor reaction functions in the presence of the zero-lower-bound—evidence for the ecb and the fed. *Economic Modelling*, 35:515–527.

Belke, A. and Polleit, T. (2007). How the ecb and the us fed set interest rates. *Applied Economics*, 39(17):2197–2209.

Belongia, M. T. and Ireland, P. N. (2016). The evolution of us monetary policy: 2000–2007. *Journal of Economic Dynamics and Control*, 73:78–93.

Benati, L. (2011). Would the bundesbank have prevented the great inflation in the united states? *Journal of Economic Dynamics and Control*, 35(7):1106–1125.

Benati, L. and Mumtaz, H. (2007). Us evolving macroeconomic dynamics: a structural investigation. *ECB Working Paper*, 746.

Benati, L. and Surico, P. (2008). Evolving us monetary policy and the decline of inflation predictability. *Journal of the European Economic Association*, 6(2-3):634–646.

Benati, L. and Surico, P. (2009). Var analysis and the great moderation. *American Economic Review*, 99(4):1636–52.

Bernanke, B. S. (2003). Constrained discretion and monetary policy. *Remarks before the Money Marketeers of New York University, New York, New York*.

Bernanke, B. S. and Blinder, A. S. (1992). The federal funds rate and the channels of monetary transmission. *American Economic Review*, 82(4):901–921.

Bernanke, B. S. and Mishkin, F. S. (1992). Central bank behavior and the strategy of monetary policy: observations from six industrialized countries. *NBER Macroeconomics Annual*, 7:183–228.

Bognanni, M. (2018). A class of time-varying parameter structural vars for inference under exact or set identification. *Federal Reserve Bank of Cleveland Working Papers*, (18-11).

Boivin, J. (2006). Has u.s. monetary policy changed? evidence from drifting coefficients and real-time data. *Journal of Money, Credit and Banking*, 38(5):1149–1173.

Boivin, J. and Giannoni, M. P. (2006). Has monetary policy become more effective? *Review of Economics and Statistics*, 88(3):445–462.

Caggiano, G., Castelnuovo, E., and Pellegrino, G. (2017). Estimating the real effects of uncertainty shocks at the zero lower bound. *European Economic Review*, 100:257–272.

Caldara, D. and Herbst, E. (2019). Monetary policy, real activity, and credit spreads: Evidence from bayesian proxy svars. *American Economic Journal: Macroeconomics*, 11(1):157–92.

Campbell, J. R., Evans, C. L., Fisher, J. D., Justiniano, A., Calomiris, C. W., and Woodford, M. (2012). Macroeconomic effects of federal reserve forward guidance. *Brookings Papers on Economic Activity*, pages 1–80.

Canova, F. and De Nicolo, G. (2002). Monetary disturbances matter for business fluctuations in the g-7. *Journal of Monetary Economics*, 49(6):1131–1159.

Canova, F. and Gambetti, L. (2009). Structural changes in the us economy: Is there a role for monetary policy? *Journal of Economic Dynamics and Control*, 33(2):477–490.

Canova, F. and Pérez Forero, F. J. (2015). Estimating overidentified, nonrecursive, time-varying coefficients structural vector autoregressions. *Quantitative Economics*, 6(2):359–384.

Caraiani, P. and Călin, A. C. (2018). The effects of monetary policy on stock market bubbles at zero lower bound: Revisiting the evidence. *Economics Letters*, 169:55–58.

Carter, C. K. and Kohn, R. (1994). On gibbs sampling for state space models. *Biometrika*, 81(3):541–553.

Castelnuovo, E. (2006). The fed's preference for policy rate smoothing: overestimation due to misspecification? *Topics in Macroeconomics*, 6(2).

Castelnuovo, E. (2007). Taylor rules and interest rate smoothing in the euro area. *The Manchester School*, 75(1):1–16.

Castelnuovo, E. and Surico, P. (2004). Model uncertainty, optimal monetary policy and the preferences of the fed. *Scottish Journal of Political Economy*, 51(1):105–126.

Chen, Q., Lombardi, M. J., Ross, A., and Zhu, F. (2017). Global impact of us and euro area unconventional monetary policies: a comparison. *BIS Working Papers*, 610.

Christensen, J. H. and Rudebusch, G. D. (2015). Estimating shadow-rate term structure models with near-zero yields. *Journal of Financial Econometrics*, 13(2):226–259.

Christiano, L., Motto, R., and Rostagno, M. (2008). Shocks, structures or monetary policies? the euro area and us after 2001. *Journal of Economic Dynamics and control*, 32(8):2476–2506.

Christiano, L. J., Eichenbaum, M., and Evans, C. (1996). The effects of monetary policy shocks: Evidence from the flow of funds. *Review of Economics and Statistics*, 78(1):16–34.

Christiano, L. J., Eichenbaum, M., and Evans, C. L. (1999). Monetary policy shocks: What have we learned and to what end? *Handbook of macroeconomics*, 1:65–148.

Christiano, L. J. and Fitzgerald, T. J. (2003). The band pass filter. *International Economic Review*, 44(2):435–465.

Clarida, R., Galí, J., and Gertler, M. (1999). The science of monetary policy: a new keynesian perspective. *Journal of Economic Literature*, 37(4):1661–1707.

Clarida, R., Galí, J., and Gertler, M. (2000). Monetary policy rules and macroeconomic stability: evidence and some theory. *The Quarterly Journal of Economics*, 115(1):147–180.

Cœuré, B. (2014). Policy coordination in a multipolar world. In *5th annual Cusco conference, Central Reserve Bank of Peru and Reinventing Bretton Woods Committee, Cusco, July*, volume 22.

Cogley, T., Primiceri, G. E., and Sargent, T. J. (2010). Inflation-gap persistence in the us. *American Economic Journal: Macroeconomics*, 2(1):43–69.

Cogley, T. and Sargent, T. J. (2005). Drifts and volatilities: monetary policies and outcomes in the post wwii us. *Review of Economic Dynamics*, 8(2):262–302.

Coibion, O. (2012). Are the effects of monetary policy shocks big or small? *American Economic Journal: Macroeconomics*, 4(2):1–32.

Creel, J. and Hubert, P. (2015). Has inflation targeting changed the conduct of monetary policy? *Macroeconomic Dynamics*, 19(1):1–21.

Crespo Cuaresma, J., Doppelhofer, G., Feldkircher, M., and Huber, F. (2019). Spillovers from us monetary policy: evidence from a time varying parameter global vector auto-regressive model. *Journal of the Royal Statistical Society: Series A (Statistics in Society)*.

Croushore, D. and Evans, C. L. (2006). Data revisions and the identification of monetary policy shocks. *Journal of Monetary Economics*, 53(6):1135–1160.

Debortoli, D., Galí, J., and Gambetti, L. (2019). On the empirical (ir) relevance ofthe zero lower bound constraint. *NBER Macroeconomics Annual 2019*, 34.

Del Negro, M. and Primiceri, G. E. (2015). Time varying structural vector autoregressions and monetary policy: a corrigendum. *The Review of Economic Studies*, 82(4):1342–1345.

Dennis, R. (2006). The policy preferences of the us federal reserve. *Journal of Applied Econometrics*, 21(1):55–77.

Fagan, G., Henry, J., and Mestre, R. (2005). An area-wide model for the euro area. *Economic Modelling*, 22(1):39–59.

Faust, J. (1998). The robustness of identified var conclusions about money. In *Carnegie-Rochester Conference Series on Public Policy*, volume 49, pages 207–244. Elsevier.

Favero, C. A. and Rovelli, R. (2003). Macroeconomic stability and the preferences of the fed: A formal analysis, 1961-98. *Journal of Money, Credit and Banking*, pages 545–556.

Fernández-Villaverde, J., Guerrón-Quintana, P., Rubio-Ramírez, J. F., and Uribe, M. (2011). Risk matters: The real effects of volatility shocks. *American Economic Review*, 101(6):2530–61.

Forbes, K., Hjortsoe, I., and Nenova, T. (2018). The shocks matter: improving our estimates of exchange rate pass-through. *Journal of International Economics*, 114:255–275.

Fourçans, A. and Vranceanu, R. (2007). The ecb monetary policy: choices and challenges. *Journal of Policy Modeling*, 29(2):181–194.

Francis, N. R., Jackson, L. E., and Owyang, M. T. (2020). How has empirical monetary policy analysis in the us changed after the financial crisis? *Economic Modelling*, 84:309–321.

Frühwirth-Schnatter, S. (1994). Data augmentation and dynamic linear models. *Journal of time series analysis*, 15(2):183–202.

Galí, J., López-Salido, J. D., and Vallés, J. (2003). Technology shocks and monetary policy: assessing the fed's performance. *Journal of Monetary Economics*, 50(4):723–743.

Garcia-Iglesias, J. M. (2007). How the european central bank decided its early monetary policy? *Applied Economics*, 39(7):927–936.

Garín, J., Lester, R., and Sims, E. (2019). Are supply shocks contractionary at the zlb? evidence from utilization-adjusted tfp data. *Review of Economics and Statistics*, 101(1):160–175.

Gavin, W. T., Keen, B. D., Richter, A. W., and Throckmorton, N. A. (2015). The zero lower bound, the dual mandate, and unconventional dynamics. *Journal of Economic Dynamics and Control*, 55:14–38.

Georgiadis, G. (2016). Determinants of global spillovers from us monetary policy. *Journal of International Money and Finance*, 67:41–61.

Gerdesmeier, D. and Roffia, B. (2004). Empirical estimates of reaction functions for the euro area. *Swiss Society of Economics and Statistics*, 140(1):37–66.

Gerlach, S. (2011). Ecb repo rate setting during the financial crisis. *Economics Letters*, 112(2):186–188.

Gerlach, S. and Lewis, J. (2014a). Ecb reaction functions and the crisis of 2008. *International Journal of Central Banking*, 10(1):137–158.

Gerlach, S. and Lewis, J. (2014b). Zero lower bound, ecb interest rate policy and the financial crisis. *Empirical Economics*, 46(3):865–886.

Gerlach, S. and Schnabel, G. (2000). The taylor rule and interest rates in the emu area. *Economics Letters*, 67(2):165–171.

Geweke, J. (1992). Evaluating the accuracy of sampling-based approaches to the calculations of posterior moments. *Bayesian statistics*, 4:641–649.

Giordani, P. (2004). An alternative explanation of the price puzzle. *Journal of Monetary Economics*, 51(6):1271–1296.

Givens, G. E. (2012). Estimating central bank preferences under commitment and discretion. *Journal of Money, Credit and Banking*, 44(6):1033–1061.

Gorter, J., Jacobs, J., and De Haan, J. (2008). Taylor rules for the ecb using expectations data. *Scandinavian Journal of Economics*, 110(3):473–488.

Gorter, J., Stolwijk, F., Jacobs, J. P., and de Haan, J. (2010). Ecb policy making and the financial crisis. *De Nederlandsche Bank Working Paper*, (272).

Halberstadt, A. and Krippner, L. (2016). The effect of conventional and unconventional euro area monetary policy on macroeconomic variables. *Bundesbank Discussion Paper*, 49.

Hamilton, J. D. (1994). *Time series analysis*. Princeton university press.

Hamilton, J. D. (2018). Why you should never use the hodrick-prescott filter. *Review of Economics and Statistics*, 100(5):831–843.

Hartmann, P. and Smets, F. (2018). The european central bank's monetary policy during its first 20 years. *Brookings Papers on Economic Activity*, 2018(2):1–146.

Hodrick, R. J. and Prescott, E. C. (1997). Postwar us business cycles: an empirical investigation. *Journal of Money, Credit and Banking*, pages 1–16.

Horvath, R. and Voslarova, K. (2016). International spillovers of ecb's unconventional monetary policy: the effect on central europe. *Applied Economics*, 49(24):2352–2364.

Hutchinson, J. and Smets, F. (2017). Monetary policy in uncertain times: Ecb monetary policy since june 2014. *The Manchester School*, 85:e1–e15.

Ilbas, P. (2012). Revealing the preferences of the us federal reserve. *Journal of Applied Econometrics*, 27(3):440–473.

Justiniano, A. and Primiceri, G. E. (2008). The time-varying volatility of macroeconomic fluctuations. *American Economic Review*, 98(3):604–41.

Kim, C.-J. and Nelson, C. R. (2006). Estimation of a forward-looking monetary policy rule: A time-varying parameter model using ex post data. *Journal of Monetary Economics*, 53(8):1949–1966.

Kim, K., Laubach, T., and Wei, M. (2020). Macroeconomic effects of large-scale asset purchases: New evidence. Technical report, Board of Governors of the Federal Reserve System (US).

Kim, S., Shephard, N., and Chib, S. (1998). Stochastic volatility: likelihood inference and comparison with arch models. *The Review of Economic Studies*, 65(3):361–393.

Koop, G., Leon-Gonzalez, R., and Strachan, R. W. (2009). On the evolution of the monetary policy transmission mechanism. *Journal of Economic Dynamics and Control*, 33(4):997–1017.

Kortela, T. and Nelimarkka, J. (2020). The effects of conventional and unconventional monetary policy: identification through the yield curve. *Bank of Finland Research Discussion Paper*, (3).

Krippner, L. (2013). Measuring the stance of monetary policy in zero lower bound environments. *Economics Letters*, 118(1):135–138.

Krippner, L. (2019). A note of caution on shadow rate estimates. *Journal of Money, Credit and Banking*, forthcoming.

Lhuissier, S., Mojon, B., and Rubio-Ramirez, J. F. (2020). Does the liquidity trap exist? *Banque de France Working Paper*, 762.

Lombardi, M. and Zhu, F. (2018). A shadow policy rate to calibrate us monetary policy at the zero lower bound. *International Journal of Central Banking*, 14(5):305–346.

Lubik, T. A. and Schorfheide, F. (2004). Testing for indeterminacy: an application to us monetary policy. *American Economic Review*, 94(1):190–217.

Lütkepohl, H. (2005). *New introduction to multiple time series analysis*. Springer Science & Business Media.

Mouabbi, S. and Sahuc, J.-g. (2019). Evaluating the macroeconomic effects of the ecb's unconventional monetary policies. *Journal of Money, Credit and Banking*, 51(4):831–858.

Mumtaz, H. and Surico, P. (2009). Time-varying yield curve dynamics and monetary policy. *Journal of Applied Econometrics*, 24(6):895–913.

Mumtaz, H. and Zanetti, F. (2013). The impact of the volatility of monetary policy shocks. *Journal of Money, Credit and Banking*, 45(4):535–558.

Newey, W. K. and West, K. D. (1987). A simple, positive semi-definite, heteroskedasticity and autocorrelation-consistent covariance matrix. *Econometrica*, 55(3):703–708.

Nikolsko-Rzhevskyy, A., Papell, D. H., and Prodan, R. (2014). Deviations from rules-based policy and their effects. *Journal of Economic Dynamics and Control*, 49:4–17.

Okun, A. (1962). Potential gnp: its measurement and significance. In *American Statistical Association: Proceedings of the Business and Economics Statistics Section*, pages 98–104.

Orphanides, A. (2001). Monetary policy rules based on real-time data. *American Economic Review*, 91(4):964–985.

Orphanides, A. (2003). Historical monetary policy analysis and the taylor rule. *Journal of monetary economics*, 50(5):983–1022.

Orphanides, A. (2004). Monetary policy rules, macroeconomic stability, and inflation: A view from the trenches. *Journal of Money, Credit and Banking*, 36(2):151–175.

Ozlale, U. (2003). Price stability vs. output stability: tales of federal reserve administrations. *Journal of Economic Dynamics and Control*, 27(9):1595–1610.

Pasricha, G. K., Falagiarda, M., Bijsterbosch, M., and Aizenman, J. (2018). Domestic and multilateral effects of capital controls in emerging markets. *Journal of International Economics*, 115:48–58.

Plante, M., Richter, A. W., and Throckmorton, N. A. (2017). The zero lower bound and endogenous uncertainty. *The Economic Journal*, 128(611):1730–1757.

Potjagailo, G. (2017). Spillover effects from euro area monetary policy across europe: A factor-augmented var approach. *Journal of International Money and Finance*, 72:127–147.

Primiceri, G. E. (2005). Time varying structural vector autoregressions and monetary policy. *The Review of Economic Studies*, 72(3):821–852.

Putnam, B. H. and Azzarello, S. (2012). A bayesian interpretation of the federal reserve's dual mandate and the taylor rule. *Review of Financial Economics*, 21(3):111–119.

Ramey, V. A. (2016). Macroeconomic shocks and their propagation. In *Handbook of macroeconomics*, volume 2, pages 71–162. Elsevier.

Rogers, J. H., Scotti, C., and Wright, J. H. (2018). Unconventional monetary policy and international risk premia. *Journal of Money, Credit and Banking*, 50(8):1827–1850.

Rubio-Ramirez, J. F., Waggoner, D. F., and Zha, T. (2010). Structural vector autoregressions: Theory of identification and algorithms for inference. *The Review of Economic Studies*, 77(2):665–696.

Rudebusch, G. D. (2001). Is the fed too timid? monetary policy in an uncertain world. *Review of Economics and Statistics*, 83(2):203–217.

Sahuc, J.-G. and Smets, F. (2008). Differences in interest rate policy at the ecb and the fed: An investigation with a medium-scale dsge model. *Journal of Money, Credit and Banking*, 40(2-3):505–521.

Sauer, S. and Sturm, J.-E. (2007). Using taylor rules to understand european central bank monetary policy. *German Economic Review*, 8(3):375–398.

Sims, C. A. (1980). Macroeconomics and reality. *Econometrica*, 48(1):1–48.

Sims, C. A. (1992). Interpreting the macroeconomic time series facts: The effects of monetary policy. *European Economic Review*, 36(5):975–1000.

Sims, E. and Wu, J. C. (2020). Are qe and conventional monetary policy substitutable? *International Journal of Central Banking*, 16(1):195–230.

Stock, J. H. and Watson, M. W. (2002). Has the business cycle changed and why? *NBER macroeconomics annual*, 17:159–218.

Stroud, J. R., Müller, P., and Polson, N. G. (2003). Nonlinear state-space models with state-dependent variances. *Journal of the American Statistical Association*, 98(462):377–386.

Surico, P. (2007a). The fed's monetary policy rule and us inflation: The case of asymmetric preferences. *Journal of Economic Dynamics and Control*, 31(1):305–324.

Surico, P. (2007b). The monetary policy of the european central bank. *Scandinavian Journal of Economics*, 109(1):115–135.

Swanson, E. T. (2018). The federal reserve is not very constrained by the lower bound on nominal interest rates. *Brookings Papers on Economic Activity*, pages 555–572.

Taylor, J. B. (1993). Discretion versus policy rules in practice. *Carnegie-Rochester conference series on public policy*, 39:195–214.

Taylor, J. B. (1999). The robustness and efficiency of monetary policy rules as guidelines for interest rate setting by the european central bank. *Journal of Monetary Economics*, 43(3):655–679.

Tchatoka, F. D., Groshenny, N., Haque, Q., and Weder, M. (2017). Monetary policy and indeterminacy after the 2001 slump. *Journal of Economic Dynamics and Control*, 82:83–95.

Uhlig, H. (2005). What are the effects of monetary policy on output? results from an agnostic identification procedure. *Journal of Monetary Economics*, 52(2):381–419.

Ullrich, K. (2005). Comparing the fed and the ecb using taylor-type rules. *Applied Economics Quarterly*, 51(3):247–266.

Vissing Jorgensen, A. and Krishnamurthy, A. (2011). The effects of quantitative easing on interest rates: Channels and implications for policy. *Brookings Papers on Economic Activity*, 43(2):215–287.

Wieland, J. F. (2019). Are negative supply shocks expansionary at the zero lower bound? *Journal of Political Economy*, 127(3):973–1007.

Woodford, M. (2001). The taylor rule and optimal monetary policy. *American Economic Review*, 91(2):232–237.

Woodford, M. (2003). Optimal interest-rate smoothing. *The Review of Economic Studies*, 70(4):861–886.

Woodford, M. et al. (2012). Methods of policy accommodation at the interest-rate lower bound. In *Proceedings-Economic Policy Symposium-Jackson Hole*, pages 185–288. Federal Reserve Bank of Kansas City.

Wu, J. C. and Xia, F. D. (2016). Measuring the macroeconomic impact of monetary policy at the zero lower bound. *Journal of Money, Credit and Banking*, 48(2-3):253–291.

Wu, J. C. and Zhang, J. (2019). A shadow rate new keynesian model. *Journal of Economic Dynamics and Control*, 107:103728.